Check for updates

Bistable Structures for Advanced Functional Systems

Yunteng Cao, Masoud Derakhshani, Yuhui Fang, Guoliang Huang, and Changyong Cao*

Bistable mechanical systems having two local minima of potential energy can rest in either of the two stable equilibrium states in the absence of external loadings. A snap-through action may occur under suitable stimuli and/or loading, during which such systems exhibit distinct properties from linear structures. Such kinds of structures have been widely exploited for designing advanced functional systems for a variety of applications. Here, the advances of bistable structures are summarized for novel advanced functional systems, including actuators, energy harvesters, microelectromechanical systems (MEMS), robotics, energy absorbers, and programmable devices as well as metamaterials. The controllable snap-through motions are highlighted in the nonlinear structures of bistability/multistability. Finally, the major principles, structures, pros and cons, and the future research directions along with its challenges are discussed.

1. Introduction

While linear mechanical systems have only one stable equilibrium state, nonlinear systems may possess more than one local minima of the potential energy, i.e., more than one stable equilibrium states to rest in. Bistable structures, which hold two stable equilibrium states, exhibit distinct properties and performances from those of linear structures, even though it is the simplest case of multistability. The two stable equilibrium states usually correspond to geometrically different configurations, indicating a snap-through action, the transition from one stable equilibrium state to the other, will cause large displacement and large deformation including remarkable curvature

Y. Cao, M. Derakhshani, Y. Fang, C. Cao
Laboratory for Soft Machines & Electronics
School of Packaging
Michigan State University
East Lansing, MI 48824, USA
E-mail: ccao@msu.edu
Y. Cao
Department of Civil and Environmental Engineering
Massachusetts Institute of Technology
Cambridge, MA 02139, USA
G. Huang
Department of Aerospace and Mechanical Engineering
University of Missouri
Columbia, MO 65211, USA
C. Cao
Departments of Mechanical Engineering, Electrical & Computer Engineering
Michigan State University
East Lansing, MI 48824, USA

changes and/or strain variations, particularly in compliant structures capable of large elastic deformation. Such displacement and deformation do not need continuous input to maintain as in linear systems. Meanwhile, the potential energy barrier for the snap-through is generally lower than that in a linear structure corresponding to such displacements and deformations. These two intrinsic features of bistable structures render them versatility and promising candidates in various applications,[1–4] such as actuators, robotics, microelectron-mechanical systems (MEMS), sensors, and energy harvesters. For instance, actuators and robotics will be able to achieve large deformations via moderate driving forces that trigger the snap-through actions by rational design where the desired motions are in coincidence with the two stable equilibrium states. Work is done by forces with limited magnitudes over large displacements in the snap-through actions, thus, energy can be absorbed, stably stored, and possibly reversely released in a rationally designed bistable system. This property enables its application for energy absorption and protection under impacts.

Over the past decade, great effort has been put into unrevealing the geometrical configurations of bistable structures from fundamental units such as beams and films/plates to more complex structures consisting of these units, followed by the topology design of bistable structures as well as multistable structures. Such efforts were originally from merely a mechanical prospective. The bistability arises intrinsically from the topology of the structures, e.g., buckled beams and plates. Recently, studies of bistable structures in other physical fields, such as electrical, magnetic, and thermal fields as well as their coupled fields, have been emerging, thanks to the advances in smart materials (e.g., shape memory materials, composite laminates, piezoelectric materials, and soft elastomers) that are responsive to specific physical stimuli. Special attention has been attracted by the design of bistable structures fabricated from smart materials that are utilized to introduce bistability and to trigger snap-through actions.

Smart materials hold a fantastic merit of being responsive to specific predefined physical factors, enabling a wide pool of choices for a variety of applications. Indeed, the diversity and versatility of smart materials significantly broaden the applications of bistable structures in advanced functional systems, including smart actuators for low-input high-output actuation purposes,[5] energy harvesters for expanding operational frequency bandwidth and maximizing output power,[6,7] soft robotics and MEMS for increasing device flexibility and

Bistable Structures for Advanced Functional Systems

Yunteng Cao, Masoud Derakhshani, Yuhui Fang, Guoliang Huang, and Changyong Cao*

Bistable mechanical systems having two local minima of potential energy can rest in either of the two stable equilibrium states in the absence of external loadings. A snap-through action may occur under suitable stimuli and/or loading, during which such systems exhibit distinct properties from linear structures. Such kinds of structures have been widely exploited for designing advanced functional systems for a variety of applications. Here, the advances of bistable structures are summarized for novel advanced functional systems, including actuators, energy harvesters, microelectromechanical systems (MEMS), robotics, energy absorbers, and programmable devices as well as metamaterials. The controllable snap-through motions are highlighted in the nonlinear structures of bistability/multistability. Finally, the major principles, structures, pros and cons, and the future research directions along with its challenges are discussed.

1. Introduction

While linear mechanical systems have only one stable equilibrium state, nonlinear systems may possess more than one local minima of the potential energy, i.e., more than one stable equilibrium states to rest in. Bistable structures, which hold two stable equilibrium states, exhibit distinct properties and performances from those of linear structures, even though it is the simplest case of multistability. The two stable equilibrium states usually correspond to geometrically different configurations, indicating a snap-through action, the transition from one stable equilibrium state to the other, will cause large displacement and large deformation including remarkable curvature

changes and/or strain variations, particularly in compliant structures capable of large elastic deformation. Such displacement and deformation do not need continuous input to maintain as in linear systems. Meanwhile, the potential energy barrier for the snap-through is generally lower than that in a linear structure corresponding to such displacements and deformations. These two intrinsic features of bistable structures render them versatility and promising candidates in various applications,[1–4] such as actuators, robotics, microelectron-mechanical systems (MEMS), sensors, and energy harvesters. For instance, actuators and robotics will be able to achieve large deformations via moderate driving forces that trigger the snap-through actions by rational design where the desired motions are in coincidence with the two stable equilibrium states. Work is done by forces with limited magnitudes over large displacements in the snap-through actions, thus, energy can be absorbed, stably stored, and possibly reversely released in a rationally designed bistable system. This property enables its application for energy absorption and protection under impacts.

Over the past decade, great effort has been put into unrevealing the geometrical configurations of bistable structures from fundamental units such as beams and films/plates to more complex structures consisting of these units, followed by the topology design of bistable structures as well as multistable structures. Such efforts were originally from merely a mechanical prospective. The bistability arises intrinsically from the topology of the structures, e.g., buckled beams and plates. Recently, studies of bistable structures in other physical fields, such as electrical, magnetic, and thermal fields as well as their coupled fields, have been emerging, thanks to the advances in smart materials (e.g., shape memory materials, composite laminates, piezoelectric materials, and soft elastomers) that are responsive to specific physical stimuli. Special attention has been attracted by the design of bistable structures fabricated from smart materials that are utilized to introduce bistability and to trigger snap-through actions.

Smart materials hold a fantastic merit of being responsive to specific predefined physical factors, enabling a wide pool of choices for a variety of applications. Indeed, the diversity and versatility of smart materials significantly broaden the applications of bistable structures in advanced functional systems, including smart actuators for low-input high-output actuation purposes,[5] energy harvesters for expanding operational frequency bandwidth and maximizing output power,[6,7] soft robotics and MEMS for increasing device flexibility and

Y. Cao, M. Derakhshani, Y. Fang, C. Cao
Laboratory for Soft Machines & Electronics
School of Packaging
Michigan State University
East Lansing, MI 48824, USA
E-mail: ccao@msu.edu
Y. Cao
Department of Civil and Environmental Engineering
Massachusetts Institute of Technology
Cambridge, MA 02139, USA
G. Huang
Department of Aerospace and Mechanical Engineering
University of Missouri
Columbia, MO 65211, USA
C. Cao
Departments of Mechanical Engineering, Electrical & Computer Engineering
Michigan State University
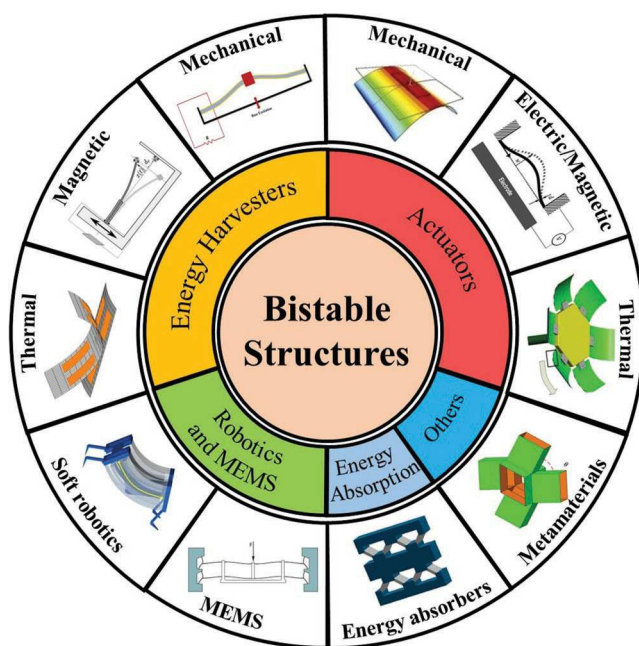East Lansing, MI 48824, USA

Figure 1. Bistable structures for advanced functional systems. They have been explored for a variety of applications, including actuators[29,45,50] energy harvesting,[3,147] robotics[79] and MEMS,[160] energy absorption,[150] and metamaterials and programmable materials.[105]

functionality,[8] energy absorption structures for enhancing energy storage capacity,[9] and programmable materials and metamaterials for unique properties like negative stiffness.[10]

In this review, we summarize the advances of bistable structures for novel advanced functional systems, categorized by their applications as actuators, robotics and MEMS, programmable devices and metamaterials, energy harvesters, and energy absorbers (**Figure 1**). Actuators, robotics and MEMS, programmable devices and metamaterials are reviewed in Section 2, 3, and 4, whose outputs are displacement and/or deformation upon energy inputs. In Section 4 and 5, energy harvesters, and energy absorbers, which harvest and store energy under displacement and/or deformation input, are discussed. The controllable snap-through actions in nonlinear structures of multistability are further highlighted. We finally discuss the major principles, pros and cons, and the future research directions and challenges.

2. Bistable Structures for Actuators

Actuators are critical parts of a device or robot/machine to generate deformation or displacement for executing specific tasks via consuming various kinds of energy. Bistable structures can enable large displacement and/or deformation by fast snap-through and have been extensively explored for developing novel actuators. Designed bistability generally result from either the topology of novel structures or the employment of smart materials. Compared with conventional actuators, such bistable structures require relatively low energy consumption to generate large displacements owing to the ease of triggering the snap-through. Smart materials, such as piezoelectric materials and shape memory materials, impart the responsive capability

of these structures to other physical stimuli (e.g., electrical, magnetic, and thermal fields) rather than mechanical interactions, broadening their potential applications. Furthermore, bistable structures can lead to a more flexible and versatile system with less design complexity. In this section, we summarize the bistable structure-based actuators, according to their actuation mechanisms, into four main categories: actuators driven by mechanical forces, by electrical fields, by magnetic interactions, and by temperature changes. The actuators with multistable structures are also briefly discussed.

2.1. Actuators Based on Mechanically Driven Bistable Structures

If designed properly with suitable topology, key fundamental units, such as buckled columns, beams, films, and plates/shells, and more complex structures consisting of these units, can exhibit intrinsic bistability that can be utilized for actuators. The snap-through of the bistable structures in actuators driven by mechanical interactions can be triggered when the applied mechanical loading is beyond a critical magnitude. The novelty of such kinds of actuators mainly relies on the structural design (e.g., complex topology) of a device and the methodology of exerting a mechanical loading. For example, Gerson et al. designed a beam-based microactuator (**Figure 2**A), where an integrated electrostatic comb driven transducer was used to apply required force for snap-through.[11] Interestingly, by serially connecting the bistable elements, a multistable actuator was created, showing controllable sequential snap-through buckling (Figure 2A). The displacement achieved was considerably enhanced while the actuation force only slightly increased, compared to those in a single beam design. It is worth noting that such a structure does not necessarily have to be at microscale as it was reported in literature. Addo-Akoto and Han proposed an actuation mechanism that utilized a twisted string and a pin driven by a DC motor to apply the bending moment and trigger the snap-through of a bistable buckled beam (Figure 2B).[12] Their design is simple and cost-effective but needs the parts to exert loading in a contact way, which increases the complexity of the entire system and hinders its miniaturization. Plates and shells are also employed in actuators driven by pneumatically or hydraulically pressure. For example, Rothemund et al. reported a type of soft valve that uses bistability of an elastomeric membrane to control the flow through channels.[13] Such bistable actuators from plates or shells share similarity to beams but facilitate application of pressure via a sealed structure.

It is noted that actuators based on conventional materials require the direct exertion of a contact loading onto the structure and usually need a complex design and control strategy, which have become the main challenges of hindering their wide applications. Therefore, more advanced actuators using smart materials are invented, allowing exertion of non-contact loading to trigger the snap-through of bistable structures. The utilization of smart materials enables exertion of mechanical loading via deformation of specific parts attached to or embedded in the bistable structures. Smart materials that are response to electrical, magnetic, and thermal fields are the main sources to introduce non-contact interactions, and related designs will be discussed later in this section. It is anticipated
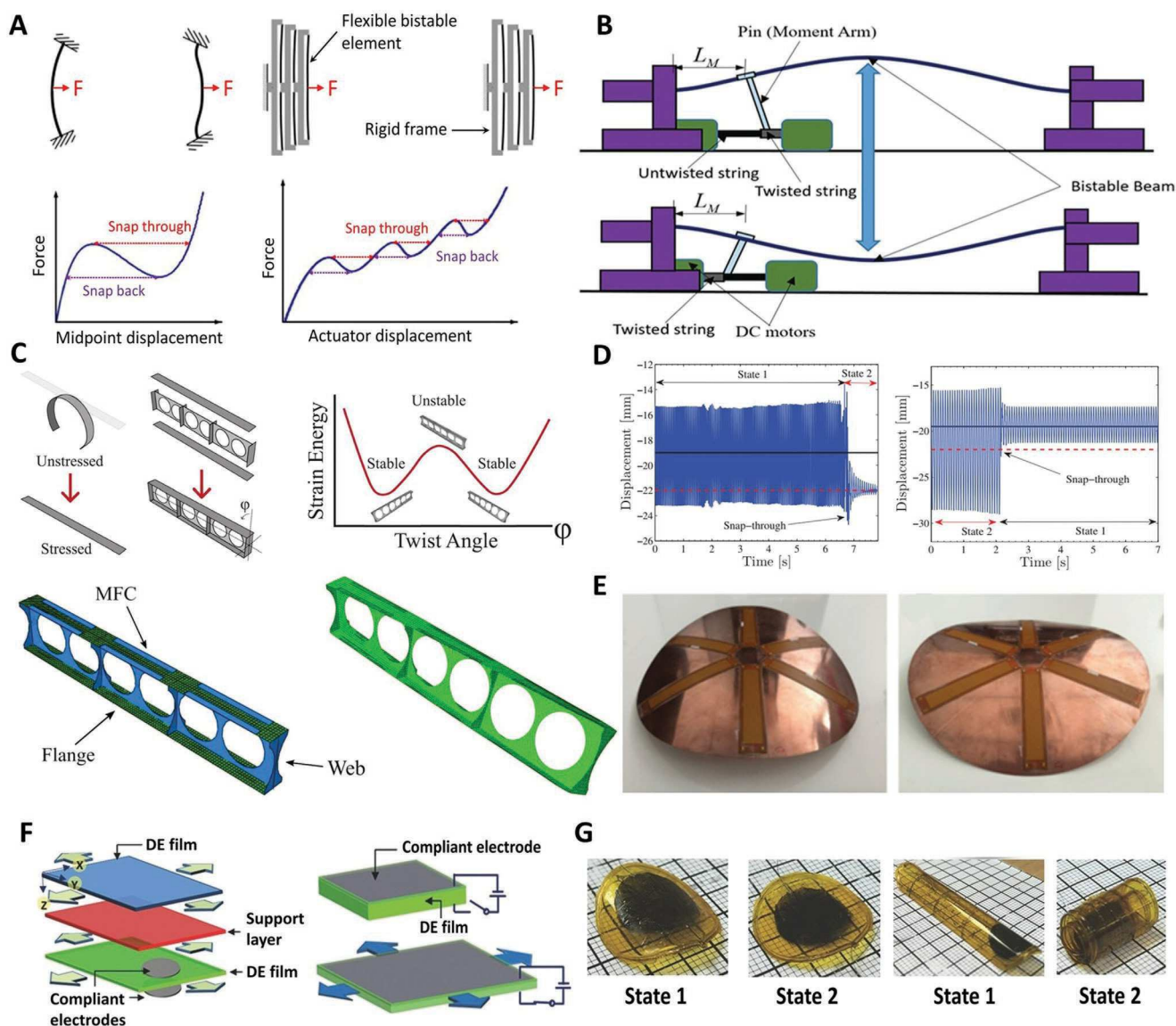
Figure 2. Actuators based on mechanically and electrically driven bistable structures. A) Conceptual design of a microscale curved beam electrostatic actuator and its expected operational performances of two configurations: a single bistable beam (left) and multiple serially connected bistable beams (right). Reproduced with permission.[1] Copyright 2012, Elsevier. B) Schematic illustration of an actuation mechanism using a bistable beam, which consists of a twisted string, a DC motor, a pin, and a moment arm for snap-through actuation. Reproduced with permission.[12] Copyright 2018, SAGE Publishing. C) Illustration of the assembly process of a pre-stressed twisting bistable structure. The curled flanges are stretched and bonded onto web and stiffeners to lock the pre-stress into the structure. The strain energy plot of the twisting bistable structure to show the structures equilibrium positions. The experimental setup and the two stable states of the twisting bistable structure. Reproduced with permission.[18] Copyright 2018, IOP Publishing. D) Displacement of dynamically induced snap-through from state 1 to state 2 (forcing frequency 28.0 Hz) and from state 2 to state 1 (forcing frequency 13.5 Hz) for a [90/0] 160 × 160 mm bi-stable specimen. Reproduced with permission.[34] Copyright 2012, SAGE Publications. E) The two stable configurations of a plastically deformed disc with the MFC actuators. Reproduced with permission.[37] Copyright 2017, The Authors, published by the Royal Society. F) A soft actuator enabled by a bistable laminate structure. The prestretched dielectric elastomer (DE) films are bonded with a support layer in the middle. The laminate can be actuated by an applied voltage from a contracted state to an expanded state. G) The disk and tape-spring actuators made of the DE composite laminate can switch between two stable states. Reproduced with permission.[5] Copyright 2018, Wiley-VCH.

that the employment of compliant and smart materials may help overcome the technical challenges while taking advantage of the topology design, as shown in the section of soft robotics.

Except the bistability induced by solid-solid interactions in response to external stimuli, the bistability triggered by solid-liquid interactions are also demonstrated by Xu et al.[14,15] For example, they propose an electrically and thermally controlled actuation system by adjusting the relative hydrophobicity of a nanoporous material/liquid system. The liquids can be continuously pumped in and out of nanopores by adjusting the electric intensity[14] or temperature field.[15] By optimizing the pore size, solid phase, and liquid phase, the energy density, power density, and efficiency of the actuation system can be tuned according to the requirements and applications.

**ADVANCED
SCIENCE NEWS**
www.advancedsciencenews.com

**ADVANCED
FUNCTIONAL
MATERIALS**
www.afm-journal.de

2.2. Actuators Based on Electrically Driven Bistable Structures

The electric actuation is attractive for many applications due to its advantages of easy control and fast response. It has been widely used for developing different kinds of electronically driven actuators. Using attraction or repulsion between charges and the responses of smart materials induced by applied electric fields are two strategies to electrically control the snap-through of bistable structure-based actuators. Piezoelectric materials generate strains when an electric field is applied, and vice versa produce charges when subjected to stresses. The combination of piezoelectric materials with bistable structures is a main approach of fabricating piezoelectric actuators. The converse piezoelectric effect forms the basis of piezoelectric actuators, which employ the deformation and displacement of piezoelectric materials under controlled external electric fields to manipulate the snap-through of the structure. For example, as shown in Figure 2C, a classic I-beam was imparted bistability by two straightened curved beam flanges, which were separated by a web.[16,17] Based on the bistable twisting I-beam, Arrieta et al. used macro fiber composites (MFC) consisting of piezoelectric materials attached to the flanges to control the snap-through, producing fast and large deflections with low strain piezoelectric materials.[18]

Composite laminates are also extensively studied as morphing structures, and the methods to introduce bistability to laminates are developed via anisotropic residual stress generated by thermal treatment[19,20] and by prestress[21–24] or via laminate design.[25] Several groups developed piezoelectric actuators by bonding MFCs to bistable composite laminates to trigger snap-through. Initial trials using a single piezoelectric MFC patch bonded to one side of a laminate demonstrated successful snap-through[26–30] but failed to trigger the reverse snap-through due to the limited actuation force of the piezoelectric MFC patch, and the changed geometry and increased stiffness resulting from the attachment of the patch. Further effort by Schultz et al. using a two-ply, [0/90]$_T$ graphite–epoxy laminate sandwiched between two piezocomposite actuators successfully demonstrated the self-resetting behaviors.[31]

Another strategy that employed narrow occurred MFC strips distributed over the entire surface was presented to replace the commonly adopted method where large rectangular MFC patches were bonded in the center of the laminates.[32] This strategy aimed to eliminate the significant influence of MFC patches on the shape of the laminates, particularly the reduction of curvature where they are bonded. Alternatively, dynamically assisted snap-through was proposed using a resonant control technique.[33–35] MFCs were used to induce resonant response of the actuator, i.e., the bi-stable composite laminate together with the attached piezoelectric MFCs. The magnitude, i.e., displacement of the actuator, would be much larger in resonant conditions than that in static or non-resonant conditions, which makes it possible to reach the critical displacement and trigger snap-through. The actuator was designed such that the two equilibrium states have distinct modal frequencies, allowing state-specific frequency being targeted and preventing chaotic oscillation arising from continuous snap-through between stable states. Once the snap-through occurred, the input from MFCs was not resonant anymore, resulting in diminishing structural displacement (Figure 2D).

Meanwhile, combining other driving mechanisms with piezoelectric actuation is used to overcome this problem. For example, Bowen et al. used a mass to demonstrate reversible transitions.[27] Shape memory alloy (NiTi) wires were used to drive reversible state switching in a bistable composite cantilever where piezoelectric MFCs triggered snap-through.[36] Interestingly, Hamouche et al. developed a bistable laminate by plastically deforming an initially flat copper disc with small imperfections based on a fully nonlinear inextensible uniform-curvature shell model (Figure 2E).[37] Distinct from those two stable configurations of laminates usually having curvatures with opposite signs, their structure showed two stable configurations with same-sign curvatures, indicating much smaller energetic gap between the equilibria. The reversible state transition was controlled by the attached MFCs electrically.

Despite these fantastic solutions, bonding piezoelectric MFC patches to bistable structures indeed introduces extra components and stiffness to the system, resulting in high working voltage, incapability of self-reverse snap-through, and sometimes even loss of bistability. An interesting thought would be: why not build bistable structures directly with piezoelectric materials so that the simplified structures are more compliant to snap through reversibly by itself? Lee et al. built such a laminate consisting of only two piezoelectric MFCs that functions as both the actuator and the primary structure.[38–40] They bonded two MFCs orthogonally in their actuated states and released the voltage post cure to create in-plane residual stresses. Recall that introducing proper prestress or residual stress is one of the key techniques to impart bistability to laminates.[21–24] The resulting [0^{MFC}/90^{MFC}]$_T$ laminate displayed a cylindrical shape, demonstrated bistability, and snapped through and back with only piezoelectric actuation.

Distinct from the rapid advances in utilizing smart materials to electrically driving actuators, the strategy that employs attraction or repulsion between charges to trigger snap-through of bistable actuators was blocked, partly due to the limited magnitude of the attraction or repulsion compared to the stiffness of the system. This is intrinsically determined by the inverse-square law, where the force between charges is inversely proportional to the square of the distance between charges that is generally larger than tens of microns in engineering. However, the development of soft materials (e.g., dielectric elastomers) and fabrication of microscale structures solved this problem. Both decrease the stiffness of the system, and the latter also allows electric interaction at a scale of the order of several micrometers. For example, a bioinspired trilayered bistable all-polymer laminate was fabricated with a supporting layer made of polyimide or polyester sandwiched by two orthogonally prestrained acrylate adhesive elastomer films as DE layers (Figure 2F).[5] Dielectric elastomer, polyacrylate film, has a thickness of 500 µm with Young's Modulus of 0.22 MPa (≈six orders lower than that of aluminum), while the supporting layer has a thickness of 25 µm with Young's Modulus of 2.5 GPa and 4.9 GPa for polyimide and polyester (≈two orders lower than that of aluminum), respectively. To actuate this laminate, electrode materials including carbon grease and PEDOT:PSS were properly placed on stretched DE layers, with lightweight carbon nanotube (CNT) yarns as soft and flexible electrical leads. As highlighted, each effort of the authors was made to decrease the

**ADVANCED
SCIENCE NEWS**
www.advancedsciencenews.com

**ADVANCED
FUNCTIONAL
MATERIALS**
www.afm-journal.de

stiffness of the system. The disk actuator displayed controlled reversible snap-through between two equilibrium states and the tape-spring actuator underwent shape transformation from one equilibrium shape to another upon activation, mimicking the retraction of a chameleon's tongue (Figure 2G).

On the other hand, the feasibility of electrostatically triggering snap-through of bistable microstructures, particularly curved micro beams, has been demonstrated theoretically and experimentally.[41–45] Electrostatic actuation is efficient at distances at the order of several micrometers between electrodes, while the typical length of microstructures ranges from tens to hundreds of micrometers. For example, the bistable structure used in Figure 2B can be triggered electrostatically by employing the beam as an electrode or attaching an electrode to the beam, instead of integration of an electrostatic comb driven transducer.[12,46] However, this adaptation may not be suitable for the multistable structure due to the limited space between the two fixed electrodes for electrostatic actuation. Thus, electrostatic actuation is promising in MEMS or NEMS, but less popular in large scale devices unless ultrahigh voltage and/or large current is used.

2.3. Actuators Based on Magnetically Driven Bistable Structures

The ubiquitous magnetic interaction is highly desired for many applications due to its attractive properties such as ease of access and control, fast response, and noncontact interaction. It has been one of the most widely used driving mechanisms for actuators and is probably the most promising method. The magnetically driven actuators take advantages of the interaction between magnetic fields, generated by currents, permanent magnets or other magnetic materials. Magnetic interaction shares similar disadvantages to electrostatic interaction; the intensity of most available magnetic fields, either natural or man-made, is limited and the magnitude of magnetic interaction decays fast with distance. Thus, employment of magnetic interaction on bistable structures composed of soft magnetic responsive composites is a feasible strategy.

Loukaides et al. reported a bistable spherical cap made of iron carbonyl-infused polydimethylsiloxane (PDMS) that was actuated remotely through permanent magnets (**Figure 3**A–C).[47] The Young's modulus and the shear modulus of the PDMS they used were 750 kPa and 250 kPa, respectively; and the thickness of the cap was 1–3 mm, retaining the compliance of the structure. Carbonyl iron microparticles ranging from 2–9 μm were uniformly distributed in the PDMS matrix, enabling the application of a magnetic force on the cap when it is close to a magnet. By decreasing the distance between a permanent magnet and the cap, the intensity of the magnetic field increased at where the cap was located, resulting in an increased force on the cap that could trigger the snap-through. It was also discovered that non-axisymmetric transition shapes had lower energy barrier and were preferred by bistable spherical caps initially tilted or with imperfection.[48] This idea was fancy, but the design could be improved from at least two aspects by a) replacement of the ferromagnetic iron microparticles by aligned permanent magnetic microparticles, and b) replacing the driving permanent magnets with electromagnets. The magnetic microparticles distributed in

the polymer can be aligned during curing process by keeping the mixture in an external magnetic field. The cured polymer matrix will become a soft permanent magnet, having a determined N and S pole (Figure 3D). This method is particularly helpful in the fabrication of complex structures using printing-based techniques (Figure 3E).[49] The magnetic field of an electromagnet is determined by the current intensity and direction, which facilitates transition between magnetic attraction and repulsion (Figure 3D). These two strategies enable reversible, remotely controlled snap-through of the cap by changing the direction and intensity of the current in the electromagnet, avoiding moving the driving magnets. For example, Hou et al. used an electromagnet, instead of a permanent magnet, to actuate a bistable curved beam composed of a silicone elastomer matrix with embedded micro-sized iron particles (Figure 3F).[50] The snap-through was triggered by the electromagnet with a current larger than a critical value. Reversible configuration transition could be achieved by combining two electromagnets on each side of the beam. It was also found that the critical current was proportional to the thickness of the beam and the distance between the beam and electromagnets and inversely proportional to the density of iron particles. It is worth noting that the critical current (voltage) was 1.8 A (12 V), much lower than the actuation voltage for dielectric elastomers, proposing a potential advantage of magnetic actuation to electric actuation via dielectric elastomers. Alternatively, the curved bistable beam was designed as conductive, having a high slenderness ratio of 12000 to enable flexibility. The current in the beam underwent a force in a magnetic field of magnets, resulting in controlled reversible snap-through (Figure 3G).[51]

Different from the studies where the bistability results from bistable structures, Li et al. reported a dielectric elastomer actuator showing tristability induced by magnetic force. They used two prestretched cone dielectric elastomer films to hold a movable magnet in the middle of two fixed magnets, creating three stable positions (Figure 3H,I).[52] Both fixed magnets exerted attraction on the movable magnet. The tensions from dielectric elastomer films and the attractions from fixed magnets were balanced when in stable position 2. By applying a voltage on dielectric elastomer film 1, electrically induced Maxwell stresses compressed the film, resulting in a reduced tension and thus the moving magnet being closer to stable position 3. Upon the applied voltage reached a critical value (2.5 kV), the moving magnet snapped through to stable position 3 from 2. Reverse snap-through from stable position 3 to 2 was achieved by removing the voltage applied on film 1 and releasing the tension in film 2 via an applied voltage. Such design combines electrostatic responsive materials and magnetic interaction, displaying a promising strategy for interaction based multistability.

2.4. Actuators Based on Thermally Driven Bistable Structures

Heat, as one of the most widely used energy forms, has been explored in bistable actuators. Despite temperature dependent material properties, the ubiquitous thermal expansion displays great potential in actuation due to thermal strain and thermal stress, which results from the difference of thermal expansion coefficients among materials that are bonded together when
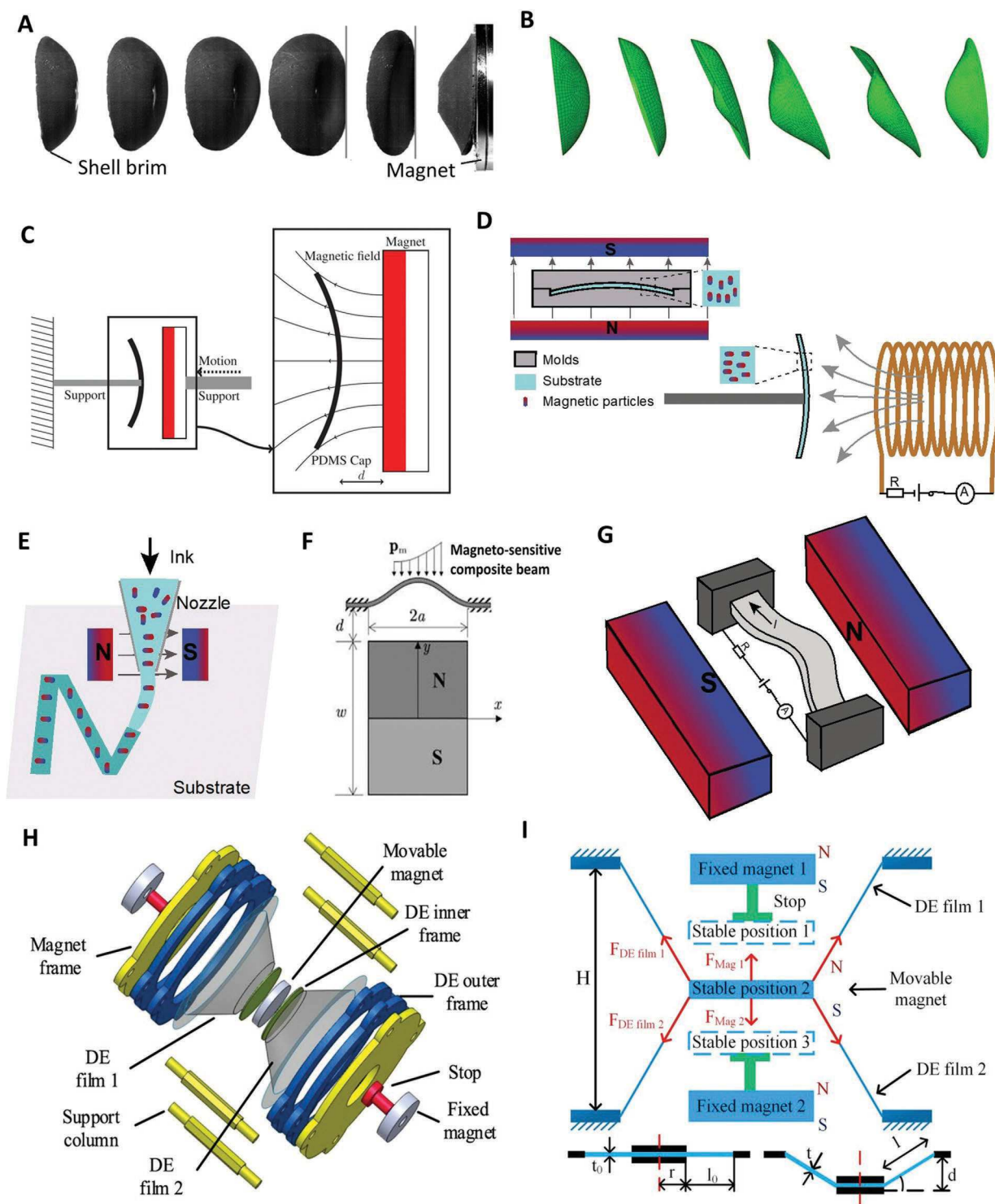
Figure 3. Actuators based on magnetically driven bistable structures. A,B) Actuation sequence of a bistable magnetic rubber composite shell from experiments and finite element modeling. Reproduced with permission.[48] Copyright 2016, IOP Publishing. C) Illustration diagram of the experimental setup for remotely actuating a PDMS spherical cap with a permanent magnet. Reproduced under the terms of the Creative Commons Attribution License.[47] Copyright 2015, The Authors, published by Taylor & Francis. D) Schematic illustration of the fabrication setup for aligning magnetic particles in a polymer substrate using an external magnetic field. Reversible and remotely controlled snap-through of the cap can be achieved by an electromagnet. E) Schematic of producing aligned magnet nanoparticles in a substrate by printing-based techniques. F) Schematic illustration of the actuation of a bistable composite beam made of a silicone elastomer with embedded iron particles. Reproduced with permission.[50] Copyright 2018, AIP Publishing. G) Schematic illustration of the experimental setup for the electromagnetic actuation of the soft beam. H) Schematic diagram of a tristable dielectric elastomer (DE) actuator consisting of two cone-shaped dielectric elastomer films, two end permanent magnets, and one central movable magnet for magnetic actuation. I) The three stable states of the magnetic-based DE actuator in (A).

**ADVANCED
SCIENCE NEWS**
www.advancedsciencenews.com

**ADVANCED
FUNCTIONAL
MATERIALS**
www.afm-journal.de

temperature changes. Thermal strain and thermal stress enable two strategies of thermally driven bistable actuators, i.e., bonding thermal strain and thermal stress generators to bistable structures and designing thermally responsive bistable structures.

Thermal strain and thermal stress generators can be built by bilayer strips made of materials with different thermal expansion coefficients or by the same material with locally heating. For example, Zhang et al. developed a solar tracking device that was composed of bistable laminates driven by a Ni36/Mn75Ni15Cu10 bimetallic strip (**Figure** 4A).[53] With the radiation from the sun, the bimetallic strips could bend and deform due to temperature change, triggering the snap-through deformation of the bistable laminates. Inversely, the decline of solar illuminance caused the decrease of temperature and the diminished deformation of the bimetallic strips, thereby the bistable laminates snapped back to their initial states (Figure 4B).

Properly designed laminates can serve as thermally driven bistable actuators. In fact, residual thermal stresses were used to impart bistability to unsymmetric laminates.[19,20] Li et al. observed the snap-through of such laminates by locally heating the middle part to relieve residual stress and induce snapping of the unheated regions, followed by a cooldown step (Figure 4C).[54] It was found that the laminated geometry and the distribution of the heated region could significantly affect the critical actuation temperature and the snap-through behavior of a bistable laminate. Therefore, it is possible coming to the plausible conclusion that the $[0_n/90_n]$ class of unsymmetric laminates are inherently incapable of displaying thermally driven snap-through behaviors when other different heating methods are utilized.[55] Eckstein et al. reported the snap-through driven by temperature change and its dependence on initial curvature using fiber–metal hybrid laminates that have high coefficient of thermal expansion mismatch between composites and metals.[55]

In addition, thermal gradients and temperature-dependent material properties were taken into consideration in thermally actuated composite laminates.[56] While it is of great importance to account for variation of material properties over a wide range of temperature, thermal gradients are usually negligible along the small thickness of thin laminates unless in rare extreme conditions and are technically challenging to apply. Clamped curved beams are another example commonly used as bistable structures. Zhou et al. reported a bistable microactuator that consisted of inverted-series-connected Cu/W-based curved beams (Figure 4D),[57,58] which bend with electrothermally induced temperature change since the thermal expansion coefficients of copper and tungsten are 17×10^{-6} and 4.3×10^{-6} °C^{-1}, respectively. The snap-through of a 1 mm long actuator enabled a displacement of more than 30 μm. Their design was significantly simplified by combining Joule heating, snap-through triggering, and bistability via the employment of conductive bi-layered beams. The two metals also have relatively high melting points and large Young's modulus, indicating a large displacement or force output. Hussein et al. created a tunable symmetric bistable actuator consisting of two opposite sets of preshaped curved beams with similar materials and dimensions that are connected to each other by a shuttle at their mid-points (Figure 4E).[59] The tunable bistability was realized by Joule heating of the two sets of conductive beams via applied voltages, which created a negative stiffness behavior at their initial position.

Other than the ubiquitous thermal expansion, some alloys, such as NiTi, CuZnAl, and CuAlNi, show unique thermal shape memory effect, that is, they can restore their original form from the deformed form when heated. Such shape memory effect results from the phase transformation between the high temperature phase (austenite structure) and low temperature phase (martensite structure).[60,61] Shape memory alloys (SMAs), especially NiTi alloy, have been extensively used for actuators, MEMS, and robotics thanks to their high actuation stress, relatively high strain, and ease to be manufactured into various formats. Using SMAs to build thermally driven bistable actuators shares analogous strategies with using piezoelectric materials to fabricate bistable actuators that are electrically driven. The feasibility of using SMA wires to trigger the snap-through of unsymmetric composite laminates was demonstrated by an approximate theory and supported with experiments. [59] Numerical models were also developed and may help solve the manufacturing problems such as a large number of SMA wires required and their distribution as well as the influence of laminates processing.[62,63] These designs used one-way shape memory effect, thus enabled only one-way snap-through. A reversible snap-through could be achieved by using additional SMA wires or other smart materials such as piezoelectric MFCs to actuate snap-back.[36] Two-way SMAs have rarely been used for bistable actuators. Even though a two-way SMA can "remember" its shapes at both high and low temperatures and might contribute to the reversible snap-through, it suffers from much lower recovery strain than a one-way SMA and quick memory loss after the initial training procedure, resulting in low reliability.

There are several other categories of materials also displayed thermally induced shape memory effect, including ceramics,[64] hydrogels,[65] and polymers.[61,66] Ceramics can be hardly used on bistable actuators due to their intrinsic brittleness. The application of hydrogels for actuations may be hindered owing to their great dependence on water and poor mechanical stability in atmosphere. These issues will be overcome by emerging hydrogels with enhanced mechanical properties for special actuators working in aqueous conditions. Despite the low thermal conductivity and Young's modulus, shape memory polymers (SMPs) manifest desiring properties including extremely high strain (up to 400%, and possibly above 800%[60]), fast and easy shape training, mild fabrication conditions, low and tunable transition temperature, and low density. SMPs have been widely used as an alternative to SMAs. Chen and Shea presented an actuator consisting of a von Mises truss based bistable structure actuated by a shape memory strip (SMS) (Figure 4F). This actuator was fabricated by 3D printing and was combined serially to achieve multistability and in other rational ways to form reconfigurable 3D structures.[67] The reconfiguration of this actuator could be triggered easily by environment temperature change since the glass transition temperature T_g of the shape memory polymer, FLX9895, is ≈30 °C, above which the SMS will recover its original shape. The activation of such a design, as claimed, was suitable to be controlled through the surrounding environment. Because Joule heating can easily overheat the structure and cause structural damage or failure without proper monitoring and a feedback mechanism will inevitably increase structural size and complexity. In addition, the maximum strain
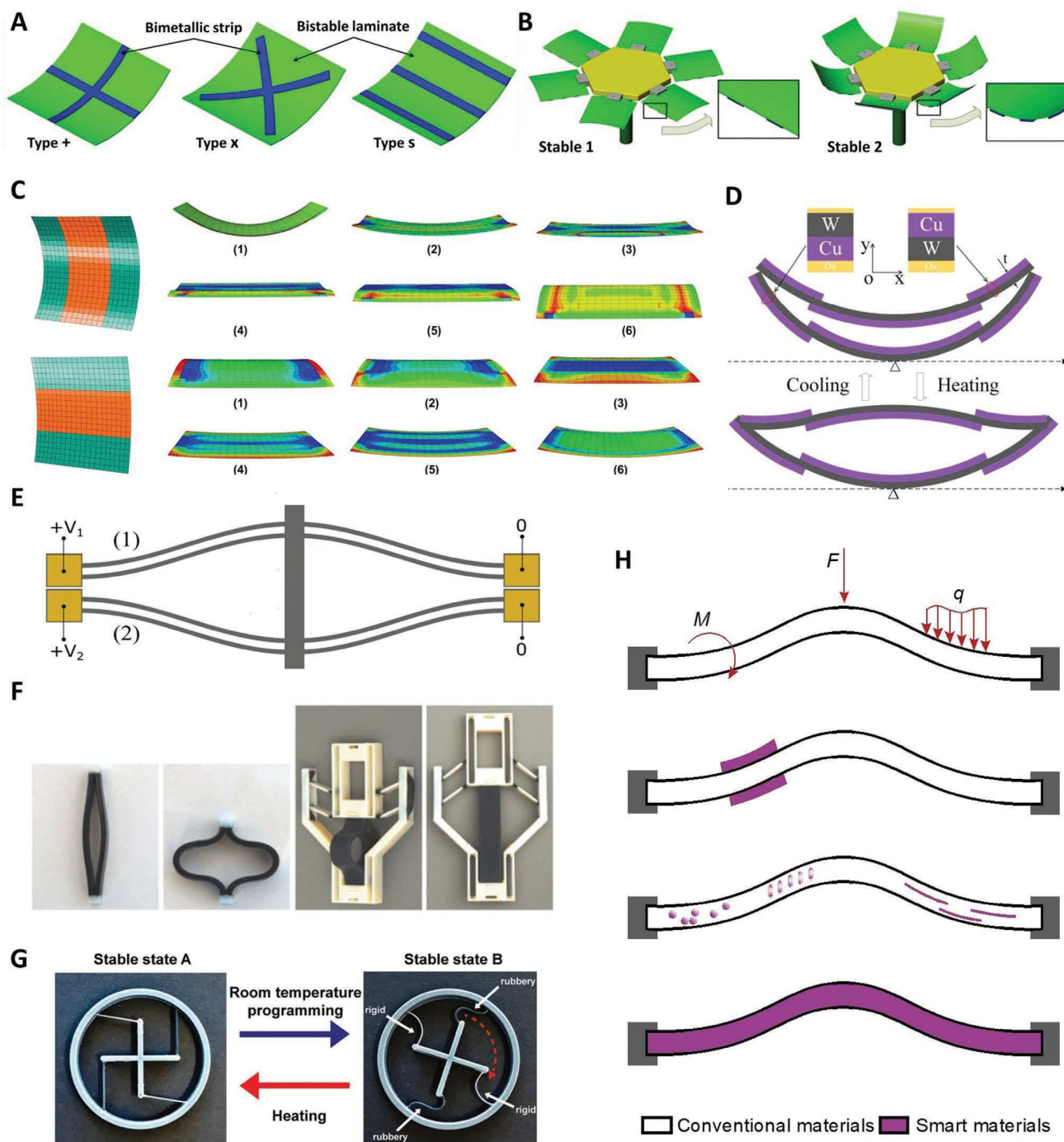
**ADVANCED
SCIENCE NEWS**
www.advancedsciencenews.com

**ADVANCED
FUNCTIONAL
MATERIALS**
www.afm-journal.de

Figure 4. Actuators based on thermally driven bistable structures. A) Bistable laminate actuators with three different layouts of bimetallic strips, bending actuated by heat to change its deformation state. B) A solar tracking device enabled by bistable actuators in (A). Reproduced with permission.[53] Copyright 2020, Elsevier. C) Sketches of residual stress-relieved regions (marked in red) of the two heating strategies on two 140 mm × 140 mm laminates and corresponding simulated snap-through process. Reproduced with permission.[54] Copyright 2012, Elsevier. D) Working principle of an electrothermal bistable microactuator. Reproduced with permission.[57] Copyright 2019, IEEE. E) The tunable symmetric bistable device. Reproduced with permission.[59] Copyright 2020, IOP Publishing. F) The printed state and programmed state of an expanded SMS and two states of the bistable actuator after assembly of the SMS. Reproduced with permission.[67] G) The original shape (state A) and rotated structure (state B) of the rotational bistable structure with two different digital SMPs (rigid and rubbery ones). Reproduced with permission.[68] Copyright 2019, Wiley-VCH. H) Four typical design strategies for bistable structure-based actuators.

within the extending and contracting SMS may reach 0.258 and 0.374, respectively, much higher than the upper limit of SMA (typically ≈8%).

In fact, the printability of SMPs is especially attractive in the fabrication of actuators with complex structures. Recently, Jeong and his colleagues designed a 4D thermally responsive

**ADVANCED
SCIENCE NEWS**
www.advancedsciencenews.com

**ADVANCED
FUNCTIONAL
MATERIALS**
www.afm-journal.de

structure, capable of large-angle rotational actuation in a highly controlled manner (Figure 4G).[68] They employed two different digital SMPs (rigid and rubbery ones) to print beams that connect the inner cross and outer circle. The rigid beams provided bistability while the rubbery beams with fixed boundary conditions act as the control knob. Multistability was also reported by aligning the actuator unit in a nesting doll manner. Note that the temporary shapes of SMP beams were obtained mechanically below T_g, which was counterintuitive. Typically, a SMP beam recovered to its initial shape from a temporary shape that was obtained by a typical heating above T_g, deforming, and cooling procedure, that is, their shape memory effect does not relate to deformation below T_g. Because SMPs are at a hard and relatively brittle "glassy" state below T_g, they undergo either small elastic deformation or fracture and cannot form a temporary shape as above T_g. The magic relies on the way the beams were prepared, i.e., mixing the SMP (VeroWhite) with a rubber-like material, TangoBlack. By the addition of rubber-like TangoBlack, the beams deformed to form a temporary configuration at room temperature below T_g without material failure and maintained the shape in the absence of external forces. Once heated up above their T_g, the beams become flexible and will minimize their potential energy by releasing deformation, i.e., reconfigure from curved beams (temporary shape) to straight ones (initial shape). In sum, the application of SMPs rendered a secondary equilibrium stable state to the structure and enabled its one-way snap-through.

In addition to the three actuation mechanisms, other smart materials that are responsive to pH,[69–71] light,[72–75] and ionic strength etc. are emerging. However, there are only a few bistable structure-based actuators reported yet. For example, Zhao et al. developed a bistable concave-shaped assembly which displayed snap-through when heated up and snapped back when pH changed from 7.0 to 2.0.[69] Most of the actuators using these smart materials do have two stable configurations, but they do not have structure-based bistability. Instead, they obtain the additional stable configuration due to the response of the smart materials to external stimuli, that is, the two stable configurations correspond to the two states of stimuli (e.g., low/high pH, with/without luminescence). The potential energy curve of the structure under stimuli is different from that without stimuli, but both of them typically have only one minimal. It should be noted that such design may have a set of continual configurations that should be maintained by application of the stimuli.

To design an actuator, two parts are essential, i.e., its structure and its actuation mechanism. We now summarize from a structural perspective coupled with the discussion on actuation mechanism to provide a thorough understanding. In conclusion, all the bistable structure-based actuators discussed were structurally designed in four typical strategies as shown in Figure 4H. The first and most fundamental design utilizes a bistable structure made of conventional materials, whose snap-through is triggered by various loadings, contact or non-contact, in a format of moments, point forces, pressures, and strains (e.g., locally heating, not shown in the figure). The application of contact moments, forces, and pressures provides sufficient loading for snap-through usually at a cost of additional components, which increases the complexity of the whole system.

Particularly, pressure can be applied via vacuum or pressured air/liquid by an external pump. Non-contact loading (e.g., the force exerted on current by a magnetic field) typically has limited magnitude and is suitable for actuators at micro scales. The second to the fourth strategies take advantage of smart materials responsive to physical stimuli, such as electric, magnetic and temperature fields, to enrich loading application methodology and/or impart bistability. By attaching components made of smart materials to (e.g., piezoelectric MFCs, SMA wires, bimetallic strips) or embedding them in (e.g., carbonyl iron microparticles) bistable structures consisting of conventional materials, the loading for snap-through triggering is applied by physical stimuli. However, smart materials and methodology to apply necessary physical stimuli as well as these strategies have inherent shortcomings that should be taken into account in the design process. While electric signals are fast responsive, an external power source and circuits are usually necessary to apply electric voltage, which makes electric voltage infeasible in the third strategy.

Temperature change and magnetic interaction are suitable for both the second and third strategies due to numerous techniques to change temperature and to generate and tune magnetic fields. For example, Joule heating, conduction, and convection have been extensively used in reported designs. Radiation, another main type of heat transfer, has yet been reported in bistable actuators despite of its high efficiency and non-contact property. Radiative heating is a promising way to change temperature locally in a controlled manner. Indeed, infrared light of specific wavelengths is used to remotely heat up embedded materials while not the substrate. (infrared heating therapy refs) Magnetically responsive micro- and nanoscale materials that can be embedded in substrates, particularly soft materials and printable materials, as shown in the third design, are the most important contributor to advances of magnetically driven actuators. The printing techniques with controlled magnetic fields will further pave the way to the fabrication of such actuators with complex structures and advanced functions.

Microactuators might still employ second structure, but the third design is not suitable owing to the size limitation of microstructures. The last strategy uses merely smart materials where they function as both structural materials and stimuli responsive parts. It significantly simplifies the structure and renders actuators possibility for more advanced functions including robots and MEMS. However, smart materials such as ceramics and metals are typically not suitable in this strategy because of the limited reversible deformation while smart polymers are great candidates.

3. Bistable Structures for Robotics and MEMS

Similar to actuators, robotics and MEMS also transform energy inputs into displacements and/or deformations. By integration of other components, they can employ bistable structures to perform more versatile functions than actuators. Soft robotics take advantages of the flexibility of the materials and structures, while MEMS and microrobotics utilize their advantages resulting from microscale sizes.

ADVANCED
SCIENCE NEWS
www.advancedsciencenews.com

ADVANCED
FUNCTIONAL
MATERIALS
www.afm-journal.de

3.1. Bistable Structures for Soft Robotics

Soft robots have demonstrated great potential in a variety of applications such as prosthetics, surgical tools, rehabilitation facilities, and medical devices thanks to their excellent environmental adaptability, user-friendliness, and safety stemming from material flexibility.[76] Efficient actuation, as one of the key issues in soft robotics, have been intensively explored in respect to employment of smart materials and structural design. Impressive advances have been reported via adoption of bistable structures and their combination with smart soft materials. Bistable structures generally are used as moveable parts due to snap-through. For example, Chen et al.[77] designed a temperature-based propulsion soft swimmer using bistable shape memory polymer (SMP) muscles (**Figure 5**A). The SMP muscle was triggered by water temperature to snap through between two stable states to generate directional propulsion (Figure 5B). By adjusting the rotational stiffness of the flexible joints, the fabricated state was more stable than the activated state which made directional actuation possible. The soft swimmer could achieve a full back and forth actuation process through two SMPs with different activation and transition temperatures (Figure 5C). When $T_1 < T_2$, by setting the temperature at T_1, the first bistable element (M_1) was actuated, while after increasing the temperature from T_1 to T_2, the second actuation process occurred (M_2).

Bistability has also been employed for agile locomotion and jumping of soft robots.[78–80] As shown in Figure 5D, the soft robot was made of a soft supporting structure (polyvinyl chloride plate (PVC)) with two thermally actuated shape memory alloys (SMA) at its top and bottom sides for achieving vertical and forward jumping, respectively.[78] The supporting layer was covered with heat-resistant sheets on both sides to eliminate the influence of temperature variation. Two different modules were fabricated: a single module for vertically jumping and a series-type module (two modules in series) for forward jumping. It was demonstrated that a 0.05 m single module could jump up to 0.13 m, and the jumping height would be further improved by adjusting bending amplitude. For the series-type module, the jumping process reduced the buckling time difference between the two modules. Tang et al. built a soft pneumatic actuator with a two-linkage structure connected by springs to provide bistable deformations for high-speed and high force tasks (Figure 5E,F).[81] The body of the soft robot was prepared by compressing the polyester sleeve through a steel rod, while the rigid frame was 3D-printed with polylactic acid (PLA). In their design, the high-speed bistable mechanism or high-force monostable (higher spring stiffness) mechanism utilized the pre-stretching of a middle spring (Figure 5G). Equipped such a bistable structure, the soft robot could run at a linear locomotion speed of 174.4 mm/s, about 4.7 times faster than the similar soft crawler without a bistable structure.

In addition, soft grippers take advantages of bistable structures, too. For example, Zhang et al. designed a bionic robotic gripper by mimicking the trapping motions of Venus flytrap using a bistable morphing structure enabled by anti-symmetric shells and the magnetic actuation.[82] The proposed design consisted of a core standing with two compliant magnetically actuated fingers for swift large deformations and strong gripping motions. More recently, Lunni et al. also developed a plant-inspired soft bistable structure made of hygroscopic electrospun nanofibers.[83] The energy barrier of the soft bistable mechanism highly depended on the geometry and the elastic properties, while the snap-through motion between the stable states was mainly governed by the active layer. Furthermore, Zhang et al. proposed a compliant bistable gripper for small-scale aerial robotic systems,[84] in which a linkage-based bistable mechanism was designed to be switchable, adjustable, and stable for grasping and holding operation. The bistable gripper consisted of four major parts: three fingers, three soft silicone tubes, a base with three vertical beams, and a contact pad. Both the analytical modeling and experimental results showed that the designed gripper can make the aerial robot perch on a horizontally hanging object.

Interestingly, Chi et al. designed pre-curved 2D beam-like bending actuators and 3D doming actuators with tunable monostability and bistability to fabricate soft robotics, which achieved high performance as energy-efficient soft gripper to holding objects, as fast-speed larva-like jumping soft crawler with average locomotion speed of 0.65 body-length s^{-1} (51.4 mm s^{-1}), and as fast swimming bistable jellyfish-like soft swimmer with an average speed of 53.3 mm s^{-1}.[85] Instead of using bistable structures directly for motion, Rothemund et al. used their soft bistable valve as an autonomous controller in grippers and crawlers,[13] which eliminates the necessity of an external programmed controller and significantly simplifies the structure of soft robotics. These studies demonstrated the versatility of bistable structures in soft robotics and the roles that bistable structures can play innovatively.

3.2. Bistable Structures for Microrobotics and MEMS

Bistable structures could simplify the design and control mechanism of microrobotics and MEMS. One representative example is the DNA-based nanostructures.[86–88] As shown in **Figure 6**A, a compliant bistable DNA nanostructure was fabricated with four links with helix bundles to predict its energy landscape for snap-through motions.[89,90] The energy plot of such a structure had two stable configurations with an asymmetric distribution and a tunable energy barrier (Figure 6B). Most of the structures were in their stable states (S_1, S_2 in Figure 6C) corresponding to the conformational energy distributions (Figure 6D). This study provided insightful knowledge for designing microscale biomedical devices such as biosensors and medical manipulators by implementing macroscale structural design into DNA nanostructures.

As the basic building blocks for many biological systems, helical structures are another kind of structures that can be combined with bistability for micro/nanorobotic applications.[91] Using FEM analysis and experimental testing, Chen et al. studied spontaneous twisting/bending of helix structures (Figure 6E),[92] demonstrating that tunable helical ribbons could be made by bonding two or three layers of pre-stretched strips. As shown in Figure 6F, a small piece of a slap bracelet composite made of stainless-steel layers and a fabric cover exhibited two stable configurations through the coupled
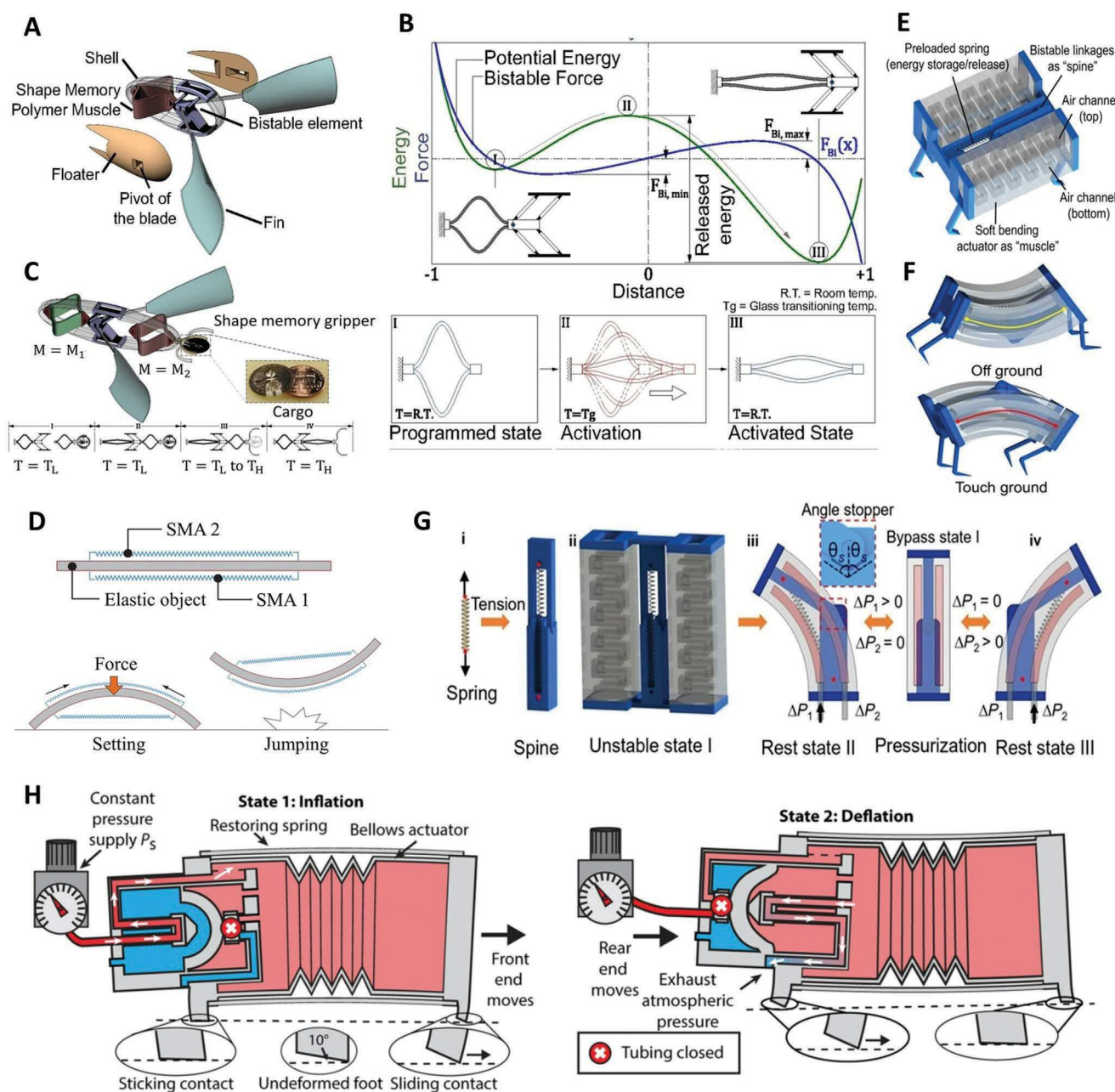
Figure 5. Bistable structures for soft robotics. A) Schematic illustration of a soft swimmer capable of directional propulsion, actuated by a shape memory polymer (SMP) bistable muscle. B) The bistable structure is actuated at the transition temperature T_g resulting in backward pulling and propulsion of robot arms. C) A full forward-backward motion mechanism via two SMP bistable actuators with different activation and transition temperature (M_2 has a higher activation temperature than M_1 to enable the full forward-backward motion). Reproduced with permission.[77] Copyright 2018, National Academy of Sciences. D) Schematic illustration of a bistable soft robot consisting of an elastic object (PVC plate) and two SMA actuators. The SMA actuators contract by heat generated by electricity, leading to snap-through deformation for jumping motions. Reproduced with permission.[78] Copyright 2018, IEEE. E) Design of a hybrid robot made of soft pneumatic actuators and a rigid bistable structure. F) Two stable states of the proposed hybrid crawler in motion. G) Schematic and work principles of the hybrid robot and its two stable configurations. Reproduced with permission.[81] Copyright 2020, American Association for the Advancement of Science.

bending/twisting behavior, which could be used for designing self-assembled microrobotics systems with different actuation mechanisms.

Beam-type bistable structures have been widely used in MEMS such as micro-switchers[93] and resonators[94] due to their nonlinear properties in improving the functionality and

reducing the design complexity of MEMS devices.[8,95] As shown in Figure 6G, the bistable micro switching device was made of curved beams with thermal actuators and two stopping blocks. The switching device could be fabricated by either microfabrication method or additive manufacturing method (Figure 6H). Design and fabrication of a novel actuation mechanism using
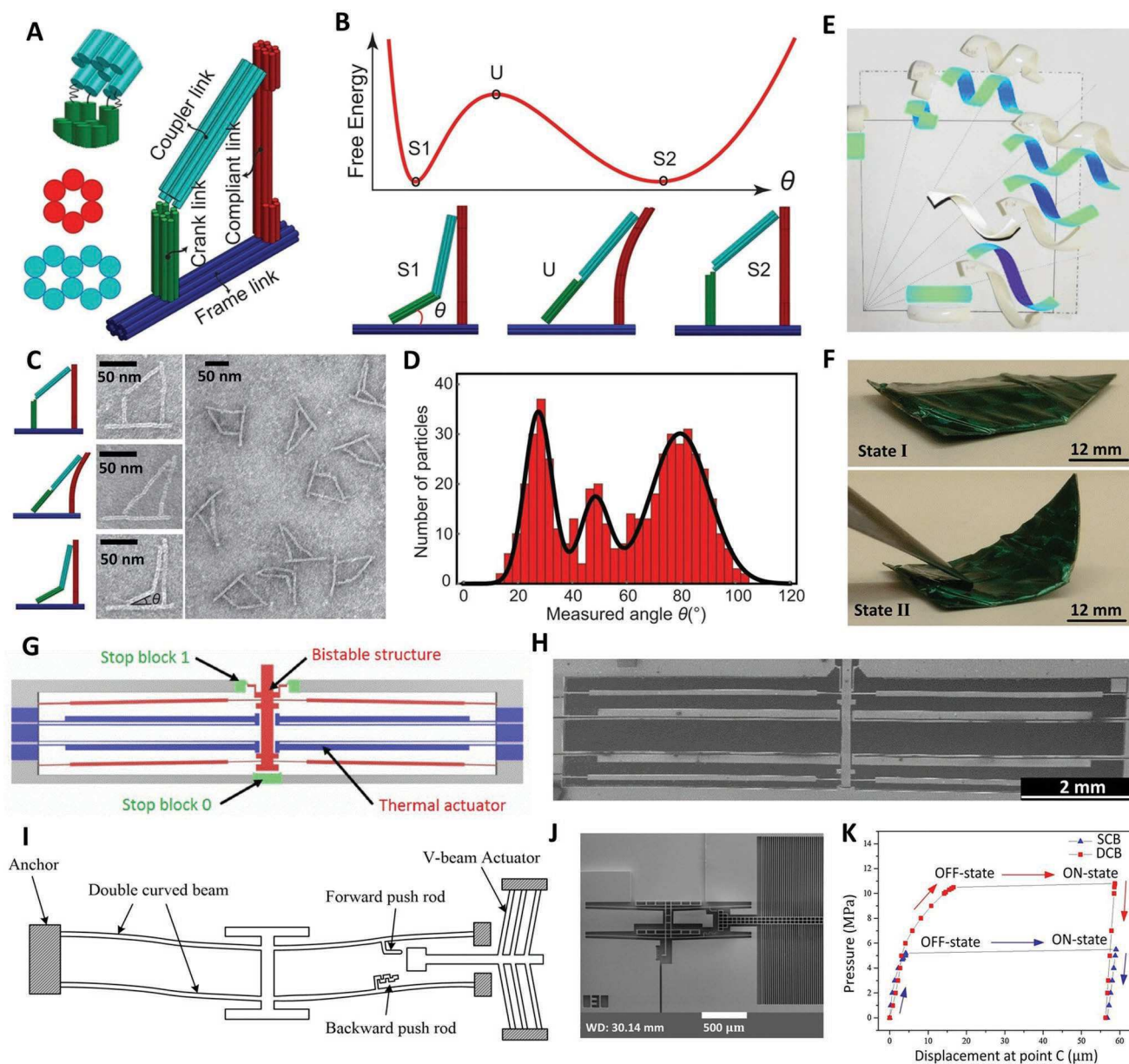
**ADVANCED
SCIENCE NEWS**

www.advancedsciencenews.com

**ADVANCED
FUNCTIONAL
MATERIALS**

www.afm-journal.de

Figure 6. Bistable structures for microrobotics and MEMS. A) Schematic illustration of a compliant DNA bistable nanostructure made of four links with helix bundles (hb). B) The energy plot of the bistable nanostructure: two stable states (S1 and S2) and one unstable state (U). C) TEM images of the designed bistable DNA structures, showing most of the structures are in their stable states (either S1 or S2). D) Distribution of the state configurations in terms of the angle between the frame link and the crank link, confirming that most of the particles stay in their stable states. Reproduced with permission.[89] Copyright 2015, American Chemical Society. E) Helix structured ribbons made by bonding two or three layers of strips with different anisotropic prestrains. F) Two stable configurations of a triangular piece of slap bracelet made of layered stainless steel wrapped by a fabric cover. Reproduced with permission.[92] Copyright 2013, IEEE. G) Schematic design of a thermally actuated bistable microswitching device. The top and bottom blocks act as a stopping mechanism for the microrobotic system. H) Image of a microfabricated bistable structure with thermal actuators and stopping blocks. Reproduced with permission.[8] Copyright 2019, Springer Science + Business Media. I) A moment-driven bistable microdevice with a curved-beam structure and a V-beam actuator. The forward and backward push rods make the switching possible via a single actuator in the absence of a stopping mechanism. J) SEM image of the fabricated microdevice. K) The pressure-displacement plot of a single curved beam (SCB) and a double curved beam (DCB) micro-actuator. As applied pressures reach the critical values, the snap-through occurs, and the bistable device switches to the ON-state. Reproduced with permission.[99] Copyright 2020, Elsevier.

a similar bistable structure were also proposed for microrobotics.[96,97] The electrothermally actuated bistable module could be optimized for use in a digital microrobotics system.[98] Also, Huang et al. designed a moment-driven bistable microdevice

with a curved-beam structure and a V-beam actuator (Figure 6I,J).[99] The forward and backward push rods made the switching possible via a single actuator with no need for a stopping mechanism. The V-beam electrothermal actuator drove

**ADVANCED
SCIENCE NEWS**

www.advancedsciencenews.com

**ADVANCED
FUNCTIONAL
MATERIALS**

www.afm-journal.de

the forward and backward pushrods to make the bistable arch beams generate reversible snap-through motions. Figure 6K shows the pressure-displacement relations of the snap-through deformations for the ON and OFF states of a single curved beam and a double-curved beam microactuator.

Additionally, many researchers also explored bistable structures for multifunctional MEMS use. For example, a clamped-clamped arch microbeam was designed to serve as a MEMS actuator and pressure sensor.[46] The arch beam accommodated between two electrodes had two stable states. The bottom driving electrode was activated by a DC voltage superimposed with an AC signal so that the beam could switch between its two stable states in a forward/backward frequency sweep, which could be detected by the topside sensing electrode powered by a DC voltage when the capacitance changed between the arch beam and the fixed electrode. In another study, Ouakad et al. performed theoretical and experimental analysis for a MEMS shallow arched beam to investigate its dynamic snap-through behaviors for filtering applications.[100] Several sharp amplitude jumps were observed for the microbeam actuated near its first and third natural frequencies. Thus, the dynamic snap-through behavior observed at certain frequency bandwidths can be potentially used for band-pass filters with a sharp transition from a passband to a stopband. Most recently, multistability designs based on bistable ferroelectric materials were studied to fabricate multistate memories with significantly high storage capacity.[2]

4. Bistable Structures for Programmable Materials/Metamaterials

Programmable structures such as origami-based structures and metamaterials have unique engineering properties including auxeticity (negative stiffness), deploy-ability, self-locking, and foldability.[10,101–104] **Figure 7**A illustrates an origami-based cube pipe structure capable of forming multiple stable configurations.[105] The unique structure consisted of six cube pipes made of polyethylene terephthalate (PET) with their hinge sections bonded with carbon fiber reinforced polymer (CFRP) shells. The shells were reconfigurable between stable states via snap-through deformation when subjected to a magnetic force on the curved edges of the pipe (Figure 7B), indicating the potential applications for non-contact smart valves. Another similar study on origami tubes with reconfigurable polygonal cross-sections was also introduced for smart pipes and microrobotics applications.[106] The foldability of origami structures enabled the shape changes of the tubes for smart functional applications. For example, Silverberg et al. used hidden DOFs to create unique features in origami structures for bistability enhancement that can be potentially used in soft grippers.[107]

Recently, Vangelatos et al. designed an architected 3D buckling structure for multistable functional materials[102] (Figure 7C). The microscale truss-based structure with bistable elements could help mechanical behavior improvement (e.g., auxeticity and yielding strength) in four different design sets (Figure 7D). It is demonstrated that an optimized lattice design could generate internal buckling in the structure to enhance

its mechanical strength. Gillman et al.[108] investigated the non-linear behavior of origami structures using a truss-based finite element model to understand the bifurcation and limit point instabilities of truss-based origami structures. They developed a theoretical framework in global coordinate system to accurately capture the nonlinear deformations and energy states of the multistable structure, resulting in a better prediction of the bifurcation points and folding paths within the system.

In a recent study, Kamrava et al. presented a novel cellular metamaterial consisting of origami building blocks.[10] By using nonlinear phenomena of origami structures, they constructed cellular elements that have highly nonlinear auxeticity, bistability, and locking behaviors. Figure 7E illustrates the first-order and second-order elements used in building the origami-based cellular metamaterials. Different possible arrangements of a cellular structure can be constructed by the basic elements to be either locked or foldable structures in one direction (Figure 7F). Bistable auxetic metamaterials capable of holding their deformed shape after being unloaded was proposed by Rafsanjani and Pasini.[109] They demonstrated that the expandability, negative Poisson's ratio, and bistability of the auxetic metamaterials could be well controlled by its structural geometry.

Origami and truss-based structures have also been utilized for locomotion and robotic applications.[103,110–113] An origami skeleton mechanism was demonstrated to create peristaltic-like locomotion by exploiting the multistability of the structure.[110] In this study, two bistable Kresling origamis were combined into a drive module to create an actuation cycle without the need for multiple actuators or a complex design. Interestingly, Pagano et al. designed a crawling robot based on origami structure[111] and showed that the crawling robot has the advantage of low power consumption with a simple controlling mechanism by using the structural bistability in the system.

At nanoscales, fluid dynamics such as evaporation have been explored for the actuation of the bistability of composite materials.[114,115] A crumpled graphene/Carbon Nanotube composite nanoparticle with large-accessible-space and high-mechanical-strength was fabricated by encapsulating carbon nanotubes (CNTs) with graphene sheets using solvent evaporation-induced assembly.[115] This method provides a facile approach to control the states of crumpling and assembling of CNTs and graphene composite nanoparticles by liquid evaporation in a large-scale and time-efficient manner.

5. Bistable Structures for Energy Harvesters

High levels of energy consumption along with the growing environmental concerns about fossil fuels have made researchers focus on harvesting energy from other sources types. Among those alternatives, mechanical vibration has played a significant role in the past decades due to the rapid advances in material science and advanced manufacturing methods. Vibration energy harvesting systems are potential candidates to replace lithium batteries and solar cells due to their ubiquitousness and high accessibility. However, so far, several limitations such as low-output density and limited frequency bandwidth are the major reasons for such devices not being able to compete with
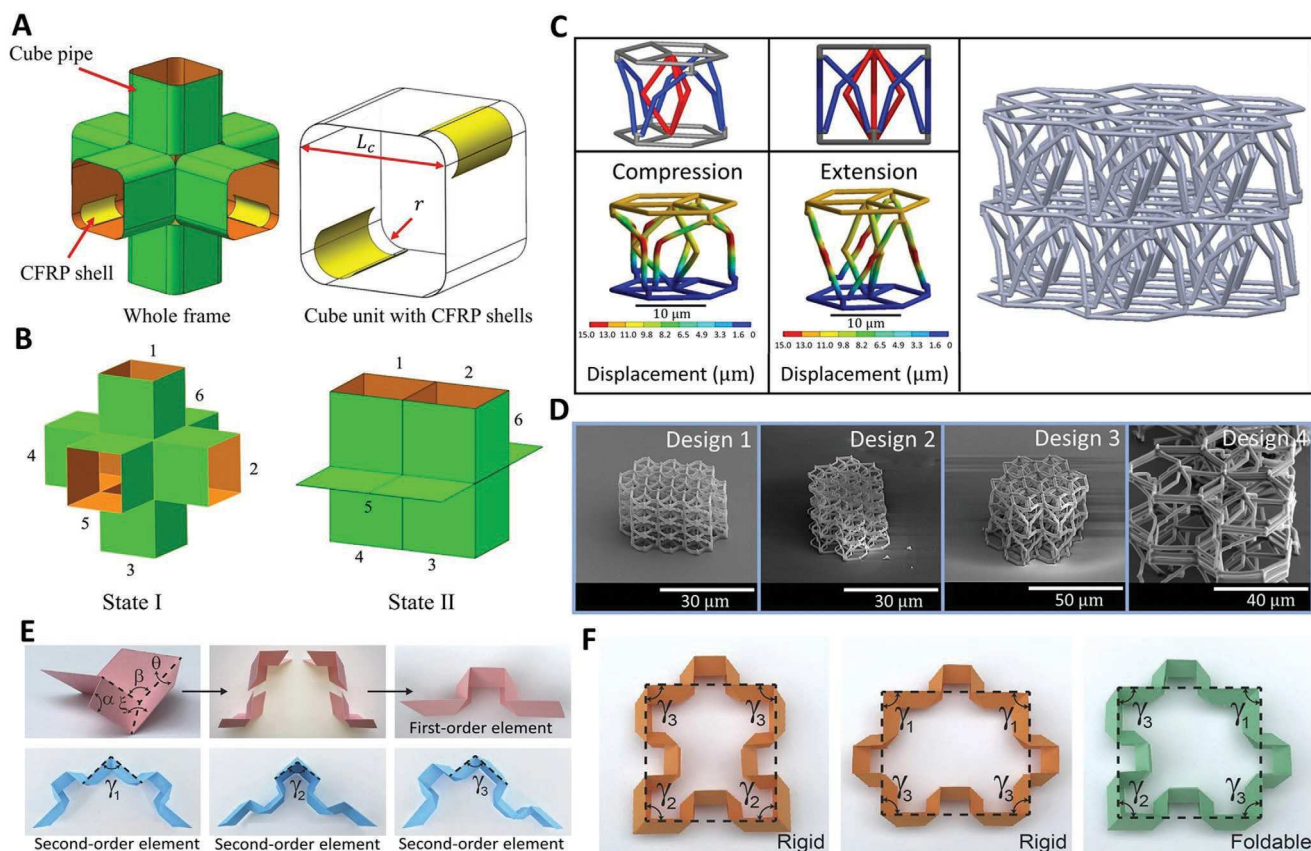
**ADVANCED
SCIENCE NEWS**
www.advancedsciencenews.com

**ADVANCED
FUNCTIONAL
MATERIALS**
www.afm-journal.de

Figure 7. Bistable structures for programmable devices/metamaterials. A) Schematic view of an origami-based programmable cube. The carbon fiber reinforced polymer (CFRP) shells are attached at the hinge sections of the cube pipe. The CFRP shells are bistable structures designed to be actuated by electromagnetic forces. B) Schematic illustration of the two stable states of a designed cube pipe. Reproduced with permission.[105] Copyright 2019, IOP Publishing. C) A microscale truss-based designed structure with bistable elements for mechanical behavior improvement, such as auxeticity and yielding strength, as a unit cell (left figures) and an assembly set (right figure). D) SEM images of the as-fabricated periodic structures consisting of 3D truss-based unit cells in four different design sets. Reproduced with permission.[102] Copyright 2019, Elsevier. E) The first-order and second-order elements used in developing an origami-based cellular metamaterial. Metamaterial constructed elements made from origami building blocks providing different engineering behaviors including bistability, foldability, auxeticity, and self-locking properties. F) Possible closed-loop elements formed by second-order units for either rigid or foldable geometry. Reproduced with permission.[10] Copyright 2017, Nature.

the other types of generators in the energy-consuming industries. Bistable and/or multistable structures have been extensively studied for energy harvesting as a promising alternative solution for such issues.[3,116–118] Significant progress is made in developing new structures and improving the output power of the devices. In this section, we review the representative bistable and multistable structures used in different kinds of energy harvesters.

5.1. Energy Harvesters Based on Mechanically Driven Bistable Structures

Figure 8A shows a simple harvester made of bistable inverted beam and an end mass.[119] The tip mass enables the bistability of the vertical cantilever beam under horizontal harmonic excitation. As a result, the bending of the cantilever beam drives the piezoelectric patches bonded on the beam to generate electricity. Friswell et al. studied the effect of the key parameters on the dynamic response and output power of the system,

including tip mass, load resistance, base amplitude, and frequency. As described in Figure 8B,C, the tip mass significantly affects the first natural frequency and bifurcation behavior of the harvester, thereby the energy harvesting performance of the harvester.

More recently, Van Blarigan and Moehlis studied the dynamic behaviors of a buckled asymmetric piezoelectric beam for energy harvesting.[120] In their work, the asymmetric buckled beam was made of a single layer and a bimorph layer. The snap-through behaviors of the beam and its transition from monostable to bistable motions were studied. Their results demonstrated the chaotic attractors related to period-doubling behavior, resulting in a much higher bandwidth of frequency compared to typical linear systems. Different from the horizontal vibration actuation, Garg and Dwivedy proposed a fixed-end beam energy harvester with one longitudinal moving end attached to a tip mass.[121] They investigated the nonlinear dynamics of the fixed beam and found that, based on the exciting frequency range, the resonance frequency of the system can be tuned by adjusting the tip mass and external
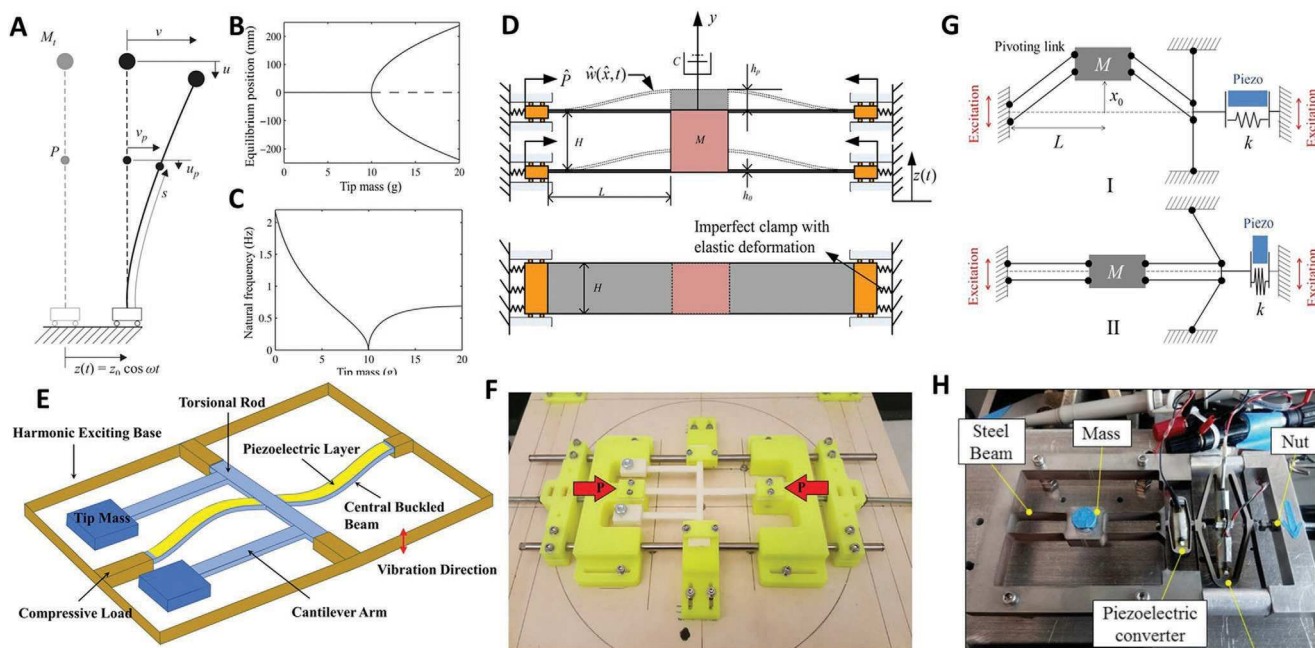
Figure 8. Mechanically driven bistable energy harvesters. A) Schematic illustration of an inverted beam harvester. The vertical cantilever beam has a tip mass to enable bistability under horizontal harmonic excitation. Piezoelectric patches are placed along the beam. B) The effect of the tip mass on the equilibrium position of the inverted beam harvester. The dashed line denotes unstable equilibrium positions. C) The effect of the tip mass on the natural frequencies for the stable equilibrium positions. Reproduced with permission.[119] Copyright 2012, SAGE Publishing. D) A bistable oscillator consisting of double buckled beams with a central mass mounted on elastic boundary conditions, in which the elastic boundary enhances the snap-through performance. Reproduced with permission.[122] Copyright 2016, IOP Publishing. E) Concept design of a unique bistable energy harvester made of a central compressive beam, a torsional rod, and two cantilevers with end masses. The cantilever arms enable snap-through motions, thereby expanding the frequency range of harvesting operation. F) The experimental setup of the bistable energy harvester mounted on a shaker table. The compressive load applied by the relative motion of the two end fixtures. Reproduced with permission.[123] Copyright 2019, Springer Nature. G) Schematic diagram of a bistable energy harvester made of a mass connected with several rigid links, demonstrating two stable states (I) and (II). (H) The experimental setup of the linkage-based mechanism with a piezoelectric generator for energy harvesting. Reproduced with permission.[124] Copyright 2019, IOP Publishing.

load. For instance, under the super-harmonic resonances, the operational frequency bandwidth of the beam can significantly increase, benefiting potential vibration energy harvesting.

Liu et al.[122] studied a nonlinear bistable oscillator made of double buckled beams with a central mass and elastic boundary conditions (Figure 8D). Based on the extended Hamilton principle, they proposed an analytical model using the Galerkin approach and showed that the clamped stiffness had a significant effect on the first mode, a moderate effect on the third mode, while no effect on the second mode. The proposed bistable harvester can broaden the operational frequency range compared to the similar linear ones. Furthermore, the elastic clamped boundary condition could be modified to improve the snap-through performance, providing new opportunities for designing bistable harvesters for vibration energy harvesting. Derakhshani et al. designed a coupled bistable structure consisting of a central buckled beam, a torsional rod, and two cantilever arms with end masses for low-frequency vibration energy harvesting (Figure 8E,F).[123] The large vibrational motions induced in the cantilever arms generated a torsional moment in the middle rod, then transferred to the central buckled beam to induce a bistable motion at the low-frequency ranges (≤30 Hz). A more accurate theoretical analysis of the nonlinear system under harmonic excitations was performed based on a component coupling approach. Special attention should be paid in the optimization of the design because

there was a tradeoff between the induced buckling level and the maximum outpower of the device.

As shown in Figure 8G, a unique linkage design was proposed for a piezoelectric bistable energy harvester to elevate the snap-through motion as the system vibrates in the vertical direction.[124] The effects of the different parameters, including load resistance, mass, stiffness, and buckling level was studied through a new theoretical model. The prototype of the harvester used lead zirconate titanate (PZT) ceramic as the piezoelectric converter (Figure 8H). The study revealed that a wider frequency bandwidth could be achieved by increasing inertial mass, adjusting stiffness to fit the frequency range on the potential frequency source, or increasing the initial stable position to cover the overlap area between the first harmonic and the following subharmonic resonances. The performance of the bistable harvester could be further optimized by adjusting the impedance match with the piezoelectric converter to maximize the outpower. In addition, Ando et al. proposed a snap-through buckling (STB) harvester made of a buckled beam with a mass located between two piezoelectric harvesters,[125,126] generating a power up to 155 Mw at the input frequency of 5 Hz. Differently, Emad et al.[127] investigated a nonlinear doubly clamped polyvinylidene fluoride (PVDF) beam with induced stretching strain for energy harvesting and found that the stretching strain can eliminate the need for a structural substrate in the design.

**ADVANCED
SCIENCE NEWS**

www.advancedsciencenews.com

**ADVANCED
FUNCTIONAL
MATERIALS**

www.afm-journal.de

5.2. Energy Harvesters Based on Magnetically Driven Bistable Structures

The main advantage of using magnetic forces for bistable energy harvesters is their high reliability to create double-welled potential systems. However, the design complexity and the need for external sources (e.g., permanent magnets) have limited their applications, in particular for MEMS and small-scale devices.[3,117] The main focuses in developing bistable energy harvesters are to broaden the frequency bandwidth and to accommodate the ambient vibration sources.[128,129] **Figure 9**A shows a bistable dual piezoelectric cantilever energy harvesting system (DPEHS) for realistic ambient vibrations.[130] In this design, the magnetic repulsive force between the two permanent magnets fixed on the tip of the cantilevers enabled the bistability of the system. The energy harvesting performance of DPEHS could be analyzed by a single degree-of-freedom (DOF) vibrational model (Figure 9B,C) that was

excited by the pink noise with intensive variations. Compared to the rigidly supported PEHS for ambient noise inputs,[131,132] the elastically supported PEHS demonstrated a superior performance under pink noise vibrations with either constant or varying intensity.

In another representative study, Yan et al. designed a bistable piezoelectric vibration energy harvester (Figure 9D) with ultra-broadband harvesting performance at low-frequency ranges.[6] The vertically placed cantilever beam has a tip magnet to repulsively interact with the other two permanent magnets fixed on the stage. Using the harmonic balance method, they developed an electromechanical coupled distributed parameter model to analyze the harvester system. Their results showed that both cubic magnetic coefficient and electric inductance can significantly improve the operational bandwidth of the harvester by creating multiple resonances and hardening or softening phenomena (Figure 9E), leading to a high-performance energy harvester suitable for a higher operating frequency of up to 40 Hz.
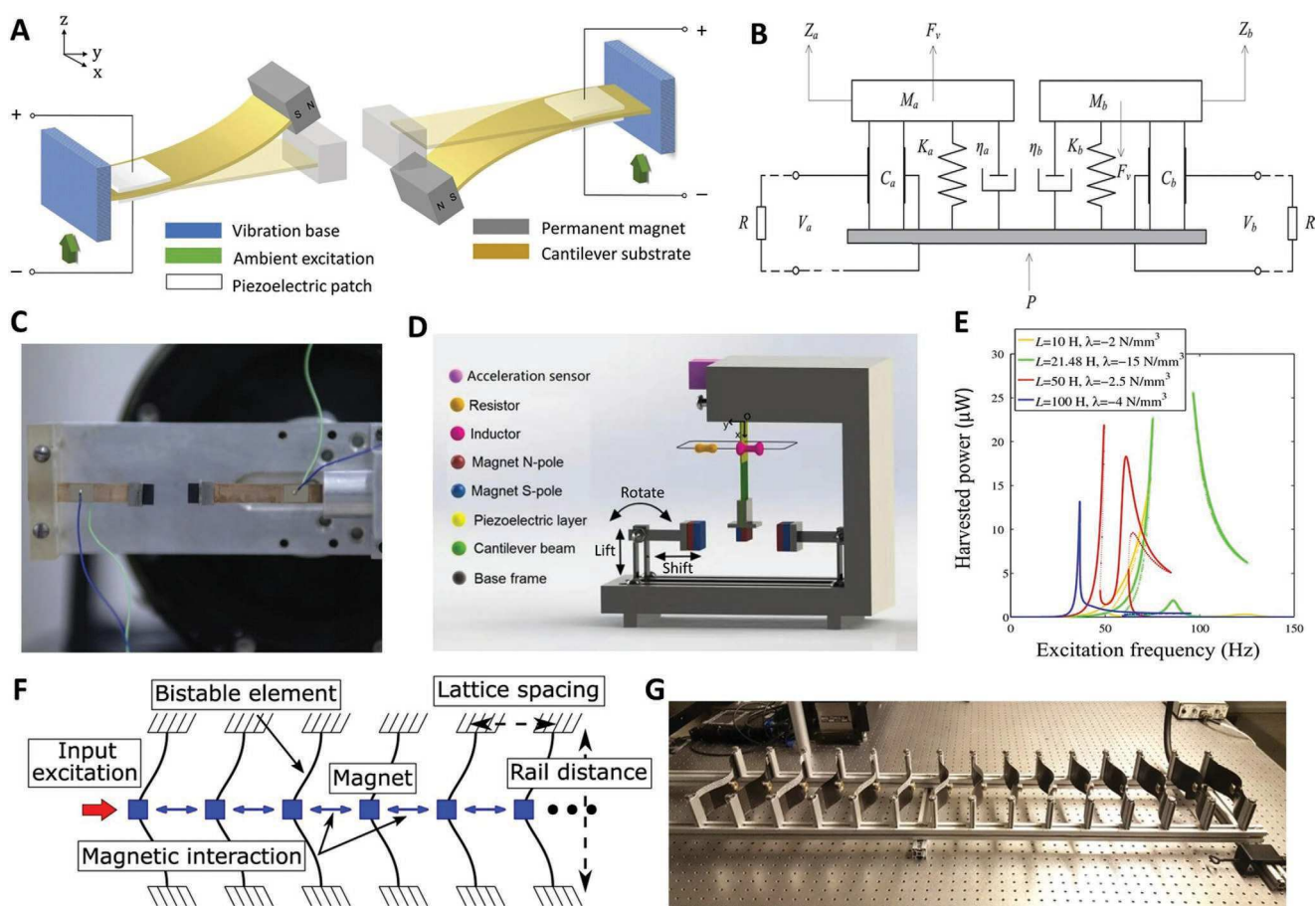

Figure 9. Magnetically driven bistable energy harvesters. A) Schematic illustration of a bistable energy harvester made of dual piezoelectric cantilevers. The bistable state change is driven by the repulsive magnetic interaction between the cantilevers tip masses. B) The equivalent single degree-of-freedom (DOF) model of the bistable harvester in (A). C) The experimental setup of a dual cantilever bistable energy harvester. Reproduced with permission.[130] Copyright 2016, IOP Publishing. D) Schematic diagram of a piezoelectric bistable energy harvester with nonlinear magnetic interaction. E) Output power-frequency response of the harvester shown in (E) with multi-hardening and multi-softening behaviors, indicating a wider range of operational frequency. Reproduced with permission.[6] Copyright 2020, Springer Nature. F) Schematic illustration of an energy harvester consisting of bistable lattice structures. The bistable unit cells are made of piezoelectric transducers and are serially connected on a frame. The magnetic interactions between the bistable cells induce the force transfer and snap-through motion.[139] G) Experimental setup of the bistable lattice. Reproduced with permission.[139] Copyright 2018, Nature.

**ADVANCED
SCIENCE NEWS**

www.advancedsciencenews.com

**ADVANCED
FUNCTIONAL
MATERIALS**

www.afm-journal.de

A mechanical adaptation was also introduced to a bistable magnetic-based piezoelectric energy harvester to improve the operational frequency bandwidth and the power output.[133] For example, a bistable harvester was made of a cantilever beam with a tip magnet interacting with another permanent magnet. The fixed permanent magnet was loaded on a spring while its motion was restricted in one-direction to improve the overall performance of the harvester. Adjusting the repulsive force between the cantilever tip magnets and the spring-loaded one enabled the bistability at low-frequency base excitations, which improved the operational frequency bandwidth and the output power of the bistable harvester.

Other approaches for improving the frequency bandwidth of magnetic-based bistable energy harvesters have been considered, including a 2-DOF cantilever bistable harvester,[134] an elastic magnifier to amplify the base excitation,[135] new arrangements to reduce the potential barrier of bistable harvesters,[136,137] and creating asymmetry in the potential functions of a bistable structure.[138] One remarkable example is a 1D lattice energy harvester shown in Figure 9F.[139] The energy harvesting system consisted of serially connected bistable elements. Each element was made of two buckled beams and one attached central magnet for transferring the snap-through motion between the biostable elements. This design has the merits of input-independent dynamics, extreme directionality, and topological energy harvesting characteristics, and has the potential to be used for building intelligent metastructures for damping and/or harvesting the unwanted energy under sudden abrupt shock inputs such as blasts or earthquakes.

Another remarkable work is a compact and flexible non-beam type bistable vibration energy harvester designed by Deng et al.[140] The energy harvesting system was made of a flexible bellows tube, an annular permanent magnet, an aluminum frame, PVDF film as the piezoelectric element, and two rectangular magnets to interact with the annular magnet for enhancing the bistability properties. The flexible bellows-type structure not only improved the energy harvesting performance of the device at low frequencies but also resolved the stress-concentration issue associated with typical beam-type structures.

5.3. Energy Harvesters Based on Thermally Driven Bistable Structures

Thermally-induced bistable structures are typically composite of several layers stretched and laminated along perpendicular directions so that they can be actuated by residual stresses induced by a thermal process for switching between two stable states.[141,142] For example, Tao et al. designed a thermally induced bistable plate made of functionally graded carbon nanotube-reinforced composite (FG-CNTRC) and piezoelectric films for energy harvesting applications (**Figure 10**A).[7] They studied the bistability and dynamic response of the energy harvester by applying a thermal field and harmonic excitations (Figure 10B). Compared to a linear plate, the nonlinear bistable composite plate can generate a wider frequency bandwidth and better output performance by softening behavior and snap-through motions. Furthermore, FG plate volume fraction could significantly affect the dynamic response of the system,

and a reduced volume fraction resulted in a low requirement of base excitation for snap-through motions. In addition, Harris et al. proposed a cantilever bistable energy harvester made of laminates and a macro fiber composite (MFC) patch as the piezoelectric generator (Figure 10C).[143] The laminate beam possessed asymmetric bistability, and thereby exhibited nonlinear features such as softening behavior and superharmonic resonances, leading to a variety of motion types from chaotic to harmonic snap-through motions (Figure 10D–F). They found that the presence of superharmonic resonances in a bistable harvester would induce snap-through motions at the low-frequency ranges, which may be used for optimizing the energy harvesting structures.

MFCs have also been utilized to combine with bistable laminates for broadband energy harvesting due to their ease of manufacture, reliability, and relatively high piezoelectricity.[144–146] For instance, Lee and Inman analyzed the nonlinear behaviors of a rectangular bistable laminate paired with MFC films for energy harvesting.[145] In their study, elastic potential energy characteristics and snap-through behaviors of the bistable plate under harmonic excitations were investigated.[144] In another study, Betts et al. considered a bistable composite with attached piezoelectric patches to harvest energy from ambient vibrations.[147,148] As shown in Figure 10G, four piezoelectric patches were attached to the composite plate where the plate was fixed on its corners. Parametric studies were performed for optimal configurations to maximize the energy harvesting performance. The key parameters included the ply orientations, piezoelectric surface area, and geometry of the plate. For example, larger piezoelectric patches could generate higher output power but sacrifice the structural compliance, thereby reduced the laminate curvature and the stress along the polarization direction of the plate.

Recently, multifunctional bistable structures to combine vibration isolation and energy harvesting have also been studied. For example, Lu and coworkers[149] proposed a bistable piezo-composite plate to simultaneously work as a vibration isolator and an energy harvester (Figure 10H). The multifunctional device was made of a central mass connected to a composite laminate with negative stiffness and a steel plate with positive stiffness. A piezoelectric strip was bonded onto a nonlinear composite laminate made of metal and carbon fiber layers. The bistable composite plate with a negative stiffness reduced the whole stiffness of the structure and consequently facilitated the transmissibility reduction, especially at higher frequency ranges. The transmissibility of the bistable structures could be reduced by 23 dB at 100 Hz while it adversely affected the energy harvesting performance.

6. Bistable Structures for Energy Absorption

Energy absorption of dissipation has attracted increasing attention due to its intensive use in a variety of applications such as structural damping, energy transferring devices, and acoustics. Recent advances in manufacturing and materials science enable structural bistability to be implemented as a promising low-cost feature for energy absorption applications. **Figure 11**A shows a possible mechanism of trapping elastic energy through
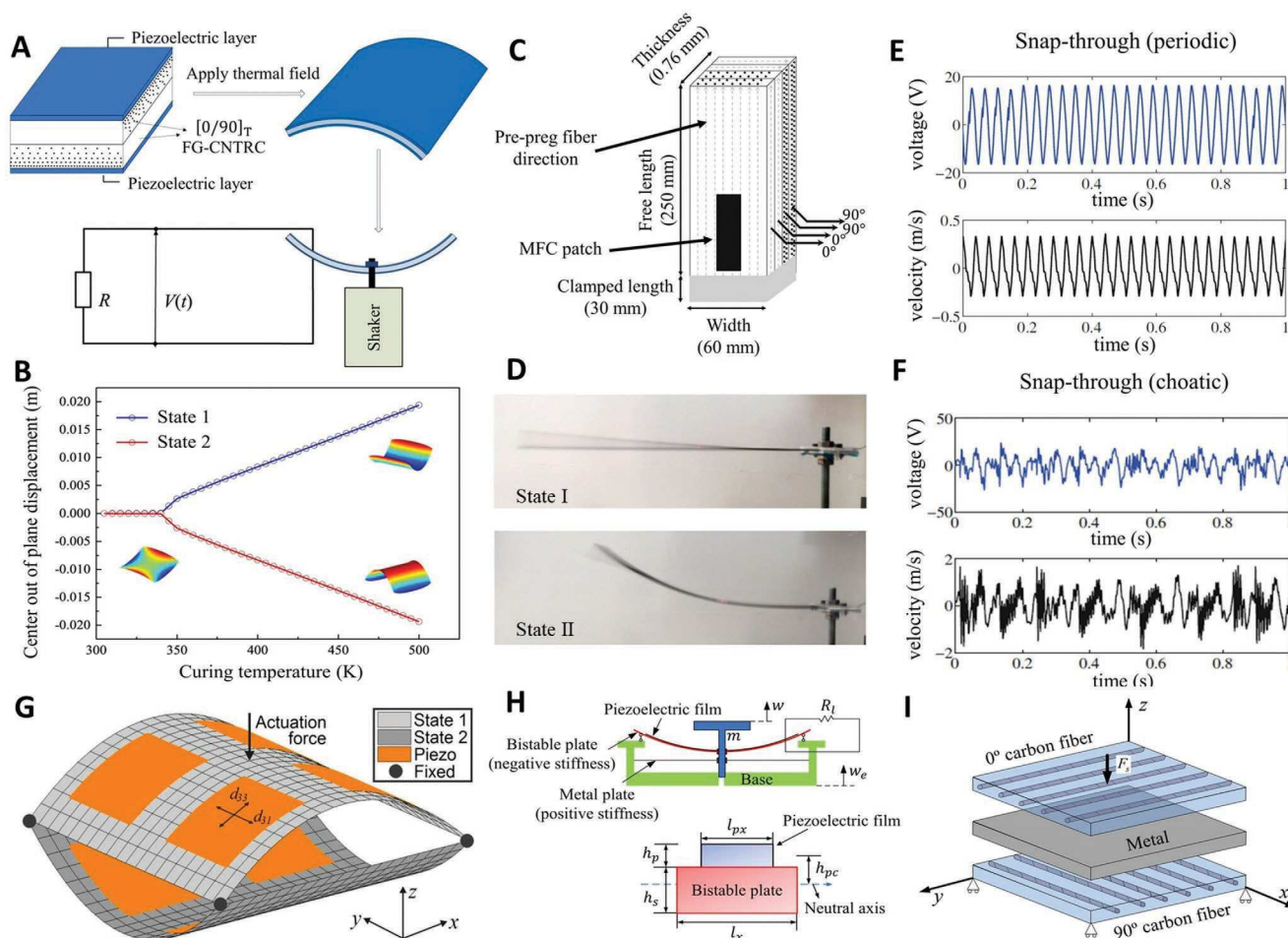
Figure 10. Thermally driven bistable energy harvesters. A) Schematic of a bistable energy harvester driven by thermal energy. It is fabricated by laminating functionally graded carbon nanotube reinforced composite with piezoelectric patches, achieving bistable change when heated up and cooled down. B) The bifurcation plot obtained by FE modeling of the FG plate under different curing temperatures. Reproduced with permission.[7] Copyright 2019, IOP Publishing. C) Schematic of a cantilever energy harvester consisting of a bistable laminate and a macro fiber composite (MFC) strip. The composite laminate generates bistable deformation under thermal actuation. D) Experimental setup of the bistable harvester, exhibiting local vibrations at its two stable states. Real-time velocity and voltage response of the bistable harvester excited by an acceleration of 4 g at two different frequencies: E) 25 Hz for periodic snap-through motion, and F) 17 Hz for chaotic snap-through motion. Reproduced with permission.[143] Copyright 2016, Springer Science + Business Media. G) Schematic of a bistable composite laminate with four piezoelectric patches attached for energy harvesting. The two laminates are bonded at the four corners and the bistability is achieved via a thermal process. Reproduced with permission.[147] Copyright 2012, AIP Publishing. H) Schematic view of a multifunctional device for vibration isolation and energy harvesting. The bistable piezo-composite plate is combined with a metal plate for negative and positive stiffness, respectively. I) Configuration of the different layers of the bistable composite laminate structure. Reproduced with permission.[149] Copyright 2019, SAGE Publishing.

the deformation of a tilted beam.[150] This unique mechanical energy trapping method stems only from the structural geometry of bistable elements and can be used in energy absorption packages. Based on the energy principle, various designs for 1D, 2D, and 3D architectured materials with embedded flexible bistable elements and rigid parts were developed (Figure 11B). For instance, Bertoldi et al. investigated the influence of the different parameters on energy absorption performance, including the tilting angle θ and the beam slenderness t/l. The energy absorbed by the system and the energy to snap back to its undeformed shape could be adjusted by tailoring θ and t/l, which allowed the beam to either remain in its deformed shape or restore to the initial shape according to the specific application requirements.

There are several other interesting studies to introduce a structural lattice for energy absorption by exploiting bistability behaviors and local snap-through motions.[151–155] For example, Tan et al.[151] proposed a reusable metamaterial structure with negative stiffness (NS) properties for energy dissipation. Unlike previous studies with elastic deformation,[156–158] this study considered energy dissipation via plastic deformation. They performed cyclic compression tests to examine the reusability of the structure. Experimental results showed that the energy absorption capacity can be improved by lowering the local energy barriers through increasing the thickness to length ratio of the beam or reducing the buckling height. Figure 11C shows a bistable tetra-beam-plate unit cell and a 3D lattice made of several single-unit cells for energy absorption use.[153] Through the
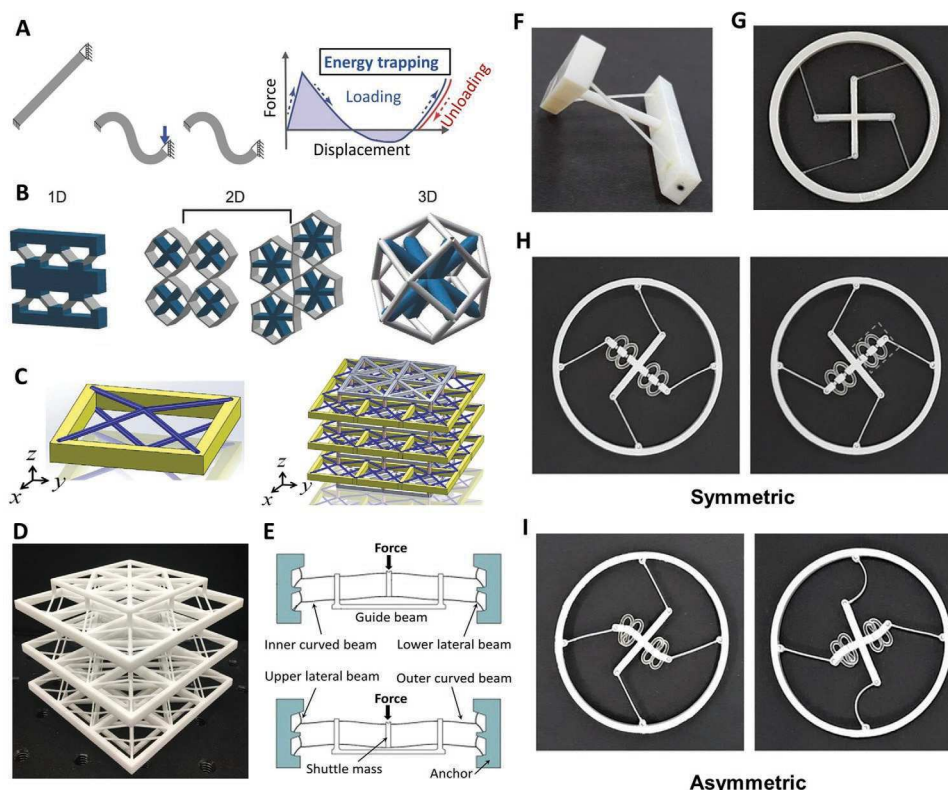
ADVANCED
SCIENCE NEWS
www.advancedsciencenews.com

ADVANCED
FUNCTIONAL
MATERIALS
www.afm-journal.de

Figure 11. Bistable structures for energy absorption. A) Schematic diagram of an elastic beam capable of energy absorption. After bending of the tilted beam, it remains in its deformed shape with potential energy trapped after unloading. B) Schematic illustrations of 1D, 2D, and 3D multistable structures capable of energy absorption. The gray and blue colors indicate the elastic bistable beams and rigid supports, respectively. Reproduced with permission.[150] Copyright 2015, Wiley-VCH. C) Schematic illustration of a tetra-beam-plate unit cell and a $3 \times 3 \times 3$ lattice consisting of the unit cells for energy absorption. The bistability of the inclined beams on the rigid frame allows energy absorption. D) A 3D-printed prototype of the $3 \times 3 \times 3$ lattice in (C) using polyamide (PA) for energy absorption. The length of each side is about 70 mm. Reproduced with permission.[153] Copyright 2018, Elsevier. E) Schematic illustration of a bistable structure for force regulation and overloading protection. The designed structure acts as a protection mechanism against high impact forces by snap-through from its initial state to an overloaded stable state. Reproduced with permission.[160] Copyright 2013, Elsevier. F) A 3D-printed twisting bistable structure. G) A 3D-printed rotational bistable structure. H) The two stable states of a tunable rotational bistable structure in a symmetric configuration. I) The two stable states of a tunable rotational bistable structure in an asymmetric configuration. Reproduced with permission.[162] Copyright 2019, Nature.

negative stiffness induced by the local snap-through deformations of the flexible beam elements, energy dissipation in a unit cell was achieved when the lattice was loaded by a compressive force (Figure 11D). The parametric analysis revealed the effects of the slenderness and tilting angle of bistable beams on the energy absorption capacity of a unit cell. The unit cells in the 3D lattice resulted in multiple energy gaps in the force-displacement plots, each of which had a certain energy trapping capacity.

Foroutan et al. recently designed a linear structure for energy absorption by coupling a tuned bistable nonlinear energy sink (TBNES) containing local potentials[9] and developed a semi-analytical model for analysis. Such a structural design can improve energy absorption performance by expanding the system's local potentials at the second mode interaction. Another theoretical study was performed on a novel adaptive bistable energy absorption mechanism,[159] in which two mainsprings were arranged on elastic boundaries for achieving tunable bistability. This adaptive design was found to outperform conventional bistable wave energy absorbers by adjusting the potential energy barrier to make it suitable for both low-amplitude and high-amplitude excitations.

Linkage-based mechanisms are another type of load-protecting system in which bistability can be used for controlling both impacts and quasi-static external forces. For example, Wang et al. designed a constant force bistable micromechanism (CFBM) for load regulation[160] (Figure 11E). A set of curved beams with flexible end fixtures enabled the snap-through deformation between its stable states for load distribution. Similarly, Cherkaev et al. proposed an impact protective structure consisting of bistable links as a shock resistance mechanism.[161] In their structure, the yielding behavior of certain links in the system (sacrificial links) was utilized as a protection for the active bistable links to improve energy absorption capacity.

The key to structural bistability in energy absorption applications is to tune the energy barrier of the system to generate adjustable snap-through transitions before the materials reach their yielding strength. In a recent study, Jeong et al. designed tunable twisting and rotational bistable structures for lowering the energy barrier level required for snap-through motions (Figure 11F,G).[162] They demonstrated that adjusting bistable structures and material properties could result in asymmetric potential energy for desired snap-through transitions.

**ADVANCED
SCIENCE NEWS**

www.advancedsciencenews.com

**ADVANCED
FUNCTIONAL
MATERIALS**

www.afm-journal.de

Figure 11H,I shows the two different stable states of the 3D-printed twisting mechanisms in the symmetric and asymmetric configurations. Tuning the energy barrier height and creating asymmetric potential wells in the potential energy plot were achieved by adjusting the length of the central link or imposing geometrical asymmetry in the mechanism, respectively. Such adjustable mechanisms could be used for switching actuators and energy absorbers.

7. Conclusion and Outlook

In summary, structural bistability has been widely used for various advanced functional systems due to snap-through and the corresponding dramatically geometrical change and potential energy change. Based on the type of applications, we categorized bistable structures as actuators, robotics and MEMS, programmable devices and metamaterials, energy harvesters, and energy absorbers and discussed the strategies used in these advances. Such strategies not only reflect the rational yet straightforward ideas, i.e., adoption of more powerful smart materials, along their emergence, into bistable structures to fulfill versatility, but also reveal the gaps among materials, structures, and functions.

While smart materials responsive to physical stimuli such as electric and magnetic fields, temperature change, and pH have demonstrated superiority over conventional materials in bistable structures, those applications are at the stage of proof-of-concept with significant drawbacks, including slow responsiveness, low sensitivity, and no reported selectivity. More physical stimuli (e.g., light, humidity, specific molecules) responsive smart materials have yet found their applications with bistable structures. Theoretical investigations on the response behaviors of bistable structures under various external stimuli have provided essential guidelines for their versatile applications. However, most studies have utilized only simple bistable structures, e.g., beams and shells/laminates, and taken little advantage of advanced structures enabled by additive manufacturing technologies in achieving advanced functions. Reliable and reversible snap-through of bistable structures in both design and manufacturing aspects is still challenging and problematic. In addition, little effort is taken to explore advanced bistable structures while beams and laminates have been exhaustively investigated theoretically and numerically. It is worth noting the pivotal role of mechanics in designing bistable structures, the snap through transition of which is essentially deformation/displacement under external applied forces and internal forces induced by physical stimuli. It is expected that the development of smart materials and advanced bistable structures and their elegant combinations will be general research opportunities.

Function-/application-oriented modification of bistable structures for real-life applications is where innovation lies. For example, it will be attractive to invent new bistable structures that can effectively respond to ambient low-intensity and low-frequency vibrational sources or low activation forces for actuators and robotics. Innovative theoretical and experimental studies for bistable laminates or composites are also highly desired for developing morphing structures and broadband energy harvesters used in aerospace, automobile, and wind energy applications. Additionally, multiscale and multifield modeling of bistable structures are still challenging and open areas for research. The rapid advances in manufacturing technologies, for instance, 3D/4D printing, will facilitate the design and fabrication of advanced bistable structures at both macro and micro scales. The accurate control of materials properties, orientation, location in the fabrication process of novel structures will enable the control of bistable threshold as necessary. Another attractive point is assigning innovative functions to bistable structures, e.g., programmable materials, metamaterials, sensing/memory devices[45] and logic controller[163] as George Whitesides and his coworkers did where they rendered a bistable actuator function as an autonomous controller for soft robots.

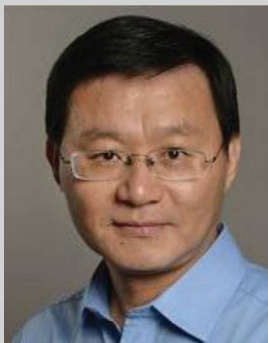## Conflict of Interest

The authors declare no conflict of interest.

[1] R. L. Harne, K.-W. Wang, *Harnessing Bistable Structural Dynamics: For Vibration Control, Energy Harvesting and Sensing*, John Wiley & Sons, Hoboken, NJ **2017**.

[2] A. Ghosh, G. Koster, G. Rijnders, *Adv. Funct. Mater.* **2016**, *26*, 5748.

[3] R. L. Harne, K. Wang, *Smart Mater. Struct.* **2013**, *22*, 023001.

[4] X. Sun, Y. Zhang, D. Kennedy, *Nonlinear Dyn.* **2019**, *95*, 3205.

[5] H. Shao, S. Wei, X. Jiang, D. P. Holmes, T. K. Ghosh, *Adv. Funct. Mater.* **2018**, *28*, 1802999.

[6] Z. Yan, W. Sun, M. R. Hajj, W. Zhang, T. Tan, *Nonlinear Dyn.* **2020**, *100*, 1057.

[7] J. Tao, X. He, S. Yi, Y. Deng, *Smart Mater. Struct.* **2019**, *28*, 095021.

[8] M. Ben Salem, H. Hussein, G. Aiche, Y. Haddab, P. Lutz, L. Rubbert, P. Renaud, *J. Micro-Bio Rob.* **2019**, *15*, 65.

[9] K. Foroutan, A. Jalali, H. Ahmadi, *J. Sound Vib.* **2019**, *447*, 155.

[10] S. Kamrava, D. Mousanezhad, H. Ebrahimi, R. Ghosh, A. Vaziri, *Sci. Rep.* **2017**, *7*, 46046.

[11] Y. Gerson, S. Krylov, B. Ilic, D. Schreiber, *Finite Elements Anal. Des.* **2012**, *49*, 58.

[12] R. Addo-Akoto, J.-H. Han, *J. Intell. Mater. Syst. Struct.* **2018**, *30*, 506.

[13] P. Rothemund, A. Ainla, L. Belding, D. J. Preston, S. Kurihara, Z. Suo, G. M. Whitesides, *Sci. Rob.* **2018**, *3*, eaar7986.

[14] B. Xu, Y. Qiao, Y. Li, Q. Zhou, X. Chen, *Appl. Phys. Lett.* **2011**, *98*, 221909.

[15] B. Xu, Y. Qiao, T. Park, M. Tak, Q. Zhou, X. Chen, *Energy Environ. Sci.* **2011**, *4*, 3632.

**ADVANCED
SCIENCE NEWS**

www.advancedsciencenews.com

**ADVANCED
FUNCTIONAL
MATERIALS**

www.afm-journal.de

[16] X. Lachenal, S. Daynes, P. M. Weaver, *J. Intell. Mater. Syst. Struct.* **2014**, *25*, 744.

[17] X. Lachenal, P. M. Weaver, S. Daynes, *Proc. R. Soc. A* **2012**, *468*, 1230.

[18] A. F. Arrieta, V. v. Gemmeren, A. J. Anderson, P. M. Weaver, *Smart Mater. Struct.* **2018**, *27*, 025006.

[19] M. W. Hyer, *J. Compos. Mater.* **1981**, *15*, 296.

[20] M. W. Hyer, *J. Compos. Mater.* **1981**, *15*, 175.

[21] V. Chillara, M. Dapino, *Composites, Part B* **2017**, *111*, 251.

[22] B. Wang, K. S. Fancey, *Mater. Lett.* **2015**, *158*, 108.

[23] S. Daynes, C. Diaconu, K. Potter, P. Weaver, *J. Compos. Mater.* **2010**, *44*, 1119.

[24] S. Daynes, K. Potter, P. Weaver, *Compos. Sci. Technol.* **2008**, *68*, 3431.

[25] H. Li, F. Dai, P. Weaver, S. Du, *Compos. Struct.* **2014**, *116*, 782.

[26] M. R. Schultz, M. W. Hyer, *J. Intell. Mater. Syst. Struct.* **2003**, *14*, 795.

[27] C. Bowen, R. Butler, R. Jervis, H. Kim, A. Salo, *J. Intell. Mater. Syst. Struct.* **2007**, *18*, 89.

[28] P. Portela, P. Camanho, P. Weaver, I. Bond, *Comput. Struct.* **2008**, *86*, 347.

[29] M. Gude, W. Hufenbach, C. Kirvel, *Compos. Struct.* **2011**, *93*, 377.

[30] P. F. Giddings, H. A. Kim, A. I. Salo, C. R. Bowen, *Mater. Lett.* **2011**, *65*, 1261.

[31] M. R. Schultz, W. K. Wilkie, R. G. Bryant, *J. Aircr.* **2007**, *44*, 1069.

[32] M.-L. Dano, M. Jean-St-Laurent, A. Fecteau, *Smart Mater. Res.* **2012**, *2012*, 695475.

[33] A. Arrieta, D. Wagg, S. Neild, *J. Intell. Mater. Syst. Struct.* **2011**, *22*, 103.

[34] A. F. Arrieta, O. Bilgen, M. I. Friswell, P. Hagedorn, *J. Intell. Mater. Syst. Struct.* **2013**, *24*, 266.

[35] O. Bilgen, A. F. Arrieta, M. I. Friswell, P. Hagedorn, *Smart Mater. Struct.* **2013**, *22*, 025020.

[36] H. A. Kim, D. N. Betts, A. I. T. Salo, C. R. Bowen, *AIAA J.* **2010**, *48*, 1265.

[37] W. Hamouche, C. Maurini, S. Vidoli, A. Vincenti, *Proc. R. Soc. A* **2017**, *473*, 20170364.

[38] A. J. Lee, A. Moosavian, D. J. Inman, *Mater. Lett.* **2017**, *190*, 123.

[39] A. J. Lee, A. Moosavian, D. J. Inman, *Smart Mater. Struct.* **2017**, *26*, 085007.

[40] A. J. Lee, A. Moosavian, D. J. Inman, presented at *Proc. SPIE 10164, Active and Passive Smart Structures and Integrated Systems*, April **2017**.

[41] S. Krylov, S. Seretensky, *J. Micromech. Microeng.* **2006**, *16*, 1382.

[42] S. Krylov, B. R. Ilic, D. Schreiber, S. Seretensky, H. Craighead, *J. Micromech. Microeng.* **2008**, *18*, 055026.

[43] L. Medina, R. Gilat, B. Ilic, S. Krylov, *Sens. Actuators, A* **2014**, *220*, 323.

[44] X. Chen, S. Meguid, *Proc. R. Soc. A* **2015**, *471*, 20150072.

[45] L. Medina, R. Gilat, S. Krylov, *Int. J. Eng. Sci.* **2017**, *110*, 15.

[46] F. Najar, M. Ghommem, A. Abdelkefi, *Int. J. Mech. Sci.* **2020**, *178*, 105624.

[47] E. G. Loukaides, S. K. Smoukov, K. A. Seffen, *Int. J. Smart Nano Mater.* **2015**, *5*, 270.

[48] K. A. Seffen, S. Vidoli, *Smart Mater. Struct.* **2016**, 25.

[49] Y. Kim, H. Yuk, R. Zhao, S. A. Chester, X. Zhao, *Nature* **2018**, *558*, 274.

[50] X. Hou, Y. Liu, G. Wan, Z. Xu, C. Wen, H. Yu, J. X. J. Zhang, J. Li, Z. Chen, *Appl. Phys. Lett.* **2018**, *113*, 221902.

[51] A. Amor, A. Fernandes, J. Pouget, *Int. J. Non-Linear Mech.* **2020**, 119.

[52] X.-Q. Li, W.-B. Li, W.-M. Zhang, H.-X. Zou, Z.-K. Peng, G. Meng, *Smart Mater. Struct.* **2017**, *26*, 105007.

[53] Z. Zhang, K. Pei, M. Sun, H. Wu, X. Yu, H. Wu, S. Jiang, F. Zhang, *Compos. Struct.* **2020**, *248*, 112506.

[54] H. Li, F. Dai, S. Du, *Compos. Sci. Technol.* **2012**, *72*, 1767.

[55] E. Eckstein, A. Pirrera, P. M. Weaver, *AIAA J.* **2016**, *54*, 1778.

[56] E. Eckstein, A. Pirrera, P. M. Weaver, *Compos. Struct.* **2013**, *100*, 363.

[57] L. Zhou, H. Xie, presented at *2019 20th Int. Conf. on Solid-State Sensors, Actuators and Microsystems & Eurosensors XXXIII (TRANSDUCERS & EUROSENSORS XXXIII)*, Berlin, Germany, June **2019**.

[58] L. Zhou, X. Zhang, Y. Sung, W.-C. Shih, H. Xie, *2018 Int. Conf. on Optical MEMS and Nanophotonics (OMN)*, IEEE, Piscataway, NJ **2018**.

[59] H. Hussein, F. Khan, M. I. Younis, *Smart Mater. Struct.* **2020**, *29*, 075033.

[60] J. M. Jani, M. Leary, A. Subic, M. A. Gibson, *Mater. Des.* **2014**, *56*, 1078.

[61] W. Huang, Z. Ding, C. Wang, J. Wei, Y. Zhao, H. Purnawali, *Mater. Today* **2010**, *13*, 54.

[62] Y. Gandhi, A. Pirondi, L. Collini, *Procedia Struct. Integr.* **2018**, *12*, 429.

[63] R. Panciroli, F. Nerilli, *Procedia Struct. Integr.* **2019**, *24*, 593.

[64] Z. Wei, R. Sandstroröm, S. Miyazaki, *J. Mater. Sci.* **1998**, *33*, 3743.

[65] Y. Osada, A. Matsuda, *Nature* **1995**, *376*, 219.

[66] A. Lendlein, S. Kelch, *Angew. Chem., Int. Ed.* **2002**, *41*, 2034.

[67] T. Chen, K. Shea, *3D Print. Addit. Manuf.* **2018**, *5*, 91.

[68] H. Y. Jeong, E. Lee, S. Ha, N. Kim, Y. C. Jun, *Adv. Mater. Technol.* **2019**, *4*, 1800495.

[69] Q. Zhao, X. Yang, C. Ma, D. Chen, H. Bai, T. Li, W. Yang, T. Xie, *Mater. Horiz.* **2016**, *3*, 422.

[70] G. Kocak, C. Tuncer, V. Bütün, *Polym. Chem.* **2017**, *8*, 144.

[71] Z. Han, P. Wang, G. Mao, T. Yin, D. Zhong, B. Yiming, X. Hu, Z. Jia, G. Nian, S. Qu, *ACS Appl. Mater. Interfaces* **2020**, *12*, 12010.

[72] M. Camacho-Lopez, H. Finkelmann, P. Palffy-Muhoray, M. Shelley, *Nat. Mater.* **2004**, *3*, 307.

[73] A. Lendlein, H. Jiang, O. Jünger, R. Langer, *Nature* **2005**, *434*, 879.

[74] A. H. Gelebart, D. J. Mulder, G. Vantomme, A. P. Schenning, D. J. Broer, *Angew. Chem., Int. Ed.* **2017**, *56*, 13436.

[75] Z. Jiang, M. L. Tan, M. Taheri, Q. Yan, T. Tsuzuki, M. G. Gardiner, B. Diggle, L. A. Connal, *Angew. Chem.* **2020**, *132*, 7115.

[76] G. Y. Gu, J. Zhu, L. M. Zhu, X. Zhu, *Bioinspir. Biomim.* **2017**, *12*, 011003.

[77] T. Chen, O. R. Bilal, K. Shea, C. Daraio, *Proc. Natl. Acad. Sci. USA* **2018**, *115*, 5698.

[78] S. Nishikawa, Y. Arai, R. Niiyama, Y. Kuniyoshi, *IEEE Rob. Autom. Lett.* **2018**, *3*, 1018.

[79] B. Gorissen, D. Melancon, N. Vasios, M. Torbati, K. Bertoldi, *Sci. Rob.* **2020**, *5*, eabb1967.

[80] S.-P. Jung, G.-P. Jung, J.-S. Koh, D.-Y. Lee, K.-J. Cho, *J. Mech. Rob.* **2015**, *7*, 021010.

[81] Y. Tang, Y. Chi, J. Sun, T.-H. Huang, O. H. Maghsoudi, A. Spence, J. Zhao, H. Su, J. Yin, *Sci. Adv.* **2020**, *6*, eaaz6912.

[82] Z. Zhang, X. Li, X. Yu, H. Chai, Y. Li, H. Wu, S. Jiang, *Compos. Struct.* **2019**, *229*, 111422.

[83] D. Lunni, M. Cianchetti, C. Filippeschi, E. Sinibaldi, B. Mazzolai, *Adv. Mater. Interfaces* **2020**, *7*, 1901310.

[84] H. Zhang, J. Sun, J. Zhao, *2019 Int. Conf. on Robotics and Automation (ICRA)*, Montréal, Canada, May **2019**.

[85] Y. Chi, Y. Tang, H. Liu, J. Yin, *Adv. Mater. Technol.* **2020**, *5*, 2000370.

[86] Y. Ke, C. Castro, J. H. Choi, *Annu. Rev. Biomed. Eng.* **2018**, *20*, 375.

[87] S. Nummelin, B. Shen, P. Piskunen, Q. Liu, M. A. Kostiainen, V. Linko, *ACS Synth. Biol.* **2020**, *9*, 1923.

[88] H. Ijas, S. Nummelin, B. Shen, M. A. Kostiainen, V. Linko, *Int. J. Mol. Sci.* **2018**, *19*, 2114.

[89] L. Zhou, A. E. Marras, H. J. Su, C. E. Castro, *Nano Lett.* **2015**, *15*, 1815.

[90] L. Zhou, A. E. Marras, C. E. Castro, H.-J. Su, *J. Mec. Rob.* **2016**, *8*, 051013.

[91] A. Ghosh, D. Paria, H. J. Singh, P. L. Venugopalan, A. Ghosh, *Phys. Rev. E: Stat., Nonlinear, Soft Matter Phys.* **2012**, *86*, 031401.

[92] Z. Chen, *2013 13th IEEE Int. Conf. on Nanotechnology (IEEE-NANO 2013)*, Beijing, China, August **2013**.

[93] J. Casals-Terre, A. Fargas-Marques, A. M. Shkel, *J. Microelectromech. Syst.* **2008**, *17*, 1082.

[94] M. A. A. Hafiz, L. Kosuru, A. Ramini, K. N. Chappanda, M. I. Younis, *Micromachines* **2016**, *7*, 191.

[95] Q. Chen, Y. Haddab, P. Lutz, presented at *2010 IEEE/RSJ Int. Conf. on Intelligent Robots and Systems*, Taipei, Taiwan, October **2010**.

[96] H. Hussein, I. Bouhadda, A. Mohand-Ousaid, G. Bourbon, P. Le Moal, Y. Haddab, P. Lutz, *Sens. Actuators, A* **2018**, *271*, 373.

[97] I. Bouhadda, A. Mohand-Ousaid, G. Bourbon, P. Le Moal, P. Lutz, H. Hussein, Y. Haddab, *2018 IEEE/RSJ Int. Conf. on Intelligent Robots and Systems (IROS)*, IEEE, Madrid, Spain, October **2018**.

[98] H. Hussein, V. Chalvet, P. Le Moal, G. Bourbon, Y. Haddab, P. Lutz, *2014 IEEE/ASME Int. Conf. on Advanced Intelligent Mechatronics*, Besançon, France, July **2014**.

[99] S.-W. Huang, F.-C. Lin, Y.-J. Yang, *Sens. Actuators, A* **2020**, *310*, 111934.

[100] H. M. Ouakad, M. I. Younis, *J. Sound Vib.* **2014**, *333*, 555.

[101] E. G. Loukaides, R. W. C. Lewis, C. R. Bowen, *Smart Mater. Struct.* **2019**, *28*, 02LT02.

[102] Z. Vangelatos, G. X. Gu, C. P. Grigoropoulos, *Extreme Mech. Lett.* **2019**, *33*, 100580.

[103] L. Wang, Y. Yang, Y. Chen, C. Majidi, F. Iida, E. Askounis, Q. Pei, *Mater. Today* **2018**, *21*, 563.

[104] J. T. Overvelde, T. A. de Jong, Y. Shevchenko, S. A. Becerra, G. M. Whitesides, J. C. Weaver, C. Hoberman, K. Bertoldi, *Nat. Commun.* **2016**, *7*, 10929.

[105] W. Ma, Z. Zhang, H. Zhang, Y. Li, H. Wu, S. Jiang, G. Chai, *Smart Mater. Struct.* **2019**, *28*, 025028.

[106] E. T. Filipov, G. Paulino, T. Tachi, *Proc. R. Soc. A* **2016**, *472*, 20150607.

[107] J. L. Silverberg, J. H. Na, A. A. Evans, B. Liu, T. C. Hull, C. D. Santangelo, R. J. Lang, R. C. Hayward, I. Cohen, *Nat. Mater.* **2015**, *14*, 389.

[108] A. Gillman, K. Fuchi, P. R. Buskohl, *Int. J. Solids Struct.* **2018**, *147*, 80.

[109] A. Rafsanjani, D. Pasini, *Extreme Mech. Lett.* **2016**, *9*, 291.

[110] P. Bhovad, J. Kaufmann, S. Li, *Extreme Mech. Lett.* **2019**, *32*, 100552.

[111] A. Pagano, T. Yan, B. Chien, A. Wissa, S. Tawfick, *Smart Mater. Struct.* **2017**, *26*, 094007.

[112] A. P. Milojević, N. D. Pavlović, *J. Intell. Mater. Syst. Struct.* **2015**, *27*, 1306.

[113] C. Jianguo, D. Xiaowei, Z. Ya, F. Jian, T. Yongming, *J. Mech. Des.* **2015**, 137.

[114] Q. Liu, J. Huang, B. Xu, *J. Mech. Phys. Solids* **2019**, *133*, 103722.

[115] Q. Liu, B. Xu, *ACS Appl. Mater. Interfaces* **2020**, *12*, 43058.

[116] M. Safaei, H. A. Sodano, S. R. Anton, *Smart Mater. Struct.* **2019**, *28*, 113001.

[117] Y. Jia, *J. Intell. Mater. Syst. Struct.* **2020**, *31*, 921.

[118] B. Kathpalia, D. Tan, I. Stern, A. Erturk, *Smart Mater. Struct.* **2017**, *27*, 015024.

[119] S. F. A. Michael I Friswell, Onur Bilgen, Sondipon Adhikari, Arthur W Lees, Grzegorz Litak, *J. Intell. Mater. Syst. Struct.* **2012**, *23*, 1505.

[120] L. Van Blarigan, J. Moehlis, *Chaos* **2016**, *26*, 033107.

[121] A. Garg, S. Dwivedy, *Proc. Eng.* **2016**, *144*, 592.

[122] W. Liu, F. Formosa, A. Badel, A. Agbossou, G. Hu, *Smart Mater. Struct.* **2016**, *25*, 115045.

[123] M. Derakhshani, T. A. Berfield, K. D. Murphy, *Nonlinear Dyn.* **2019**, *96*, 1429.

[124] T. Huguet, A. Badel, M. Lallart, *Smart Mater. Struct.* **2019**, *28*, 115009.

[125] B. Andò, S. Baglio, A. R. Bulsara, V. Marletta, A. Pistorio, *IEEE Trans. Instrum. Meas.* **2017**, *66*, 1067.

[126] B. Andò, S. Baglio, A. Bulsara, V. Marletta, A. Pistorio, *Proc. Eng.* **2015**, *120*, 1024.

[127] A. Emad, M. A. Mahmoud, M. Ghoneima, M. Dessouky, *Smart Mater. Struct.* **2016**, *25*, 115006.

[128] A. Erturk, D. J. Inman, *J. Sound Vib.* **2011**, *330*, 2339.

[129] A. S. De Paula, D. J. Inman, M. A. Savi, *Mech. Syst. Signal Process.* **2015**, *54*, 405.

[130] Y. Gao, Y. Leng, A. Javey, D. Tan, J. Liu, S. Fan, Z. Lai, *Smart Mater. Struct.* **2016**, *25*, 115032.

[131] Y. Leng, Y. Gao, D. Tan, S. Fan, Z. Lai, *J. Appl. Phys.* **2015**, *117*, 064901.

[132] Y. Gao, Y. Leng, S. Fan, Z. Lai, *Smart Mater. Struct.* **2014**, *23*, 095003.

[133] K. A. Singh, M. Pathak, R. J. Weber, R. Kumar, *IEEE Trans. Sonics Ultrason.* **2018**, *65*, 2184.

[134] D. Zhao, M. Gan, C. Zhang, J. Wei, S. Liu, T. Wang, *Mater. Res. Express* **2018**, *5*, 085704.

[135] G. Wang, W.-H. Liao, B. Yang, X. Wang, W. Xu, X. Li, *Mech. Syst. Signal Process.* **2018**, *105*, 427.

[136] C. Lan, W. Qin, *Mech. Syst. Signal Process.* **2017**, *85*, 71.

[137] P. Podder, D. Mallick, A. Amann, S. Roy, *Sci. Rep.* **2016**, *6*, 37292.

[138] W. Wang, J. Cao, C. R. Bowen, D. J. Inman, J. Lin, *Appl. Phys. Lett.* **2018**, *112*, 213903.

[139] M. Hwang, A. F. Arrieta, *Sci. Rep.* **2018**, *8*, 3630.

[140] H. Deng, Z. Wang, Y. Du, J. Zhang, M. Ma, X. Zhong, *IEEE/ASME Trans. Mechatronics* **2019**, *24*, 282.

[141] S. A. Emam, D. J. Inman, *Appl. Mech. Rev.* **2015**, *67*, 060803.

[142] R. Xu, S. Kim, *J. Phys.: Conf. Ser.* **2015**, *660*, 012013.

[143] P. Harris, C. R. Bowen, H. A. Kim, G. Litak, *Eur. Phys. J. Plus* **2016**, *131*, 109.

[144] A. J. Lee, D. J. Inman, *J. Intell. Mater. Syst. Struct.* **2018**, *29*, 2528.

[145] A. J. Lee, D. J. Inman, *J. Sound Vib.* **2019**, *446*, 326.

[146] A. F. Arrieta, P. Hagedorn, A. Erturk, D. J. Inman, *Appl. Phys. Lett.* **2010**, *97*, 104102.

[147] D. N. Betts, H. A. Kim, C. R. Bowen, D. J. Inman, *Appl. Phys. Lett.* **2012**, *100*, 114104.

[148] D. Betts, H. Kim, C. Bowen, D. Inman, presented at 53rd AIAA/ASME/ASCE/AHS/ASC Structures, Structural Dynamics and Materials Conf. 20th AIAA/ASME/AHS Adaptive Structures Conference 14th AIAA, Honolulu, Hawaii, USA, April **2012**.

[149] Z.-Q. Lu, D. Shao, Z.-W. Fang, H. Ding, L.-Q. Chen, *J. Vib. Control* **2019**, *26*, 779.

[150] S. Shan, S. H. Kang, J. R. Raney, P. Wang, L. Fang, F. Candido, J. A. Lewis, K. Bertoldi, *Adv. Mater.* **2015**, *27*, 4296.

[151] X. Tan, S. Chen, S. Zhu, B. Wang, P. Xu, K. Yao, Y. Sun, *Int. J. Mech. Sci.* **2019**, *155*, 509.

[152] J. Hua, H.-s. Lei, C.-f. Gao, D.-n. Fang, presented at *2019 13th Symposium on Piezoelectrcity, Acoustic Waves and Device Applications (SPAWDA)*, Harbin, China, January **2019**.

[153] C. S. Ha, R. S. Lakes, M. E. Plesha, *Mater. Des.* **2018**, *141*, 426.

[154] C. Winkelmann, S. S. Kim, V. La Saponara, *Compos. Struct.* **2010**, *93*, 171.

[155] M. J. Frazier, D. M. Kochmann, *J. Sound Vib.* **2017**, *388*, 315.

[156] C. Ren, D. Yang, H. Qin, *Materials* **2018**, *11*, 1078.

[157] B. Haghpanah, L. Salari-Sharif, P. Pourrajab, J. Hopkins, L. Valdevit, *Adv. Mater.* **2016**, *28*, 7915.

[158] A. Rafsanjani, A. Akbarzadeh, D. Pasini, *Adv. Mater.* **2015**, *27*, 5931.

[159] X. Zhang, X. Tian, L. Xiao, X. Li, L. Chen, *Appl. Energy* **2018**, *228*, 450.

[160] D.-A. Wang, J.-H. Chen, H.-T. Pham, *Sens. Actuators, A* **2013**, *189*, 481.

[161] A. Cherkaev, S. Leelavanichkul, *Int. J. Damage Mech.* **2011**, *21*, 697.

[162] H. Y. Jeong, S. C. An, I. C. Seo, E. Lee, S. Ha, N. Kim, Y. C. Jun, *Sci. Rep.* **2019**, *9*, 324.

[163] V. Vetriselvi, M. Geetha, K. Dhanalakshmi, presented at *2018 8th IEEE India Int. Conf. on Power Electronics (IICPE)*, Jaipur, India, December **2018**.

Yunteng Cao is currently a Ph.D. candidate in the Department of Civil and Environmental Engineering at Massachusetts Institute of Technology (MIT). He received his B.E. degree in Engineering Mechanics from Shanghai Jiao Tong University (China) in 2013 and M.E. in solid mechanics from Xi'an Jiaotong University (China) in 2016. His research focuses on advanced materials and structures, biopolymers and material delivery to plants and precision agriculture.

Guoliang Huang is currently a Huber and Hellen Croft Chair professor of mechanical and aerospace engineering at University of Missouri-Columbia. He received his Ph.D. degree from University of Alberta, Canada, in 2004. Dr. Huang works in the broad area of Solid Mechanics and Architected Materials in particular the new frontiers of structural dynamics, topological mechanics, wave propagation, and dynamical behaviors of composite materials, both man-made and formed naturally. Dr. Huang's research has been funded by NSF, Air Force of Scientific Research, Army Research Office, Office of Naval Research, Department of Energy, NASA, and major industries.

Changyong Cao is currently an Assistant Professor of Packaging, Mechanical Engineering, and Electrical & Computer Engineering at Michigan State University, where he is directing the *Laboratory for Soft Machines & Electronics*. He received his Ph.D. degree in Mechanical Engineering and Materials Science from the Australian National University (ANU) in 2014, and then worked as a postdoctoral associate for three years at Duke University, USA. His research interests include solid mechanics, soft (active) materials, soft/hybrid robotics, flexible and stretchable electronics, energy devices, and 3D/4D printing of multifunctional materials.
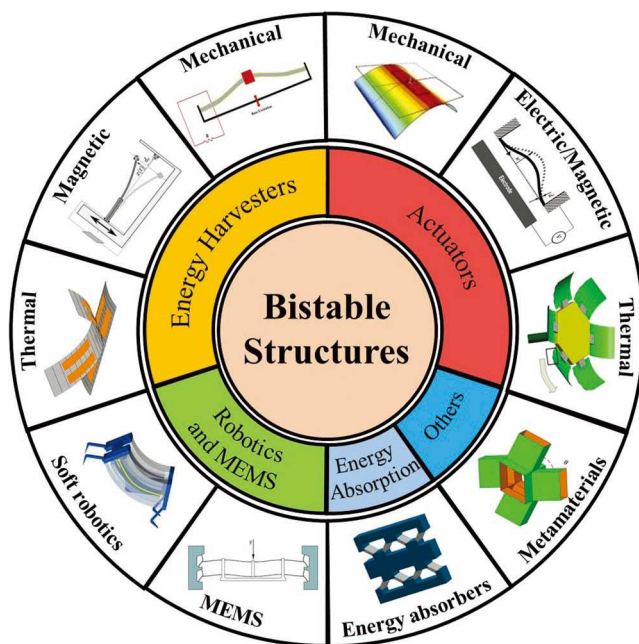
**ADVANCED
SCIENCE NEWS**
www.advancedsciencenews.com

**ADVANCED
FUNCTIONAL
MATERIALS**
www.afm-journal.de

Figure 1. Bistable structures for advanced functional systems. They have been explored for a variety of applications, including actuators[29,45,50] energy harvesting,[3,147] robotics[79] and MEMS,[160] energy absorption,[150] and metamaterials and programmable materials.[105]

functionality,[8] energy absorption structures for enhancing energy storage capacity,[9] and programmable materials and metamaterials for unique properties like negative stiffness.[10]

In this review, we summarize the advances of bistable structures for novel advanced functional systems, categorized by their applications as actuators, robotics and MEMS, programmable devices and metamaterials, energy harvesters, and energy absorbers (**Figure 1**). Actuators, robotics and MEMS, programmable devices and metamaterials are reviewed in Section 2, 3, and 4, whose outputs are displacement and/or deformation upon energy inputs. In Section 4 and 5, energy harvesters, and energy absorbers, which harvest and store energy under displacement and/or deformation input, are discussed. The controllable snap-through actions in nonlinear structures of multistability are further highlighted. We finally discuss the major principles, pros and cons, and the future research directions and challenges.

2. Bistable Structures for Actuators

Actuators are critical parts of a device or robot/machine to generate deformation or displacement for executing specific tasks via consuming various kinds of energy. Bistable structures can enable large displacement and/or deformation by fast snap-through and have been extensively explored for developing novel actuators. Designed bistability generally result from either the topology of novel structures or the employment of smart materials. Compared with conventional actuators, such bistable structures require relatively low energy consumption to generate large displacements owing to the ease of triggering the snap-through. Smart materials, such as piezoelectric materials and shape memory materials, impart the responsive capability

of these structures to other physical stimuli (e.g., electrical, magnetic, and thermal fields) rather than mechanical interactions, broadening their potential applications. Furthermore, bistable structures can lead to a more flexible and versatile system with less design complexity. In this section, we summarize the bistable structure-based actuators, according to their actuation mechanisms, into four main categories: actuators driven by mechanical forces, by electrical fields, by magnetic interactions, and by temperature changes. The actuators with multistable structures are also briefly discussed.

2.1. Actuators Based on Mechanically Driven Bistable Structures

If designed properly with suitable topology, key fundamental units, such as buckled columns, beams, films, and plates/shells, and more complex structures consisting of these units, can exhibit intrinsic bistability that can be utilized for actuators. The snap-through of the bistable structures in actuators driven by mechanical interactions can be triggered when the applied mechanical loading is beyond a critical magnitude. The novelty of such kinds of actuators mainly relies on the structural design (e.g., complex topology) of a device and the methodology of exerting a mechanical loading. For example, Gerson et al. designed a beam-based microactuator (**Figure 2**A), where an integrated electrostatic comb driven transducer was used to apply required force for snap-through.[11] Interestingly, by serially connecting the bistable elements, a multistable actuator was created, showing controllable sequential snap-through buckling (Figure 2A). The displacement achieved was considerably enhanced while the actuation force only slightly increased, compared to those in a single beam design. It is worth noting that such a structure does not necessarily have to be at microscale as it was reported in literature. Addo-Akoto and Han proposed an actuation mechanism that utilized a twisted string and a pin driven by a DC motor to apply the bending moment and trigger the snap-through of a bistable buckled beam (Figure 2B).[12] Their design is simple and cost-effective but needs the parts to exert loading in a contact way, which increases the complexity of the entire system and hinders its miniaturization. Plates and shells are also employed in actuators driven by pneumatically or hydraulically pressure. For example, Rothemund et al. reported a type of soft valve that uses bistability of an elastomeric membrane to control the flow through channels.[13] Such bistable actuators from plates or shells share similarity to beams but facilitate application of pressure via a sealed structure.

It is noted that actuators based on conventional materials require the direct exertion of a contact loading onto the structure and usually need a complex design and control strategy, which have become the main challenges of hindering their wide applications. Therefore, more advanced actuators using smart materials are invented, allowing exertion of non-contact loading to trigger the snap-through of bistable structures. The utilization of smart materials enables exertion of mechanical loading via deformation of specific parts attached to or embedded in the bistable structures. Smart materials that are response to electrical, magnetic, and thermal fields are the main sources to introduce non-contact interactions, and related designs will be discussed later in this section. It is anticipated
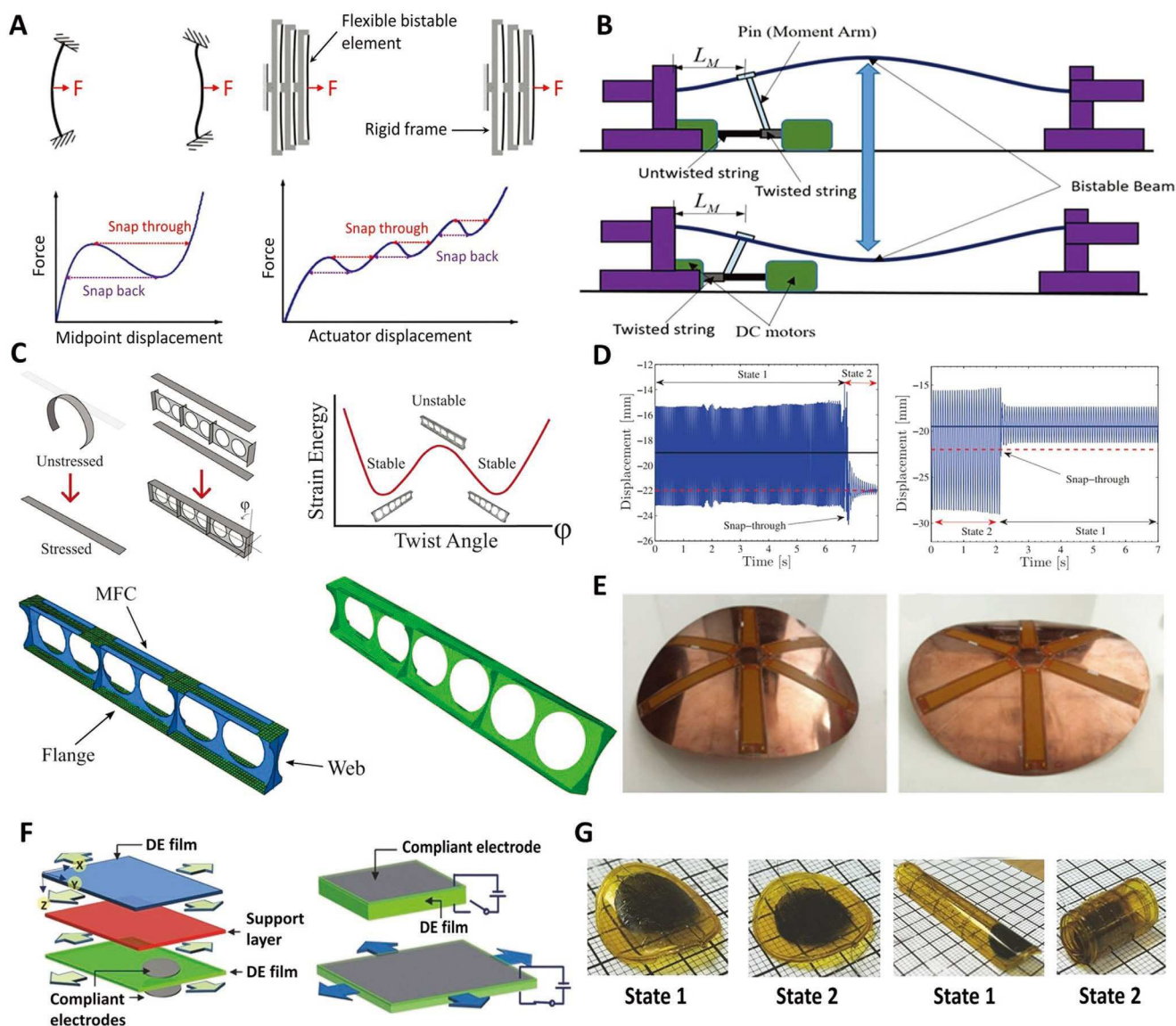
Figure 2. Actuators based on mechanically and electrically driven bistable structures. A) Conceptual design of a microscale curved beam electrostatic actuator and its expected operational performances of two configurations: a single bistable beam (left) and multiple serially connected bistable beams (right). Reproduced with permission.[11] Copyright 2012, Elsevier. B) Schematic illustration of an actuation mechanism using a bistable beam, which consists of a twisted string, a DC motor, a pin, and a moment arm for snap-through actuation. Reproduced with permission.[12] Copyright 2018, SAGE Publishing. C) Illustration of the assembly process of a pre-stressed twisting bistable structure. The curled flanges are stretched and bonded onto web and stiffeners to lock the pre-stress into the structure. The strain energy plot of the twisting bistable structure to show the structures equilibrium positions. The experimental setup and the two stable states of the twisting bistable structure. Reproduced with permission.[18] Copyright 2018, IOP Publishing. D) Displacement of dynamically induced snap-through from state 1 to state 2 (forcing frequency 28.0 Hz) and from state 2 to state 1 (forcing frequency 13.5 Hz) for a [90/0] 160 × 160 mm bi-stable specimen. Reproduced with permission.[34] Copyright 2012, SAGE Publications. E) The two stable configurations of a plastically deformed disc with the MFC actuators. Reproduced with permission.[37] Copyright 2017, The Authors, published by the Royal Society. F) A soft actuator enabled by a bistable laminate structure. The prestretched dielectric elastomer (DE) films are bonded with a support layer in the middle. The laminate can be actuated by an applied voltage from a contracted state to an expanded state. G) The disk and tape-spring actuators made of the DE composite laminate can switch between two stable states. Reproduced with permission.[5] Copyright 2018, Wiley-VCH.

that the employment of compliant and smart materials may help overcome the technical challenges while taking advantage of the topology design, as shown in the section of soft robotics.

Except the bistability induced by solid-solid interactions in response to external stimuli, the bistability triggered by solid-liquid interactions are also demonstrated by Xu et al.[14,15] For example, they propose an electrically and thermally controlled actuation system by adjusting the relative hydrophobicity of a nanoporous material/liquid system. The liquids can be continuously pumped in and out of nanopores by adjusting the electric intensity[14] or temperature field.[15] By optimizing the pore size, solid phase, and liquid phase, the energy density, power density, and efficiency of the actuation system can be tuned according to the requirements and applications.

ADVANCED
SCIENCE NEWS
www.advancedsciencenews.com

ADVANCED
FUNCTIONAL
MATERIALS
www.afm-journal.de

2.2. Actuators Based on Electrically Driven Bistable Structures

The electric actuation is attractive for many applications due to its advantages of easy control and fast response. It has been widely used for developing different kinds of electronically driven actuators. Using attraction or repulsion between charges and the responses of smart materials induced by applied electric fields are two strategies to electrically control the snap-through of bistable structure-based actuators. Piezoelectric materials generate strains when an electric field is applied, and vice versa produce charges when subjected to stresses. The combination of piezoelectric materials with bistable structures is a main approach of fabricating piezoelectric actuators. The converse piezoelectric effect forms the basis of piezoelectric actuators, which employ the deformation and displacement of piezoelectric materials under controlled external electric fields to manipulate the snap-through of the structure. For example, as shown in Figure 2C, a classic I-beam was imparted bistability by two straightened curved beam flanges, which were separated by a web.[16,17] Based on the bistable twisting I-beam, Arrieta et al. used macro fiber composites (MFC) consisting of piezoelectric materials attached to the flanges to control the snap-through, producing fast and large deflections with low strain piezoelectric materials.[18]

Composite laminates are also extensively studied as morphing structures, and the methods to introduce bistability to laminates are developed via anisotropic residual stress generated by thermal treatment[19,20] and by prestress[21–24] or via laminate design.[25] Several groups developed piezoelectric actuators by bonding MFCs to bistable composite laminates to trigger snap-through. Initial trials using a single piezoelectric MFC patch bonded to one side of a laminate demonstrated successful snap-through[26–30] but failed to trigger the reverse snap-through due to the limited actuation force of the piezoelectric MFC patch, and the changed geometry and increased stiffness resulting from the attachment of the patch. Further effort by Schultz et al. using a two-ply, $[0/90]_T$ graphite–epoxy laminate sandwiched between two piezocomposite actuators successfully demonstrated the self-resetting behaviors.[31]

Another strategy that employed narrow occurred MFC strips distributed over the entire surface was presented to replace the commonly adopted method where large rectangular MFC patches were bonded in the center of the laminates.[32] This strategy aimed to eliminate the significant influence of MFC patches on the shape of the laminates, particularly the reduction of curvature where they are bonded. Alternatively, dynamically assisted snap-through was proposed using a resonant control technique.[33–35] MFCs were used to induce resonant response of the actuator, i.e., the bi-stable composite laminate together with the attached piezoelectric MFCs. The magnitude, i.e., displacement of the actuator, would be much larger in resonant conditions than that in static or non-resonant conditions, which makes it possible to reach the critical displacement and trigger snap-through. The actuator was designed such that the two equilibrium states have distinct modal frequencies, allowing state-specific frequency being targeted and preventing chaotic oscillation arising from continuous snap-through between stable states. Once the snap-through occurred, the input from MFCs was not resonant anymore, resulting in diminishing structural displacement (Figure 2D).

Meanwhile, combining other driving mechanisms with piezoelectric actuation is used to overcome this problem. For example, Bowen et al. used a mass to demonstrate reversible transitions.[27] Shape memory alloy (NiTi) wires were used to drive reversible state switching in a bistable composite cantilever where piezoelectric MFCs triggered snap-through.[36] Interestingly, Hamouche et al. developed a bistable laminate by plastically deforming an initially flat copper disc with small imperfections based on a fully nonlinear inextensible uniform-curvature shell model (Figure 2E).[37] Distinct from those two stable configurations of laminates usually having curvatures with opposite signs, their structure showed two stable configurations with same-sign curvatures, indicating much smaller energetic gap between the equilibria. The reversible state transition was controlled by the attached MFCs electrically.

Despite these fantastic solutions, bonding piezoelectric MFC patches to bistable structures indeed introduces extra components and stiffness to the system, resulting in high working voltage, incapability of self-reverse snap-through, and sometimes even loss of bistability. An interesting thought would be: why not build bistable structures directly with piezoelectric materials so that the simplified structures are more compliant to snap through reversibly by itself? Lee et al. built such a laminate consisting of only two piezoelectric MFCs that functions as both the actuator and the primary structure.[38–40] They bonded two MFCs orthogonally in their actuated states and released the voltage post cure to create in-plane residual stresses. Recall that introducing proper prestress or residual stress is one of the key techniques to impart bistability to laminates.[21–24] The resulting $[0^{MFC}/90^{MFC}]_T$ laminate displayed a cylindrical shape, demonstrated bistability, and snapped through and back with only piezoelectric actuation.

Distinct from the rapid advances in utilizing smart materials to electrically driving actuators, the strategy that employs attraction or repulsion between charges to trigger snap-through of bistable actuators was blocked, partly due to the limited magnitude of the attraction or repulsion compared to the stiffness of the system. This is intrinsically determined by the inverse-square law, where the force between charges is inversely proportional to the square of the distance between charges that is generally larger than tens of microns in engineering. However, the development of soft materials (e.g., dielectric elastomers) and fabrication of microscale structures solved this problem. Both decrease the stiffness of the system, and the latter also allows electric interaction at a scale of the order of several micrometers. For example, a bioinspired trilayered bistable all-polymer laminate was fabricated with a supporting layer made of polyimide or polyester sandwiched by two orthogonally prestrained acrylate adhesive elastomer films as DE layers (Figure 2F).[5] Dielectric elastomer, polyacrylate film, has a thickness of 500 µm with Young's Modulus of 0.22 MPa (≈six orders lower than that of aluminum), while the supporting layer has a thickness of 25 µm with Young's Modulus of 2.5 GPa and 4.9 GPa for polyimide and polyester (≈two orders lower than that of aluminum), respectively. To actuate this laminate, electrode materials including carbon grease and PEDOT:PSS were properly placed on stretched DE layers, with lightweight carbon nanotube (CNT) yarns as soft and flexible electrical leads. As highlighted, each effort of the authors was made to decrease the

stiffness of the system. The disk actuator displayed controlled reversible snap-through between two equilibrium states and the tape-spring actuator underwent shape transformation from one equilibrium shape to another upon activation, mimicking the retraction of a chameleon's tongue (Figure 2G).

On the other hand, the feasibility of electrostatically triggering snap-through of bistable microstructures, particularly curved micro beams, has been demonstrated theoretically and experimentally.[41–45] Electrostatic actuation is efficient at distances at the order of several micrometers between electrodes, while the typical length of microstructures ranges from tens to hundreds of micrometers. For example, the bistable structure used in Figure 2B can be triggered electrostatically by employing the beam as an electrode or attaching an electrode to the beam, instead of integration of an electrostatic comb driven transducer.[12,46] However, this adaptation may not be suitable for the multistable structure due to the limited space between the two fixed electrodes for electrostatic actuation. Thus, electrostatic actuation is promising in MEMS or NEMS, but less popular in large scale devices unless ultrahigh voltage and/or large current is used.

2.3. Actuators Based on Magnetically Driven Bistable Structures

The ubiquitous magnetic interaction is highly desired for many applications due to its attractive properties such as ease of access and control, fast response, and noncontact interaction. It has been one of the most widely used driving mechanisms for actuators and is probably the most promising method. The magnetically driven actuators take advantages of the interaction between magnetic fields, generated by currents, permanent magnets or other magnetic materials. Magnetic interaction shares similar disadvantages to electrostatic interaction; the intensity of most available magnetic fields, either natural or man-made, is limited and the magnitude of magnetic interaction decays fast with distance. Thus, employment of magnetic interaction on bistable structures composed of soft magnetic responsive composites is a feasible strategy.
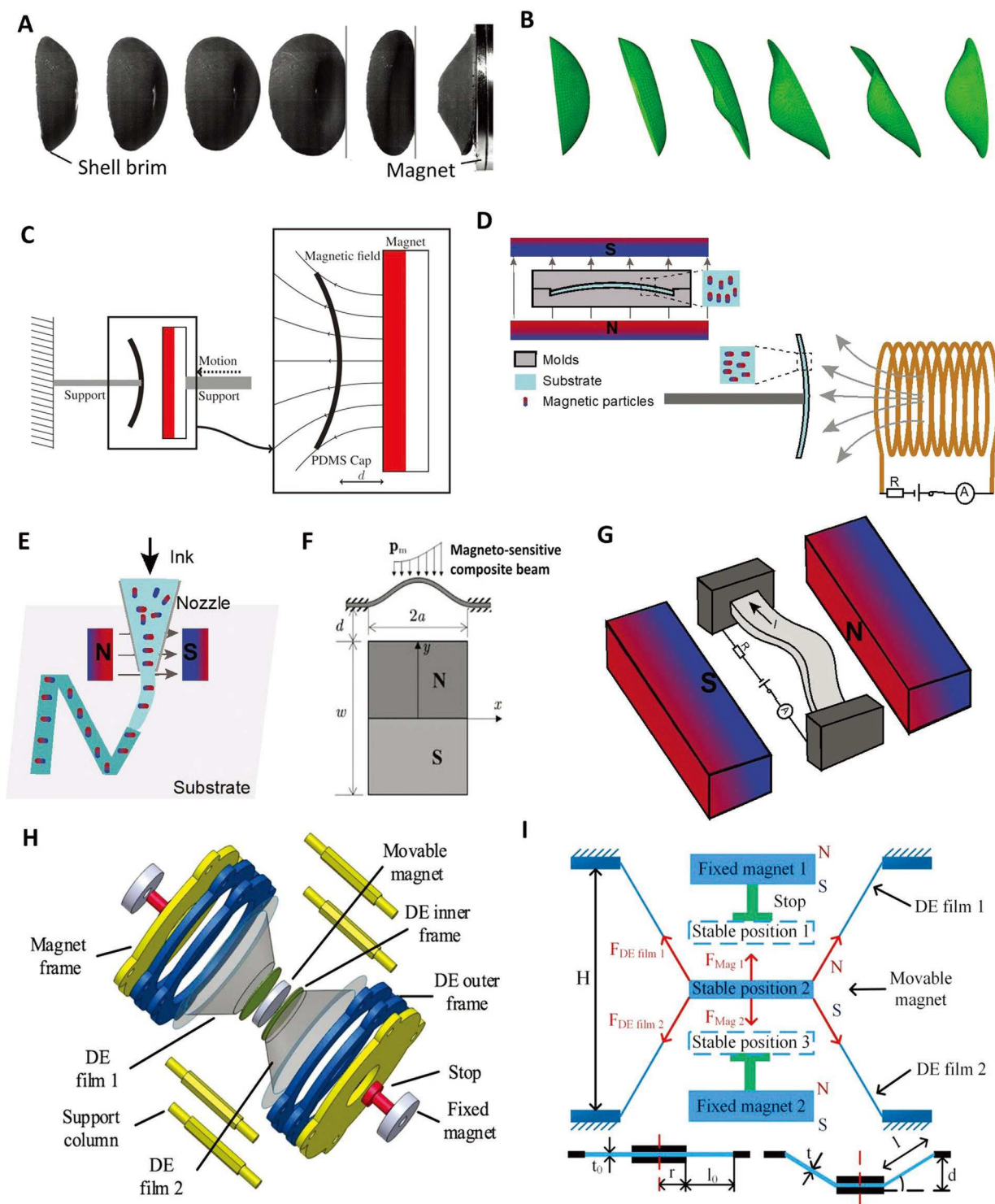
Loukaides et al. reported a bistable spherical cap made of iron carbonyl-infused polydimethylsiloxane (PDMS) that was actuated remotely through permanent magnets (**Figure 3**A–C).[47] The Young's modulus and the shear modulus of the PDMS they used were 750 kPa and 250 kPa, respectively; and the thickness of the cap was 1–3 mm, retaining the compliance of the structure. Carbonyl iron microparticles ranging from 2–9 µm were uniformly distributed in the PDMS matrix, enabling the application of a magnetic force on the cap when it is close to a magnet. By decreasing the distance between a permanent magnet and the cap, the intensity of the magnetic field increased at where the cap was located, resulting in an increased force on the cap that could trigger the snap-through. It was also discovered that non-axisymmetric transition shapes had lower energy barrier and were preferred by bistable spherical caps initially tilted or with imperfection.[48] This idea was fancy, but the design could be improved from at least two aspects by a) replacement of the ferromagnetic iron microparticles by aligned permanent magnetic microparticles, and b) replacing the driving permanent magnets with electromagnets. The magnetic microparticles distributed in

the polymer can be aligned during curing process by keeping the mixture in an external magnetic field. The cured polymer matrix will become a soft permanent magnet, having a determined N and S pole (Figure 3D). This method is particularly helpful in the fabrication of complex structures using printing-based techniques (Figure 3E).[49] The magnetic field of an electromagnet is determined by the current intensity and direction, which facilitates transition between magnetic attraction and repulsion (Figure 3D). These two strategies enable reversible, remotely controlled snap-through of the cap by changing the direction and intensity of the current in the electromagnet, avoiding moving the driving magnets. For example, Hou et al. used an electromagnet, instead of a permanent magnet, to actuate a bistable curved beam composed of a silicone elastomer matrix with embedded micro-sized iron particles (Figure 3F).[50] The snap-through was triggered by the electromagnet with a current larger than a critical value. Reversible configuration transition could be achieved by combining two electromagnets on each side of the beam. It was also found that the critical current was proportional to the thickness of the beam and the distance between the beam and electromagnets and inversely proportional to the density of iron particles. It is worth noting that the critical current (voltage) was 1.8 A (12 V), much lower than the actuation voltage for dielectric elastomers, proposing a potential advantage of magnetic actuation to electric actuation via dielectric elastomers. Alternatively, the curved bistable beam was designed as conductive, having a high slenderness ratio of 12000 to enable flexibility. The current in the beam underwent a force in a magnetic field of magnets, resulting in controlled reversible snap-through (Figure 3G).[51]

Different from the studies where the bistability results from bistable structures, Li et al. reported a dielectric elastomer actuator showing tristability induced by magnetic force. They used two prestretched cone dielectric elastomer films to hold a movable magnet in the middle of two fixed magnets, creating three stable positions (Figure 3H,I).[52] Both fixed magnets exerted attraction on the movable magnet. The tensions from dielectric elastomer films and the attractions from fixed magnets were balanced when in stable position 2. By applying a voltage on dielectric elastomer film 1, electrically induced Maxwell stresses compressed the film, resulting in a reduced tension and thus the moving magnet being closer to stable position 3. Upon the applied voltage reached a critical value (2.5 kV), the moving magnet snapped through to stable position 3 from 2. Reverse snap-through from stable position 3 to 2 was achieved by removing the voltage applied on film 1 and releasing the tension in film 2 via an applied voltage. Such design combines electrostatic responsive materials and magnetic interaction, displaying a promising strategy for interaction based multistability.

2.4. Actuators Based on Thermally Driven Bistable Structures

Heat, as one of the most widely used energy forms, has been explored in bistable actuators. Despite temperature dependent material properties, the ubiquitous thermal expansion displays great potential in actuation due to thermal strain and thermal stress, which results from the difference of thermal expansion coefficients among materials that are bonded together when

**ADVANCED
SCIENCE NEWS**

www.advancedsciencenews.com

**ADVANCED
FUNCTIONAL
MATERIALS**

www.afm-journal.de

Figure 3. Actuators based on magnetically driven bistable structures. A,B) Actuation sequence of a bistable magnetic rubber composite shell from experiments and finite element modeling. Reproduced with permission.[48] Copyright 2016, IOP Publishing. C) Illustration diagram of the experimental setup for remotely actuating a PDMS spherical cap with a permanent magnet. Reproduced under the terms of the Creative Commons Attribution License.[47] Copyright 2015, The Authors, published by Taylor & Francis. D) Schematic illustration of the fabrication setup for aligning magnetic particles in a polymer substrate using an external magnetic field. Reversible and remotely controlled snap-through of the cap can be achieved by an electromagnet. E) Schematic of producing aligned magnet nanoparticles in a substrate by printing-based techniques. F) Schematic illustration of the actuation of a bistable composite beam made of a silicone elastomer with embedded iron particles. Reproduced with permission.[50] Copyright 2018, AIP Publishing. G) Schematic illustration of the experimental setup for the electromagnetic actuation of the soft beam. H) Schematic diagram of a tristable dielectric elastomer (DE) actuator consisting of two cone-shaped dielectric elastomer films, two end permanent magnets, and one central movable magnet for magnetic actuation. I) The three stable states of the magnetic-based DE actuator in (A).

**ADVANCED
SCIENCE NEWS**
www.advancedsciencenews.com

**ADVANCED
FUNCTIONAL
MATERIALS**
www.afm-journal.de

temperature changes. Thermal strain and thermal stress enable two strategies of thermally driven bistable actuators, i.e., bonding thermal strain and thermal stress generators to bistable structures and designing thermally responsive bistable structures.

Thermal strain and thermal stress generators can be built by bilayer strips made of materials with different thermal expansion coefficients or by the same material with locally heating. For example, Zhang et al. developed a solar tracking device that was composed of bistable laminates driven by a Ni36/Mn75Ni15Cu10 bimetallic strip (**Figure** 4A).[53] With the radiation from the sun, the bimetallic strips could bend and deform due to temperature change, triggering the snap-through deformation of the bistable laminates. Inversely, the decline of solar illuminance caused the decrease of temperature and the diminished deformation of the bimetallic strips, thereby the bistable laminates snapped back to their initial states (Figure 4B).

Properly designed laminates can serve as thermally driven bistable actuators. In fact, residual thermal stresses were used to impart bistability to unsymmetric laminates.[19,20] Li et al. observed the snap-through of such laminates by locally heating the middle part to relieve residual stress and induce snapping of the unheated regions, followed by a cooldown step (Figure 4C).[54] It was found that the laminated geometry and the distribution of the heated region could significantly affect the critical actuation temperature and the snap-through behavior of a bistable laminate. Therefore, it is possible coming to the plausible conclusion that the $[0_n/90_n]$ class of unsymmetric laminates are inherently incapable of displaying thermally driven snap-through behaviors when other different heating methods are utilized.[55] Eckstein et al. reported the snap-through driven by temperature change and its dependence on initial curvature using fiber–metal hybrid laminates that have high coefficient of thermal expansion mismatch between composites and metals.[55]

In addition, thermal gradients and temperature-dependent material properties were taken into consideration in thermally actuated composite laminates.[56] While it is of great importance to account for variation of material properties over a wide range of temperature, thermal gradients are usually negligible along the small thickness of thin laminates unless in rare extreme conditions and are technically challenging to apply. Clamped curved beams are another example commonly used as bistable structures. Zhou et al. reported a bistable microactuator that consisted of inverted-series-connected Cu/W-based curved beams (Figure 4D),[57,58] which bend with electrothermally induced temperature change since the thermal expansion coefficients of copper and tungsten are 17×10^{-6} and 4.3×10^{-6} °C^{-1}, respectively. The snap-through of a 1 mm long actuator enabled a displacement of more than 30 μm. Their design was significantly simplified by combining Joule heating, snap-through triggering, and bistability via the employment of conductive bi-layered beams. The two metals also have relatively high melting points and large Young's modulus, indicating a large displacement or force output. Hussein et al. created a tunable symmetric bistable actuator consisting of two opposite sets of preshaped curved beams with similar materials and dimensions that are connected to each other by a shuttle at their mid-points (Figure 4E).[59] The tunable bistability was realized by Joule heating of the two sets of conductive beams via applied voltages, which created a negative stiffness behavior at their initial position.

Other than the ubiquitous thermal expansion, some alloys, such as NiTi, CuZnAl, and CuAlNi, show unique thermal shape memory effect, that is, they can restore their original form from the deformed form when heated. Such shape memory effect results from the phase transformation between the high temperature phase (austenite structure) and low temperature phase (martensite structure).[60,61] Shape memory alloys (SMAs), especially NiTi alloy, have been extensively used for actuators, MEMS, and robotics thanks to their high actuation stress, relatively high strain, and ease to be manufactured into various formats. Using SMAs to build thermally driven bistable actuators shares analogous strategies with using piezoelectric materials to fabricate bistable actuators that are electrically driven. The feasibility of using SMA wires to trigger the snap-through of unsymmetric composite laminates was demonstrated by an approximate theory and supported with experiments. [59] Numerical models were also developed and may help solve the manufacturing problems such as a large number of SMA wires required and their distribution as well as the influence of laminates processing.[62,63] These designs used one-way shape memory effect, thus enabled only one-way snap-through. A reversible snap-through could be achieved by using additional SMA wires or other smart materials such as piezoelectric MFCs to actuate snap-back.[36] Two-way SMAs have rarely been used for bistable actuators. Even though a two-way SMA can "remember" its shapes at both high and low temperatures and might contribute to the reversible snap-through, it suffers from much lower recovery strain than a one-way SMA and quick memory loss after the initial training procedure, resulting in low reliability.

There are several other categories of materials also displayed thermally induced shape memory effect, including ceramics,[64] hydrogels,[65] and polymers.[61,66] Ceramics can be hardly used on bistable actuators due to their intrinsic brittleness. The application of hydrogels for actuations may be hindered owing to their great dependence on water and poor mechanical stability in atmosphere. These issues will be overcome by emerging hydrogels with enhanced mechanical properties for special actuators working in aqueous conditions. Despite the low thermal conductivity and Young's modulus, shape memory polymers (SMPs) manifest desiring properties including extremely high strain (up to 400%, and possibly above 800%[60]), fast and easy shape training, mild fabrication conditions, low and tunable transition temperature, and low density. SMPs have been widely used as an alternative to SMAs. Chen and Shea presented an actuator consisting of a von Mises truss based bistable structure actuated by a shape memory strip (SMS) (Figure 4F). This actuator was fabricated by 3D printing and was combined serially to achieve multistability and in other rational ways to form reconfigurable 3D structures.[67] The reconfiguration of this actuator could be triggered easily by environment temperature change since the glass transition temperature T_g of the shape memory polymer, FLX9895, is ≈30 °C, above which the SMS will recover its original shape. The activation of such a design, as claimed, was suitable to be controlled through the surrounding environment. Because Joule heating can easily overheat the structure and cause structural damage or failure without proper monitoring and a feedback mechanism will inevitably increase structural size and complexity. In addition, the maximum strain
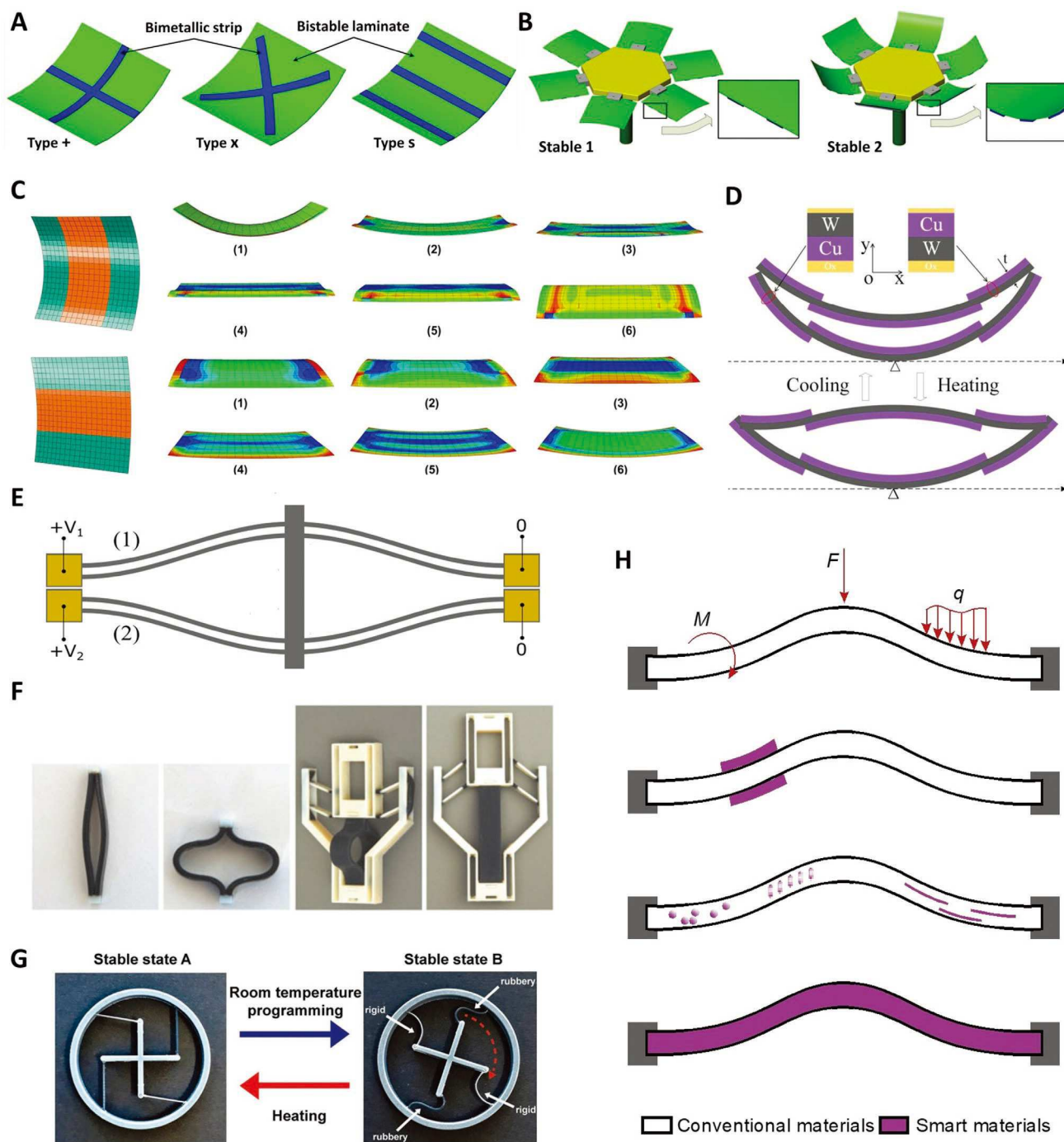
**ADVANCED
SCIENCE NEWS**
www.advancedsciencenews.com

**ADVANCED
FUNCTIONAL
MATERIALS**
www.afm-journal.de

Figure 4. Actuators based on thermally driven bistable structures. A) Bistable laminate actuators with three different layouts of bimetallic strips, bending actuated by heat to change its deformation state. B) A solar tracking device enabled by bistable actuators in (A). Reproduced with permission.[53] Copyright 2020, Elsevier. C) Sketches of residual stress-relieved regions (marked in red) of the two heating strategies on two 140 mm × 140 mm laminates and corresponding simulated snap-through process. Reproduced with permission.[54] Copyright 2012, Elsevier. D) Working principle of an electrothermal bistable microactuator. Reproduced with permission.[57] Copyright 2019, IEEE. E) The tunable symmetric bistable device. Reproduced with permission.[59] Copyright 2020, IOP Publishing. F) The printed state and programmed state of an expanded SMS and two states of the bistable actuator after assembly of the SMS. Reproduced with permission.[67] G) The original shape (state A) and rotated structure (state B) of the rotational bistable structure with two different digital SMPs (rigid and rubbery ones). Reproduced with permission.[68] Copyright 2019, Wiley-VCH. H) Four typical design strategies for bistable structure-based actuators.

within the extending and contracting SMS may reach 0.258 and 0.374, respectively, much higher than the upper limit of SMA (typically ≈8%).

In fact, the printability of SMPs is especially attractive in the fabrication of actuators with complex structures. Recently, Jeong and his colleagues designed a 4D thermally responsive

**ADVANCED
SCIENCE NEWS**
www.advancedsciencenews.com

**ADVANCED
FUNCTIONAL
MATERIALS**
www.afm-journal.de

structure, capable of large-angle rotational actuation in a highly controlled manner (Figure 4G).[68] They employed two different digital SMPs (rigid and rubbery ones) to print beams that connect the inner cross and outer circle. The rigid beams provided bistability while the rubbery beams with fixed boundary conditions act as the control knob. Multistability was also reported by aligning the actuator unit in a nesting doll manner. Note that the temporary shapes of SMP beams were obtained mechanically below T_g, which was counterintuitive. Typically, a SMP beam recovered to its initial shape from a temporary shape that was obtained by a typical heating above T_g, deforming, and cooling procedure, that is, their shape memory effect does not relate to deformation below T_g. Because SMPs are at a hard and relatively brittle "glassy" state below T_g, they undergo either small elastic deformation or fracture and cannot form a temporary shape as above T_g. The magic relies on the way the beams were prepared, i.e., mixing the SMP (VeroWhite) with a rubber-like material, TangoBlack. By the addition of rubber-like TangoBlack, the beams deformed to form a temporary configuration at room temperature below T_g without material failure and maintained the shape in the absence of external forces. Once heated up above their T_g, the beams become flexible and will minimize their potential energy by releasing deformation, i.e., reconfigure from curved beams (temporary shape) to straight ones (initial shape). In sum, the application of SMPs rendered a secondary equilibrium stable state to the structure and enabled its one-way snap-through.

In addition to the three actuation mechanisms, other smart materials that are responsive to pH,[69–71] light,[72–75] and ionic strength etc. are emerging. However, there are only a few bistable structure-based actuators reported yet. For example, Zhao et al. developed a bistable concave-shaped assembly which displayed snap-through when heated up and snapped back when pH changed from 7.0 to 2.0.[69] Most of the actuators using these smart materials do have two stable configurations, but they do not have structure-based bistability. Instead, they obtain the additional stable configuration due to the response of the smart materials to external stimuli, that is, the two stable configurations correspond to the two states of stimuli (e.g., low/high pH, with/without luminescence). The potential energy curve of the structure under stimuli is different from that without stimuli, but both of them typically have only one minimal. It should be noted that such design may have a set of continual configurations that should be maintained by application of the stimuli.

To design an actuator, two parts are essential, i.e., its structure and its actuation mechanism. We now summarize from a structural perspective coupled with the discussion on actuation mechanism to provide a thorough understanding. In conclusion, all the bistable structure-based actuators discussed were structurally designed in four typical strategies as shown in Figure 4H. The first and most fundamental design utilizes a bistable structure made of conventional materials, whose snap-through is triggered by various loadings, contact or non-contact, in a format of moments, point forces, pressures, and strains (e.g., locally heating, not shown in the figure). The application of contact moments, forces, and pressures provides sufficient loading for snap-through usually at a cost of additional components, which increases the complexity of the whole system.

Particularly, pressure can be applied via vacuum or pressured air/liquid by an external pump. Non-contact loading (e.g., the force exerted on current by a magnetic field) typically has limited magnitude and is suitable for actuators at micro scales. The second to the fourth strategies take advantage of smart materials responsive to physical stimuli, such as electric, magnetic and temperature fields, to enrich loading application methodology and/or impart bistability. By attaching components made of smart materials to (e.g., piezoelectric MFCs, SMA wires, bimetallic strips) or embedding them in (e.g., carbonyl iron microparticles) bistable structures consisting of conventional materials, the loading for snap-through triggering is applied by physical stimuli. However, smart materials and methodology to apply necessary physical stimuli as well as these strategies have inherent shortcomings that should be taken into account in the design process. While electric signals are fast responsive, an external power source and circuits are usually necessary to apply electric voltage, which makes electric voltage infeasible in the third strategy.

Temperature change and magnetic interaction are suitable for both the second and third strategies due to numerous techniques to change temperature and to generate and tune magnetic fields. For example, Joule heating, conduction, and convection have been extensively used in reported designs. Radiation, another main type of heat transfer, has yet been reported in bistable actuators despite of its high efficiency and non-contact property. Radiative heating is a promising way to change temperature locally in a controlled manner. Indeed, infrared light of specific wavelengths is used to remotely heat up embedded materials while not the substrate. (infrared heating therapy refs) Magnetically responsive micro- and nanoscale materials that can be embedded in substrates, particularly soft materials and printable materials, as shown in the third design, are the most important contributor to advances of magnetically driven actuators. The printing techniques with controlled magnetic fields will further pave the way to the fabrication of such actuators with complex structures and advanced functions.

Microactuators might still employ second structure, but the third design is not suitable owing to the size limitation of microstructures. The last strategy uses merely smart materials where they function as both structural materials and stimuli responsive parts. It significantly simplifies the structure and renders actuators possibility for more advanced functions including robots and MEMS. However, smart materials such as ceramics and metals are typically not suitable in this strategy because of the limited reversible deformation while smart polymers are great candidates.

3. Bistable Structures for Robotics and MEMS

Similar to actuators, robotics and MEMS also transform energy inputs into displacements and/or deformations. By integration of other components, they can employ bistable structures to perform more versatile functions than actuators. Soft robotics take advantages of the flexibility of the materials and structures, while MEMS and microrobotics utilize their advantages resulting from microscale sizes.

3.1. Bistable Structures for Soft Robotics

Soft robots have demonstrated great potential in a variety of applications such as prosthetics, surgical tools, rehabilitation facilities, and medical devices thanks to their excellent environmental adaptability, user-friendliness, and safety stemming from material flexibility.[76] Efficient actuation, as one of the key issues in soft robotics, have been intensively explored in respect to employment of smart materials and structural design. Impressive advances have been reported via adoption of bistable structures and their combination with smart soft materials. Bistable structures generally are used as moveable parts due to snap-through. For example, Chen et al.[77] designed a temperature-based propulsion soft swimmer using bistable shape memory polymer (SMP) muscles (**Figure 5**A). The SMP muscle was triggered by water temperature to snap through between two stable states to generate directional propulsion (Figure 5B). By adjusting the rotational stiffness of the flexible joints, the fabricated state was more stable than the activated state which made directional actuation possible. The soft swimmer could achieve a full back and forth actuation process through two SMPs with different activation and transition temperatures (Figure 5C). When $T_1 < T_2$, by setting the temperature at T_1, the first bistable element (M_1) was actuated, while after increasing the temperature from T_1 to T_2, the second actuation process occurred (M_2).

Bistability has also been employed for agile locomotion and jumping of soft robots.[78–80] As shown in Figure 5D, the soft robot was made of a soft supporting structure (polyvinyl chloride plate (PVC)) with two thermally actuated shape memory alloys (SMA) at its top and bottom sides for achieving vertical and forward jumping, respectively.[78] The supporting layer was covered with heat-resistant sheets on both sides to eliminate the influence of temperature variation. Two different modules were fabricated: a single module for vertically jumping and a series-type module (two modules in series) for forward jumping. It was demonstrated that a 0.05 m single module could jump up to 0.13 m, and the jumping height would be further improved by adjusting bending amplitude. For the series-type module, the jumping process reduced the buckling time difference between the two modules. Tang et al. built a soft pneumatic actuator with a two-linkage structure connected by springs to provide bistable deformations for high-speed and high force tasks (Figure 5E,F).[81] The body of the soft robot was prepared by compressing the polyester sleeve through a steel rod, while the rigid frame was 3D-printed with polylactic acid (PLA). In their design, the high-speed bistable mechanism or high-force monostable (higher spring stiffness) mechanism utilized the pre-stretching of a middle spring (Figure 5G). Equipped such a bistable structure, the soft robot could run at a linear locomotion speed of 174.4 mm/s, about 4.7 times faster than the similar soft crawler without a bistable structure.

In addition, soft grippers take advantages of bistable structures, too. For example, Zhang et al. designed a bionic robotic gripper by mimicking the trapping motions of Venus flytrap using a bistable morphing structure enabled by anti-symmetric shells and the magnetic actuation.[82] The proposed design consisted of a core standing with two compliant magnetically actuated fingers for swift large deformations and strong gripping motions. More recently, Lunni et al. also developed a plant-inspired soft bistable structure made of hygroscopic electrospun nanofibers.[83] The energy barrier of the soft bistable mechanism highly depended on the geometry and the elastic properties, while the snap-through motion between the stable states was mainly governed by the active layer. Furthermore, Zhang et al. proposed a compliant bistable gripper for small-scale aerial robotic systems,[84] in which a linkage-based bistable mechanism was designed to be switchable, adjustable, and stable for grasping and holding operation. The bistable gripper consisted of four major parts: three fingers, three soft silicone tubes, a base with three vertical beams, and a contact pad. Both the analytical modeling and experimental results showed that the designed gripper can make the aerial robot perch on a horizontally hanging object.

Interestingly, Chi et al. designed pre-curved 2D beam-like bending actuators and 3D doming actuators with tunable monostability and bistability to fabricate soft robotics, which achieved high performance as energy-efficient soft gripper to holding objects, as fast-speed larva-like jumping soft crawler with average locomotion speed of 0.65 body-length s^{-1} (51.4 mm s^{-1}), and as fast swimming bistable jellyfish-like soft swimmer with an average speed of 53.3 mm s^{-1}.[85] Instead of using bistable structures directly for motion, Rothemund et al. used their soft bistable valve as an autonomous controller in grippers and crawlers,[13] which eliminates the necessity of an external programmed controller and significantly simplifies the structure of soft robotics. These studies demonstrated the versatility of bistable structures in soft robotics and the roles that bistable structures can play innovatively.

3.2. Bistable Structures for Microrobotics and MEMS

Bistable structures could simplify the design and control mechanism of microrobotics and MEMS. One representative example is the DNA-based nanostructures.[86–88] As shown in **Figure 6**A, a compliant bistable DNA nanostructure was fabricated with four links with helix bundles to predict its energy landscape for snap-through motions.[89,90] The energy plot of such a structure had two stable configurations with an asymmetric distribution and a tunable energy barrier (Figure 6B). Most of the structures were in their stable states (S_1, S_2 in Figure 6C) corresponding to the conformational energy distributions (Figure 6D). This study provided insightful knowledge for designing microscale biomedical devices such as biosensors and medical manipulators by implementing macroscale structural design into DNA nanostructures.

As the basic building blocks for many biological systems, helical structures are another kind of structures that can be combined with bistability for micro/nanorobotic applications.[91] Using FEM analysis and experimental testing, Chen et al. studied spontaneous twisting/bending of helix structures (Figure 6E),[92] demonstrating that tunable helical ribbons could be made by bonding two or three layers of pre-stretched strips. As shown in Figure 6F, a small piece of a slap bracelet composite made of stainless-steel layers and a fabric cover exhibited two stable configurations through the coupled
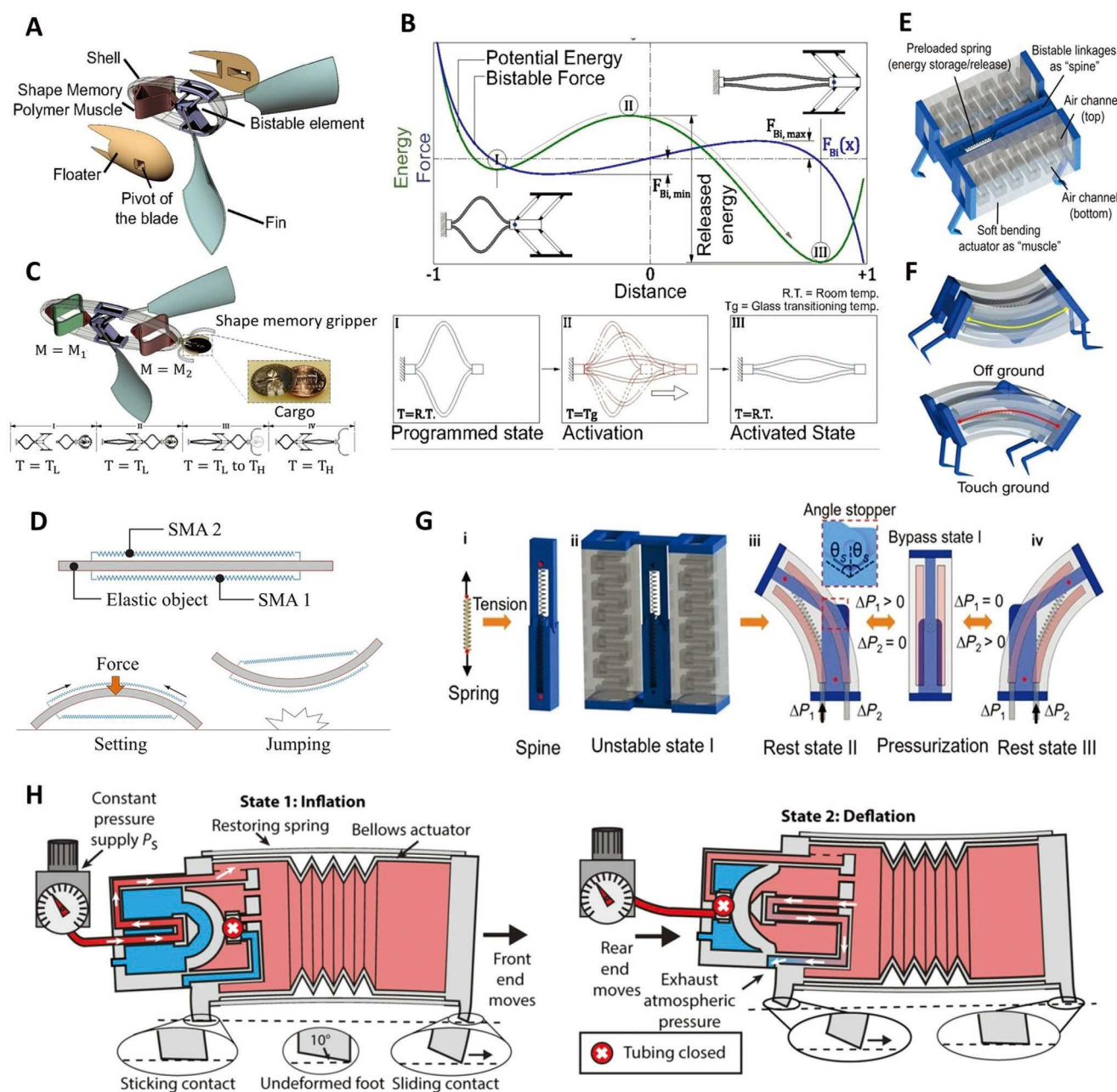
Figure 5. Bistable structures for soft robotics. A) Schematic illustration of a soft swimmer capable of directional propulsion, actuated by a shape memory polymer (SMP) bistable muscle. B) The bistable structure is actuated at the transition temperature T_g resulting in backward pulling and propulsion of robot arms. C) A full forward-backward motion mechanism via two SMP bistable actuators with different activation and transition temperature (M_2 has a higher activation temperature than M_1 to enable the full forward-backward motion). Reproduced with permission.[77] Copyright 2018, National Academy of Sciences. D) Schematic illustration of a bistable soft robot consisting of an elastic object (PVC plate) and two SMA actuators. The SMA actuators contract by heat generated by electricity, leading to snap-through deformation for jumping motions. Reproduced with permission.[78] Copyright 2018, IEEE. E) Design of a hybrid robot made of soft pneumatic actuators and a rigid bistable structure. F) Two stable states of the proposed hybrid crawler in motion. G) Schematic and work principles of the hybrid robot and its two stable configurations. Reproduced with permission.[81] Copyright 2020, American Association for the Advancement of Science.

bending/twisting behavior, which could be used for designing self-assembled microrobotics systems with different actuation mechanisms.

Beam-type bistable structures have been widely used in MEMS such as micro-switchers[93] and resonators[94] due to their nonlinear properties in improving the functionality and

reducing the design complexity of MEMS devices.[8,95] As shown in Figure 6G, the bistable micro switching device was made of curved beams with thermal actuators and two stopping blocks. The switching device could be fabricated by either microfabrication method or additive manufacturing method (Figure 6H). Design and fabrication of a novel actuation mechanism using
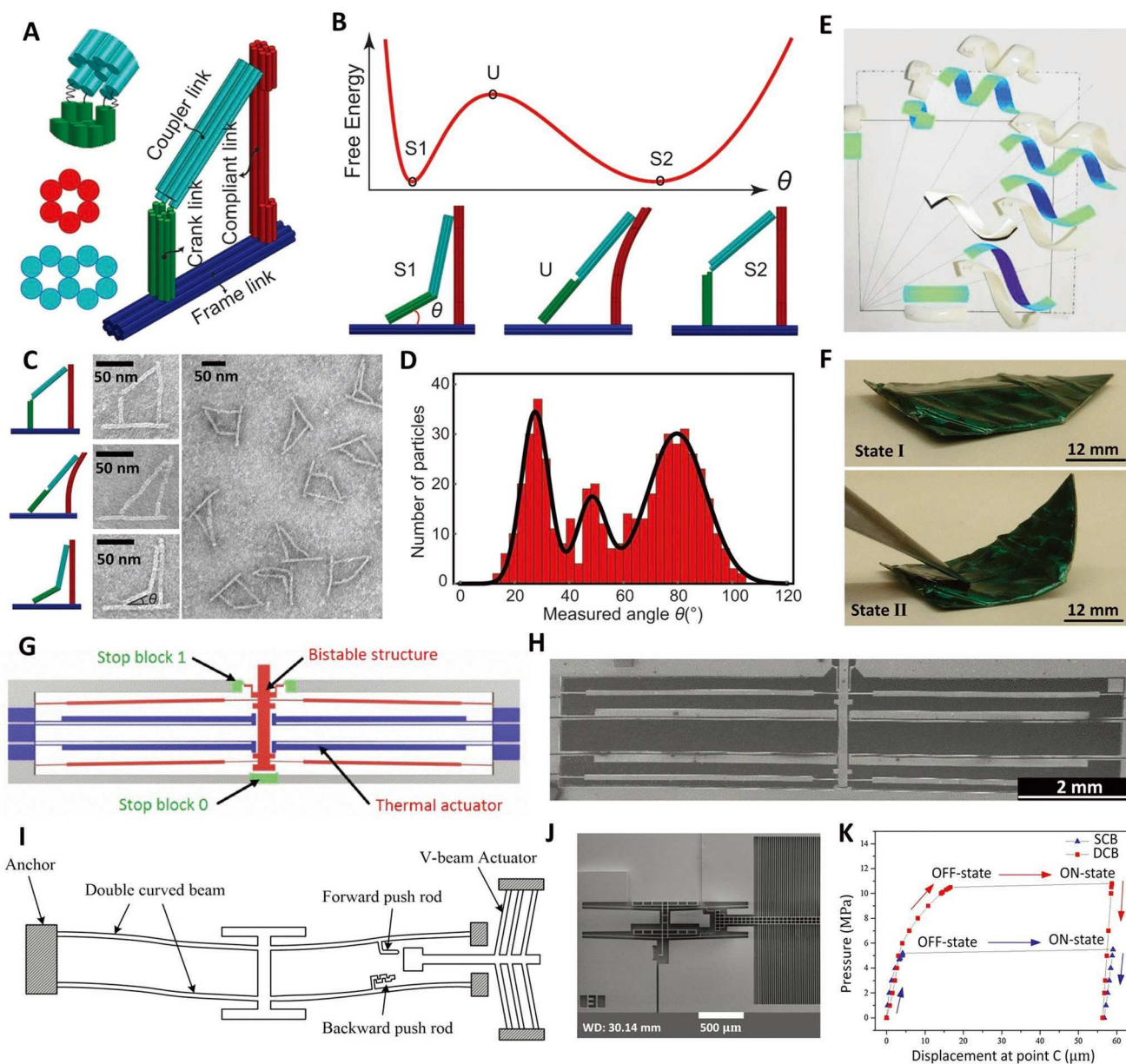
Figure 6. Bistable structures for microrobotics and MEMS. A) Schematic illustration of a compliant DNA bistable nanostructure made of four links with helix bundles (hb). B) The energy plot of the bistable nanostructure: two stable states (S1 and S2) and one unstable state (U). C) TEM images of the designed bistable DNA structures, showing most of the structures are in their stable states (either S1 or S2). D) Distribution of the state configurations in terms of the angle between the frame link and the crank link, confirming that most of the particles stay in their stable states. Reproduced with permission.[89] Copyright 2015, American Chemical Society. E) Helix structured ribbons made by bonding two or three layers of strips with different anisotropic prestrains. F) Two stable configurations of a triangular piece of slap bracelet made of layered stainless steel wrapped by a fabric cover. Reproduced with permission.[92] Copyright 2013, IEEE. G) Schematic design of a thermally actuated bistable microswitching device. The top and bottom blocks act as a stopping mechanism for the microrobotic system. H) Image of a microfabricated bistable structure with thermal actuators and stopping blocks. Reproduced with permission.[8] Copyright 2019, Springer Science + Business Media. I) A moment-driven bistable microdevice with a curved-beam structure and a V-beam actuator. The forward and backward push rods make the switching possible via a single actuator in the absence of a stopping mechanism. J) SEM image of the fabricated microdevice. K) The pressure-displacement plot of a single curved beam (SCB) and a double curved beam (DCB) micro-actuator. As applied pressures reach the critical values, the snap-through occurs, and the bistable device switches to the ON-state. Reproduced with permission.[99] Copyright 2020, Elsevier.

a similar bistable structure were also proposed for microrobotics.[96,97] The electrothermally actuated bistable module could be optimized for use in a digital microrobotics system.[98] Also, Huang et al. designed a moment-driven bistable microdevice

with a curved-beam structure and a V-beam actuator (Figure 6I,J).[99] The forward and backward push rods made the switching possible via a single actuator with no need for a stopping mechanism. The V-beam electrothermal actuator drove

**ADVANCED
SCIENCE NEWS**

www.advancedsciencenews.com

**ADVANCED
FUNCTIONAL
MATERIALS**

www.afm-journal.de

the forward and backward pushrods to make the bistable arch beams generate reversible snap-through motions. Figure 6K shows the pressure-displacement relations of the snap-through deformations for the ON and OFF states of a single curved beam and a double-curved beam microactuator.

Additionally, many researchers also explored bistable structures for multifunctional MEMS use. For example, a clamped-clamped arch microbeam was designed to serve as a MEMS actuator and pressure sensor.[46] The arch beam accommodated between two electrodes had two stable states. The bottom driving electrode was activated by a DC voltage superimposed with an AC signal so that the beam could switch between its two stable states in a forward/backward frequency sweep, which could be detected by the topside sensing electrode powered by a DC voltage when the capacitance changed between the arch beam and the fixed electrode. In another study, Ouakad et al. performed theoretical and experimental analysis for a MEMS shallow arched beam to investigate its dynamic snap-through behaviors for filtering applications.[100] Several sharp amplitude jumps were observed for the microbeam actuated near its first and third natural frequencies. Thus, the dynamic snap-through behavior observed at certain frequency bandwidths can be potentially used for band-pass filters with a sharp transition from a passband to a stopband. Most recently, multistability designs based on bistable ferroelectric materials were studied to fabricate multistate memories with significantly high storage capacity.[2]

4. Bistable Structures for Programmable Materials/Metamaterials

Programmable structures such as origami-based structures and metamaterials have unique engineering properties including auxeticity (negative stiffness), deploy-ability, self-locking, and foldability.[10,101–104] **Figure 7**A illustrates an origami-based cube pipe structure capable of forming multiple stable configurations.[105] The unique structure consisted of six cube pipes made of polyethylene terephthalate (PET) with their hinge sections bonded with carbon fiber reinforced polymer (CFRP) shells. The shells were reconfigurable between stable states via snap-through deformation when subjected to a magnetic force on the curved edges of the pipe (Figure 7B), indicating the potential applications for non-contact smart valves. Another similar study on origami tubes with reconfigurable polygonal cross-sections was also introduced for smart pipes and microrobotics applications.[106] The foldability of origami structures enabled the shape changes of the tubes for smart functional applications. For example, Silverberg et al. used hidden DOFs to create unique features in origami structures for bistability enhancement that can be potentially used in soft grippers.[107]

Recently, Vangelatos et al. designed an architected 3D buckling structure for multistable functional materials[102] (Figure 7C). The microscale truss-based structure with bistable elements could help mechanical behavior improvement (e.g., auxeticity and yielding strength) in four different design sets (Figure 7D). It is demonstrated that an optimized lattice design could generate internal buckling in the structure to enhance

its mechanical strength. Gillman et al.[108] investigated the nonlinear behavior of origami structures using a truss-based finite element model to understand the bifurcation and limit point instabilities of truss-based origami structures. They developed a theoretical framework in global coordinate system to accurately capture the nonlinear deformations and energy states of the multistable structure, resulting in a better prediction of the bifurcation points and folding paths within the system.

In a recent study, Kamrava et al. presented a novel cellular metamaterial consisting of origami building blocks.[10] By using nonlinear phenomena of origami structures, they constructed cellular elements that have highly nonlinear auxeticity, bistability, and locking behaviors. Figure 7E illustrates the first-order and second-order elements used in building the origami-based cellular metamaterials. Different possible arrangements of a cellular structure can be constructed by the basic elements to be either locked or foldable structures in one direction (Figure 7F). Bistable auxetic metamaterials capable of holding their deformed shape after being unloaded was proposed by Rafsanjani and Pasini.[109] They demonstrated that the expandability, negative Poisson's ratio, and bistability of the auxetic metamaterials could be well controlled by its structural geometry.

Origami and truss-based structures have also been utilized for locomotion and robotic applications.[103,110–113] An origami skeleton mechanism was demonstrated to create peristaltic-like locomotion by exploiting the multistability of the structure.[110] In this study, two bistable Kresling origamis were combined into a drive module to create an actuation cycle without the need for multiple actuators or a complex design. Interestingly, Pagano et al. designed a crawling robot based on origami structure[111] and showed that the crawling robot has the advantage of low power consumption with a simple controlling mechanism by using the structural bistability in the system.

At nanoscales, fluid dynamics such as evaporation have been explored for the actuation of the bistability of composite materials.[114,115] A crumpled graphene/Carbon Nanotube composite nanoparticle with large-accessible-space and high-mechanical-strength was fabricated by encapsulating carbon nanotubes (CNTs) with graphene sheets using solvent evaporation-induced assembly.[115] This method provides a facile approach to control the states of crumpling and assembling of CNTs and graphene composite nanoparticles by liquid evaporation in a large-scale and time-efficient manner.

5. Bistable Structures for Energy Harvesters

High levels of energy consumption along with the growing environmental concerns about fossil fuels have made researchers focus on harvesting energy from other sources types. Among those alternatives, mechanical vibration has played a significant role in the past decades due to the rapid advances in material science and advanced manufacturing methods. Vibration energy harvesting systems are potential candidates to replace lithium batteries and solar cells due to their ubiquitousness and high accessibility. However, so far, several limitations such as low-output density and limited frequency bandwidth are the major reasons for such devices not being able to compete with
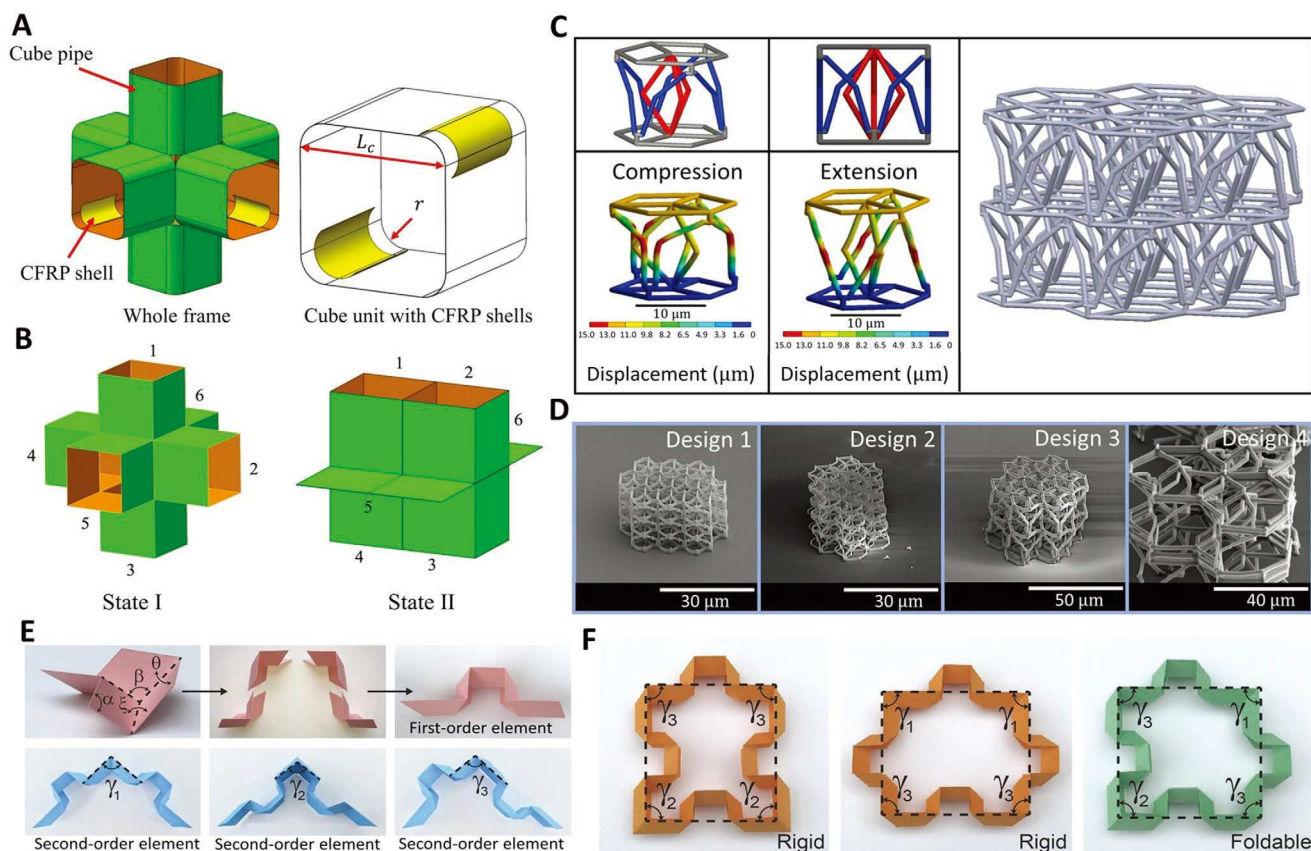
**ADVANCED
SCIENCE NEWS**
www.advancedsciencenews.com

**ADVANCED
FUNCTIONAL
MATERIALS**
www.afm-journal.de

Figure 7. Bistable structures for programmable devices/metamaterials. A) Schematic view of an origami-based programmable cube. The carbon fiber reinforced polymer (CFRP) shells are attached at the hinge sections of the cube pipe. The CFRP shells are bistable structures designed to be actuated by electromagnetic forces. B) Schematic illustration of the two stable states of a designed cube pipe. Reproduced with permission.[105] Copyright 2019, IOP Publishing. C) A microscale truss-based designed structure with bistable elements for mechanical behavior improvement, such as auxeticity and yielding strength, as a unit cell (left figures) and an assembly set (right figure). D) SEM images of the as-fabricated periodic structures consisting of 3D truss-based unit cells in four different design sets. Reproduced with permission.[102] Copyright 2019, Elsevier. E) The first-order and second-order elements used in developing an origami-based cellular metamaterial. Metamaterial constructed elements made from origami building blocks providing different engineering behaviors including bistability, foldability, auxeticity, and self-locking properties. F) Possible closed-loop elements formed by second-order units for either rigid or foldable geometry. Reproduced with permission.[10] Copyright 2017, Nature.

the other types of generators in the energy-consuming industries. Bistable and/or multistable structures have been extensively studied for energy harvesting as a promising alternative solution for such issues.[3,116–118] Significant progress is made in developing new structures and improving the output power of the devices. In this section, we review the representative bistable and multistable structures used in different kinds of energy harvesters.

5.1. Energy Harvesters Based on Mechanically Driven Bistable Structures

Figure 8A shows a simple harvester made of bistable inverted beam and an end mass.[119] The tip mass enables the bistability of the vertical cantilever beam under horizontal harmonic excitation. As a result, the bending of the cantilever beam drives the piezoelectric patches bonded on the beam to generate electricity. Friswell et al. studied the effect of the key parameters on the dynamic response and output power of the system,

including tip mass, load resistance, base amplitude, and frequency. As described in Figure 8B,C, the tip mass significantly affects the first natural frequency and bifurcation behavior of the harvester, thereby the energy harvesting performance of the harvester.

More recently, Van Blarigan and Moehlis studied the dynamic behaviors of a buckled asymmetric piezoelectric beam for energy harvesting.[120] In their work, the asymmetric buckled beam was made of a single layer and a bimorph layer. The snap-through behaviors of the beam and its transition from monostable to bistable motions were studied. Their results demonstrated the chaotic attractors related to period-doubling behavior, resulting in a much higher bandwidth of frequency compared to typical linear systems. Different from the horizontal vibration actuation, Garg and Dwivedy proposed a fixed-end beam energy harvester with one longitudinal moving end attached to a tip mass.[121] They investigated the nonlinear dynamics of the fixed beam and found that, based on the exciting frequency range, the resonance frequency of the system can be tuned by adjusting the tip mass and external
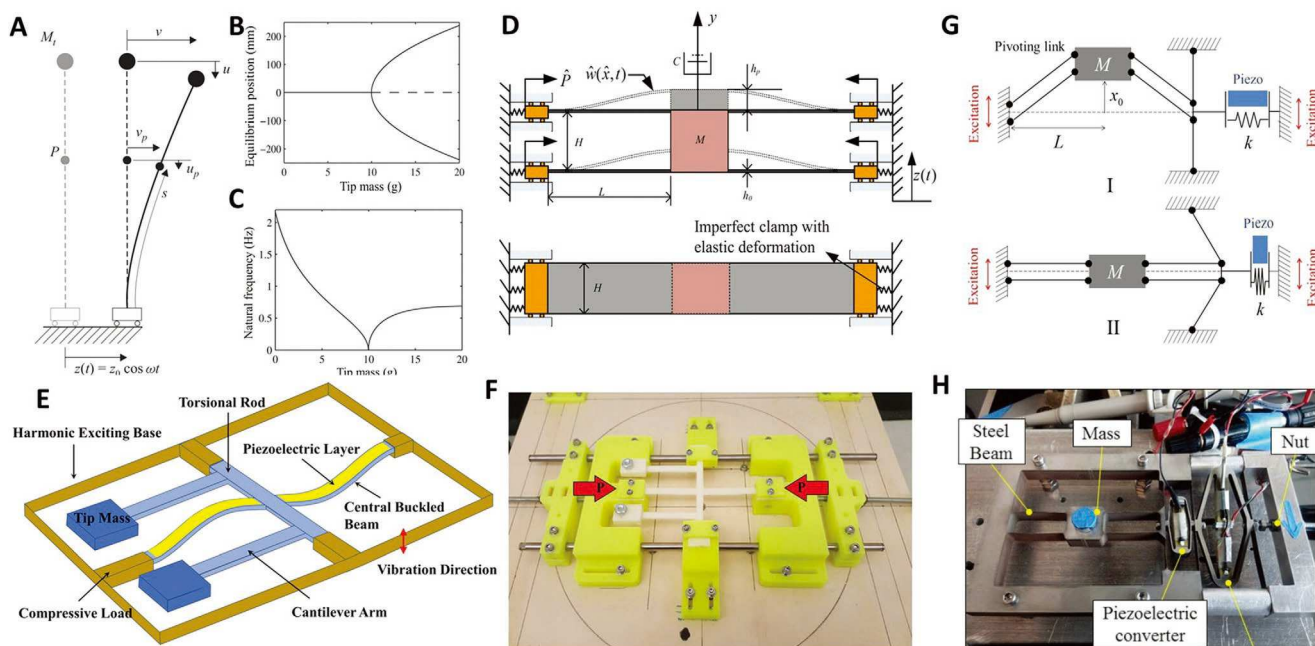
Figure 8. Mechanically driven bistable energy harvesters. A) Schematic illustration of an inverted beam harvester. The vertical cantilever beam has a tip mass to enable bistability under horizontal harmonic excitation. Piezoelectric patches are placed along the beam. B) The effect of the tip mass on the equilibrium position of the inverted beam harvester. The dashed line denotes unstable equilibrium positions. C) The effect of the tip mass on the natural frequencies for the stable equilibrium positions. Reproduced with permission.[119] Copyright 2012, SAGE Publishing. D) A bistable oscillator consisting of double buckled beams with a central mass mounted on elastic boundary conditions, in which the elastic boundary enhances the snap-through performance. Reproduced with permission.[122] Copyright 2016, IOP Publishing. E) Concept design of a unique bistable energy harvester made of a central compressive beam, a torsional rod, and two cantilevers with end masses. The cantilever arms enable snap-through motions, thereby expanding the frequency range of harvesting operation. F) The experimental setup of the bistable energy harvester mounted on a shaker table. The compressive load applied by the relative motion of the two end fixtures. Reproduced with permission.[123] Copyright 2019, Springer Nature. G) Schematic diagram of a bistable energy harvester made of a mass connected with several rigid links, demonstrating two stable states (I) and (II). (H) The experimental setup of the linkage-based mechanism with a piezoelectric generator for energy harvesting. Reproduced with permission.[124] Copyright 2019, IOP Publishing.

load. For instance, under the super-harmonic resonances, the operational frequency bandwidth of the beam can significantly increase, benefiting potential vibration energy harvesting.

Liu et al.[122] studied a nonlinear bistable oscillator made of double buckled beams with a central mass and elastic boundary conditions (Figure 8D). Based on the extended Hamilton principle, they proposed an analytical model using the Galerkin approach and showed that the clamped stiffness had a significant effect on the first mode, a moderate effect on the third mode, while no effect on the second mode. The proposed bistable harvester can broaden the operational frequency range compared to the similar linear ones. Furthermore, the elastic clamped boundary condition could be modified to improve the snap-through performance, providing new opportunities for designing bistable harvesters for vibration energy harvesting. Derakhshani et al. designed a coupled bistable structure consisting of a central buckled beam, a torsional rod, and two cantilever arms with end masses for low-frequency vibration energy harvesting (Figure 8E,F).[123] The large vibrational motions induced in the cantilever arms generated a torsional moment in the middle rod, then transferred to the central buckled beam to induce a bistable motion at the low-frequency ranges (≤30 Hz). A more accurate theoretical analysis of the nonlinear system under harmonic excitations was performed based on a component coupling approach. Special attention should be paid in the optimization of the design because

there was a tradeoff between the induced buckling level and the maximum outpower of the device.

As shown in Figure 8G, a unique linkage design was proposed for a piezoelectric bistable energy harvester to elevate the snap-through motion as the system vibrates in the vertical direction.[124] The effects of the different parameters, including load resistance, mass, stiffness, and buckling level was studied through a new theoretical model. The prototype of the harvester used lead zirconate titanate (PZT) ceramic as the piezoelectric converter (Figure 8H). The study revealed that a wider frequency bandwidth could be achieved by increasing inertial mass, adjusting stiffness to fit the frequency range on the potential frequency source, or increasing the initial stable position to cover the overlap area between the first harmonic and the following subharmonic resonances. The performance of the bistable harvester could be further optimized by adjusting the impedance match with the piezoelectric converter to maximize the outpower. In addition, Ando et al. proposed a snap-through buckling (STB) harvester made of a buckled beam with a mass located between two piezoelectric harvesters,[125,126] generating a power up to 155 Mw at the input frequency of 5 Hz. Differently, Emad et al.[127] investigated a nonlinear doubly clamped polyvinylidene fluoride (PVDF) beam with induced stretching strain for energy harvesting and found that the stretching strain can eliminate the need for a structural substrate in the design.

5.2. Energy Harvesters Based on Magnetically Driven Bistable Structures

The main advantage of using magnetic forces for bistable energy harvesters is their high reliability to create double-welled potential systems. However, the design complexity and the need for external sources (e.g., permanent magnets) have limited their applications, in particular for MEMS and small-scale devices.[3,117] The main focuses in developing bistable energy harvesters are to broaden the frequency bandwidth and to accommodate the ambient vibration sources.[128,129] **Figure 9**A shows a bistable dual piezoelectric cantilever energy harvesting system (DPEHS) for realistic ambient vibrations.[130] In this design, the magnetic repulsive force between the two permanent magnets fixed on the tip of the cantilevers enabled the bistability of the system. The energy harvesting performance of DPEHS could be analyzed by a single degree-of-freedom (DOF) vibrational model (Figure 9B,C) that was

excited by the pink noise with intensive variations. Compared to the rigidly supported PEHS for ambient noise inputs,[131,132] the elastically supported PEHS demonstrated a superior performance under pink noise vibrations with either constant or varying intensity.

In another representative study, Yan et al. designed a bistable piezoelectric vibration energy harvester (Figure 9D) with ultra-broadband harvesting performance at low-frequency ranges.[6] The vertically placed cantilever beam has a tip magnet to repulsively interact with the other two permanent magnets fixed on the stage. Using the harmonic balance method, they developed an electromechanical coupled distributed parameter model to analyze the harvester system. Their results showed that both cubic magnetic coefficient and electric inductance can significantly improve the operational bandwidth of the harvester by creating multiple resonances and hardening or softening phenomena (Figure 9E), leading to a high-performance energy harvester suitable for a higher operating frequency of up to 40 Hz.
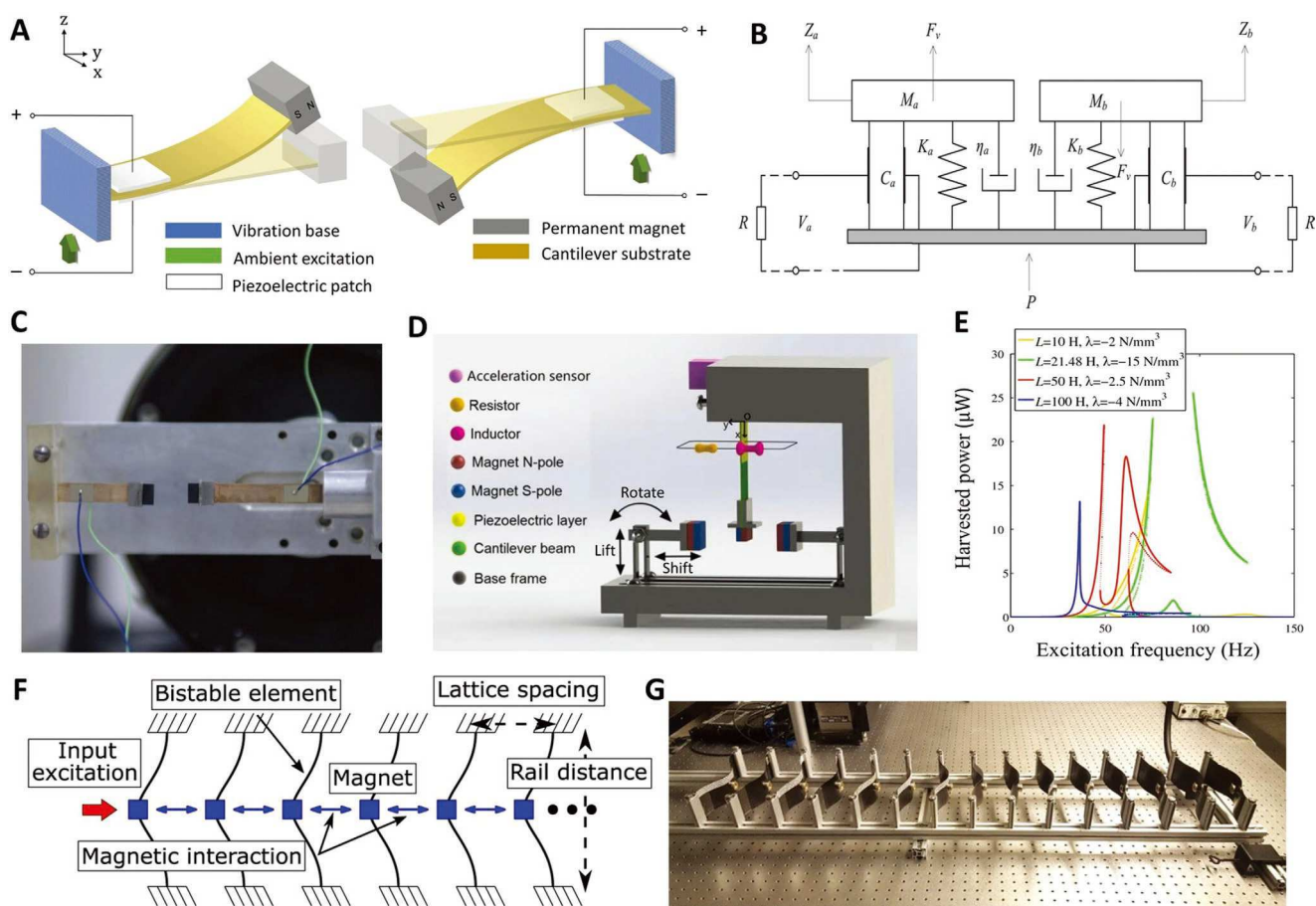

Figure 9. Magnetically driven bistable energy harvesters. A) Schematic illustration of a bistable energy harvester made of dual piezoelectric cantilevers. The bistable state change is driven by the repulsive magnetic interaction between the cantilevers tip masses. B) The equivalent single degree-of-freedom (DOF) model of the bistable harvester in (A). C) The experimental setup of a dual cantilever bistable energy harvester. Reproduced with permission.[130] Copyright 2016, IOP Publishing. D) Schematic diagram of a piezoelectric bistable energy harvester with nonlinear magnetic interaction. E) Output power-frequency response of the harvester shown in (E) with multi-hardening and multi-softening behaviors, indicating a wider range of operational frequency. Reproduced with permission.[6] Copyright 2020, Springer Nature. F) Schematic illustration of an energy harvester consisting of bistable lattice structures. The bistable unit cells are made of piezoelectric transducers and are serially connected on a frame. The magnetic interactions between the bistable cells induce the force transfer and snap-through motion. G) Experimental setup of the bistable lattice. Reproduced with permission.[139] Copyright 2018, Nature.

**ADVANCED
SCIENCE NEWS**
www.advancedsciencenews.com

**ADVANCED
FUNCTIONAL
MATERIALS**
www.afm-journal.de

A mechanical adaptation was also introduced to a bistable magnetic-based piezoelectric energy harvester to improve the operational frequency bandwidth and the power output.[133] For example, a bistable harvester was made of a cantilever beam with a tip magnet interacting with another permanent magnet. The fixed permanent magnet was loaded on a spring while its motion was restricted in one-direction to improve the overall performance of the harvester. Adjusting the repulsive force between the cantilever tip magnets and the spring-loaded one enabled the bistability at low-frequency base excitations, which improved the operational frequency bandwidth and the output power of the bistable harvester.

Other approaches for improving the frequency bandwidth of magnetic-based bistable energy harvesters have been considered, including a 2-DOF cantilever bistable harvester,[134] an elastic magnifier to amplify the base excitation,[135] new arrangements to reduce the potential barrier of bistable harvesters,[136,137] and creating asymmetry in the potential functions of a bistable structure.[138] One remarkable example is a 1D lattice energy harvester shown in Figure 9F.[139] The energy harvesting system consisted of serially connected bistable elements. Each element was made of two buckled beams and one attached central magnet for transferring the snap-through motion between the biostable elements. This design has the merits of input-independent dynamics, extreme directionality, and topological energy harvesting characteristics, and has the potential to be used for building intelligent metastructures for damping and/or harvesting the unwanted energy under sudden abrupt shock inputs such as blasts or earthquakes.

Another remarkable work is a compact and flexible non-beam type bistable vibration energy harvester designed by Deng et al.[140] The energy harvesting system was made of a flexible bellows tube, an annular permanent magnet, an aluminum frame, PVDF film as the piezoelectric element, and two rectangular magnets to interact with the annular magnet for enhancing the bistability properties. The flexible bellows-type structure not only improved the energy harvesting performance of the device at low frequencies but also resolved the stress-concentration issue associated with typical beam-type structures.

5.3. Energy Harvesters Based on Thermally Driven Bistable Structures

Thermally-induced bistable structures are typically composite of several layers stretched and laminated along perpendicular directions so that they can be actuated by residual stresses induced by a thermal process for switching between two stable states.[141,142] For example, Tao et al. designed a thermally induced bistable plate made of functionally graded carbon nanotube-reinforced composite (FG-CNTRC) and piezoelectric films for energy harvesting applications (**Figure 10**A).[7] They studied the bistability and dynamic response of the energy harvester by applying a thermal field and harmonic excitations (Figure 10B). Compared to a linear plate, the nonlinear bistable composite plate can generate a wider frequency bandwidth and better output performance by softening behavior and snap-through motions. Furthermore, FG plate volume fraction could significantly affect the dynamic response of the system,

and a reduced volume fraction resulted in a low requirement of base excitation for snap-through motions. In addition, Harris et al. proposed a cantilever bistable energy harvester made of laminates and a macro fiber composite (MFC) patch as the piezoelectric generator (Figure 10C).[143] The laminate beam possessed asymmetric bistability, and thereby exhibited non-linear features such as softening behavior and superharmonic resonances, leading to a variety of motion types from chaotic to harmonic snap-through motions (Figure 10D–F). They found that the presence of superharmonic resonances in a bistable harvester would induce snap-through motions at the low-frequency ranges, which may be used for optimizing the energy harvesting structures.

MFCs have also been utilized to combine with bistable laminates for broadband energy harvesting due to their ease of manufacture, reliability, and relatively high piezoelectricity.[144–146] For instance, Lee and Inman analyzed the nonlinear behaviors of a rectangular bistable laminate paired with MFC films for energy harvesting.[145] In their study, elastic potential energy characteristics and snap-through behaviors of the bistable plate under harmonic excitations were investigated.[144] In another study, Betts et al. considered a bistable composite with attached piezoelectric patches to harvest energy from ambient vibrations.[147,148] As shown in Figure 10G, four piezoelectric patches were attached to the composite plate where the plate was fixed on its corners. Parametric studies were performed for optimal configurations to maximize the energy harvesting performance. The key parameters included the ply orientations, piezoelectric surface area, and geometry of the plate. For example, larger piezoelectric patches could generate higher output power but sacrifice the structural compliance, thereby reduced the laminate curvature and the stress along the polarization direction of the plate.

Recently, multifunctional bistable structures to combine vibration isolation and energy harvesting have also been studied. For example, Lu and coworkers[149] proposed a bistable piezo-composite plate to simultaneously work as a vibration isolator and an energy harvester (Figure 10H). The multifunctional device was made of a central mass connected to a composite laminate with negative stiffness and a steel plate with positive stiffness. A piezoelectric strip was bonded onto a nonlinear composite laminate made of metal and carbon fiber layers. The bistable composite plate with a negative stiffness reduced the whole stiffness of the structure and consequently facilitated the transmissibility reduction, especially at higher frequency ranges. The transmissibility of the bistable structures could be reduced by 23 dB at 100 Hz while it adversely affected the energy harvesting performance.

6. Bistable Structures for Energy Absorption

Energy absorption of dissipation has attracted increasing attention due to its intensive use in a variety of applications such as structural damping, energy transferring devices, and acoustics. Recent advances in manufacturing and materials science enable structural bistability to be implemented as a promising low-cost feature for energy absorption applications. **Figure 11**A shows a possible mechanism of trapping elastic energy through

ADVANCED
SCIENCE NEWS
www.advancedsciencenews.com

ADVANCED
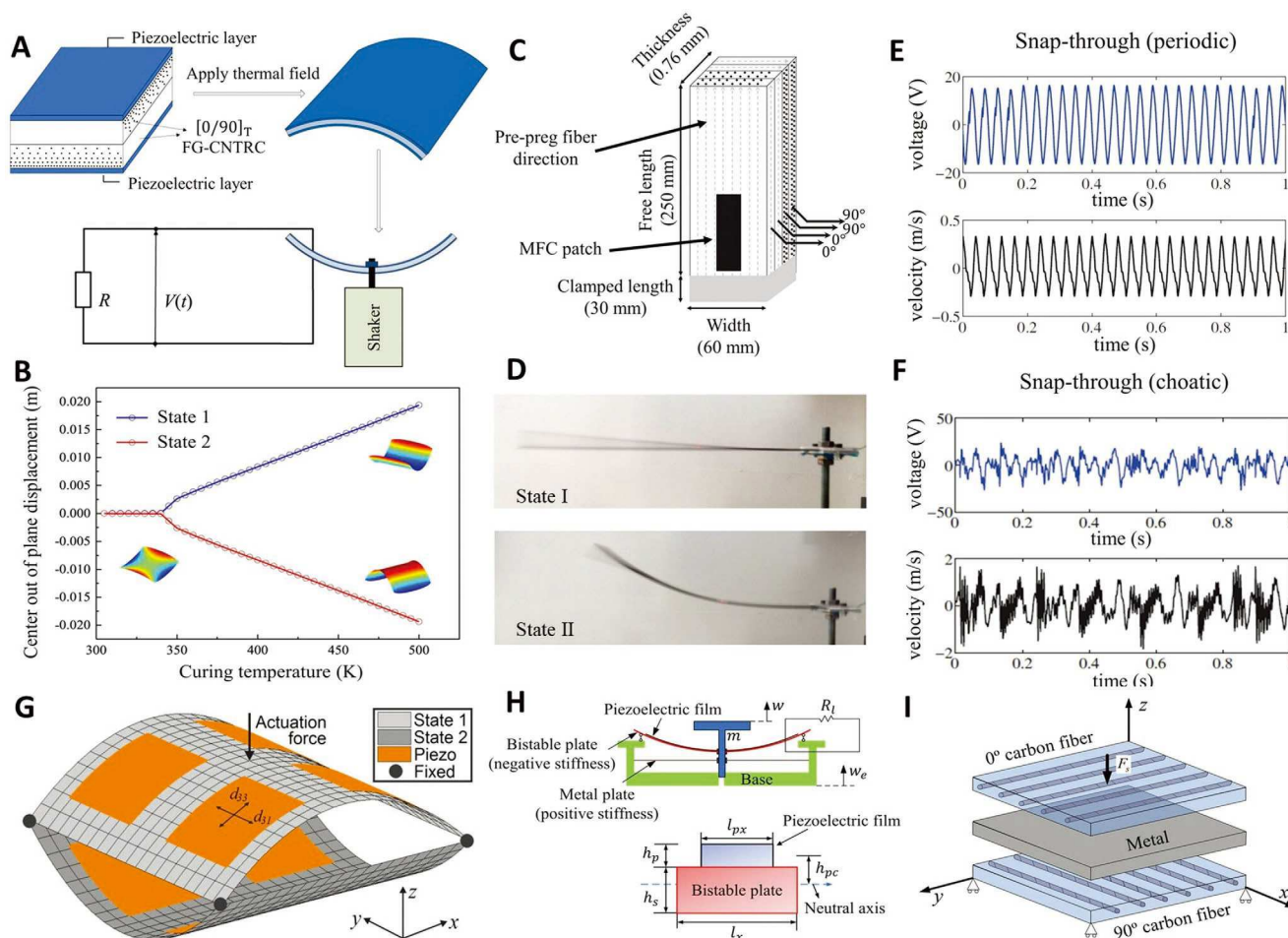**FUNCTIONAL**
MATERIALS
www.afm-journal.de

Figure 10. Thermally driven bistable energy harvesters. A) Schematic of a bistable energy harvester driven by thermal energy. It is fabricated by laminating functionally graded carbon nanotube reinforced composite with piezoelectric patches, achieving bistable change when heated up and cooled down. B) The bifurcation plot obtained by FE modeling of the FG plate under different curing temperatures. Reproduced with permission.[7] Copyright 2019, IOP Publishing. C) Schematic of a cantilever energy harvester consisting of a bistable laminate and a macro fiber composite (MFC) strip. The composite laminate generates bistable deformation under thermal actuation. D) Experimental setup of the bistable harvester, exhibiting local vibrations at its two stable states. Real-time velocity and voltage response of the bistable harvester excited by an acceleration of 4 g at two different frequencies: E) 25 Hz for periodic snap-through motion, and F) 17 Hz for chaotic snap-through motion. Reproduced with permission.[143] Copyright 2016, Springer Science + Business Media. G) Schematic of a bistable composite laminate with four piezoelectric patches attached for energy harvesting. The two laminates are bonded at the four corners and the bistability is achieved via a thermal process. Reproduced with permission.[147] Copyright 2012, AIP Publishing. H) Schematic view of a multifunctional device for vibration isolation and energy harvesting. The bistable piezo-composite plate is combined with a metal plate for negative and positive stiffness, respectively. I) Configuration of the different layers of the bistable composite laminate structure. Reproduced with permission.[149] Copyright 2019, SAGE Publishing.

the deformation of a tilted beam.[150] This unique mechanical energy trapping method stems only from the structural geometry of bistable elements and can be used in energy absorption packages. Based on the energy principle, various designs for 1D, 2D, and 3D architectured materials with embedded flexible bistable elements and rigid parts were developed (Figure 11B). For instance, Bertoldi et al. investigated the influence of the different parameters on energy absorption performance, including the tilting angle θ and the beam slenderness t/l. The energy absorbed by the system and the energy to snap back to its undeformed shape could be adjusted by tailoring θ and t/l, which allowed the beam to either remain in its deformed shape or restore to the initial shape according to the specific application requirements.

There are several other interesting studies to introduce a structural lattice for energy absorption by exploiting bistability behaviors and local snap-through motions.[151–155] For example, Tan et al.[151] proposed a reusable metamaterial structure with negative stiffness (NS) properties for energy dissipation. Unlike previous studies with elastic deformation,[156–158] this study considered energy dissipation via plastic deformation. They performed cyclic compression tests to examine the reusability of the structure. Experimental results showed that the energy absorption capacity can be improved by lowering the local energy barriers through increasing the thickness to length ratio of the beam or reducing the buckling height. Figure 11C shows a bistable tetra-beam-plate unit cell and a 3D lattice made of several single-unit cells for energy absorption use.[153] Through the
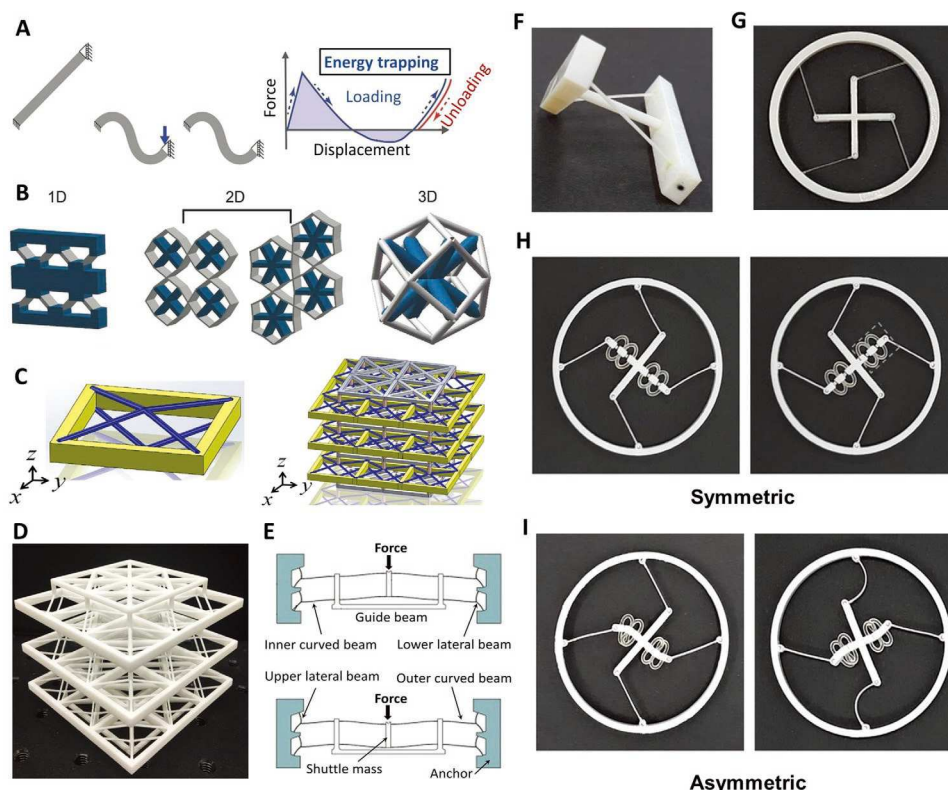
**ADVANCED
SCIENCE NEWS**
www.advancedsciencenews.com

**ADVANCED
FUNCTIONAL
MATERIALS**
www.afm-journal.de

Figure 11. Bistable structures for energy absorption. A) Schematic diagram of an elastic beam capable of energy absorption. After bending of the tilted beam, it remains in its deformed shape with potential energy trapped after unloading. B) Schematic illustrations of 1D, 2D, and 3D multistable structures capable of energy absorption. The gray and blue colors indicate the elastic bistable beams and rigid supports, respectively. Reproduced with permission.[150] Copyright 2015, Wiley-VCH. C) Schematic illustration of a tetra-beam-plate unit cell and a 3 × 3 × 3 lattice consisting of the unit cells for energy absorption. The bistability of the inclined beams on the rigid frame allows energy absorption. D) A 3D-printed prototype of the 3 × 3 × 3 lattice in (C) using polyamide (PA) for energy absorption. The length of each side is about 70 mm. Reproduced with permission.[153] Copyright 2018, Elsevier. E) Schematic illustration of a bistable structure for force regulation and overloading protection. The designed structure acts as a protection mechanism against high impact forces by snap-through from its initial state to an overloaded stable state. Reproduced with permission.[160] Copyright 2013, Elsevier. F) A 3D-printed twisting bistable structure. G) A 3D-printed rotational bistable structure. H) The two stable states of a tunable rotational bistable structure in a symmetric configuration. I) The two stable states of a tunable rotational bistable structure in an asymmetric configuration. Reproduced with permission.[162] Copyright 2019, Nature.

negative stiffness induced by the local snap-through deformations of the flexible beam elements, energy dissipation in a unit cell was achieved when the lattice was loaded by a compressive force (Figure 11D). The parametric analysis revealed the effects of the slenderness and tilting angle of bistable beams on the energy absorption capacity of a unit cell. The unit cells in the 3D lattice resulted in multiple energy gaps in the force-displacement plots, each of which had a certain energy trapping capacity.

Foroutan et al. recently designed a linear structure for energy absorption by coupling a tuned bistable nonlinear energy sink (TBNES) containing local potentials[9] and developed a semi-analytical model for analysis. Such a structural design can improve energy absorption performance by expanding the system's local potentials at the second mode interaction. Another theoretical study was performed on a novel adaptive bistable energy absorption mechanism,[159] in which two mainsprings were arranged on elastic boundaries for achieving tunable bistability. This adaptive design was found to outperform conventional bistable wave energy absorbers by adjusting the potential energy barrier to make it suitable for both low-amplitude and high-amplitude excitations.

Linkage-based mechanisms are another type of load-protecting system in which bistability can be used for controlling both impacts and quasi-static external forces. For example, Wang et al. designed a constant force bistable micromechanism (CFBM) for load regulation[160] (Figure 11E). A set of curved beams with flexible end fixtures enabled the snap-through deformation between its stable states for load distribution. Similarly, Cherkaev et al. proposed an impact protective structure consisting of bistable links as a shock resistance mechanism.[161] In their structure, the yielding behavior of certain links in the system (sacrificial links) was utilized as a protection for the active bistable links to improve energy absorption capacity.

The key to structural bistability in energy absorption applications is to tune the energy barrier of the system to generate adjustable snap-through transitions before the materials reach their yielding strength. In a recent study, Jeong et al. designed tunable twisting and rotational bistable structures for lowering the energy barrier level required for snap-through motions (Figure 11F,G).[162] They demonstrated that adjusting bistable structures and material properties could result in asymmetric potential energy for desired snap-through transitions.

**ADVANCED
SCIENCE NEWS**
www.advancedsciencenews.com

**ADVANCED
FUNCTIONAL
MATERIALS**
www.afm-journal.de

Figure 11H,I shows the two different stable states of the 3D-printed twisting mechanisms in the symmetric and asymmetric configurations. Tuning the energy barrier height and creating asymmetric potential wells in the potential energy plot were achieved by adjusting the length of the central link or imposing geometrical asymmetry in the mechanism, respectively. Such adjustable mechanisms could be used for switching actuators and energy absorbers.

7. Conclusion and Outlook

In summary, structural bistability has been widely used for various advanced functional systems due to snap-through and the corresponding dramatically geometrical change and potential energy change. Based on the type of applications, we categorized bistable structures as actuators, robotics and MEMS, programmable devices and metamaterials, energy harvesters, and energy absorbers and discussed the strategies used in these advances. Such strategies not only reflect the rational yet straightforward ideas, i.e., adoption of more powerful smart materials, along their emergence, into bistable structures to fulfill versatility, but also reveal the gaps among materials, structures, and functions.

While smart materials responsive to physical stimuli such as electric and magnetic fields, temperature change, and pH have demonstrated superiority over conventional materials in bistable structures, those applications are at the stage of proof-of-concept with significant drawbacks, including slow responsiveness, low sensitivity, and no reported selectivity. More physical stimuli (e.g., light, humidity, specific molecules) responsive smart materials have yet found their applications with bistable structures. Theoretical investigations on the response behaviors of bistable structures under various external stimuli have provided essential guidelines for their versatile applications. However, most studies have utilized only simple bistable structures, e.g., beams and shells/laminates, and taken little advantage of advanced structures enabled by additive manufacturing technologies in achieving advanced functions. Reliable and reversible snap-through of bistable structures in both design and manufacturing aspects is still challenging and problematic. In addition, little effort is taken to explore advanced bistable structures while beams and laminates have been exhaustively investigated theoretically and numerically. It is worth noting the pivotal role of mechanics in designing bistable structures, the snap through transition of which is essentially deformation/displacement under external applied forces and internal forces induced by physical stimuli. It is expected that the development of smart materials and advanced bistable structures and their elegant combinations will be general research opportunities.

Function-/application-oriented modification of bistable structures for real-life applications is where innovation lies. For example, it will be attractive to invent new bistable structures that can effectively respond to ambient low-intensity and low-frequency vibrational sources or low activation forces for actuators and robotics. Innovative theoretical and experimental studies for bistable laminates or composites are also highly desired for developing morphing structures and broadband energy harvesters used in aerospace, automobile, and wind energy

applications. Additionally, multiscale and multifield modeling of bistable structures are still challenging and open areas for research. The rapid advances in manufacturing technologies, for instance, 3D/4D printing, will facilitate the design and fabrication of advanced bistable structures at both macro and micro scales. The accurate control of materials properties, orientation, location in the fabrication process of novel structures will enable the control of bistable threshold as necessary. Another attractive point is assigning innovative functions to bistable structures, e.g., programmable materials, metamaterials, sensing/memory devices[45] and logic controller[163] as George Whitesides and his coworkers did where they rendered a bistable actuator function as an autonomous controller for soft robots.

Conflict of Interest

The authors declare no conflict of interest.

[1] R. L. Harne, K.-W. Wang, *Harnessing Bistable Structural Dynamics: For Vibration Control, Energy Harvesting and Sensing*, John Wiley & Sons, Hoboken, NJ **2017**.
[2] A. Ghosh, G. Koster, G. Rijnders, *Adv. Funct. Mater.* **2016**, *26*, 5748.
[3] R. L. Harne, K. Wang, *Smart Mater. Struct.* **2013**, *22*, 023001.
[4] X. Sun, Y. Zhang, D. Kennedy, *Nonlinear Dyn.* **2019**, *95*, 3205.
[5] H. Shao, S. Wei, X. Jiang, D. P. Holmes, T. K. Ghosh, *Adv. Funct. Mater.* **2018**, *28*, 1802999.
[6] Z. Yan, W. Sun, M. R. Hajj, W. Zhang, T. Tan, *Nonlinear Dyn.* **2020**, *100*, 1057.
[7] J. Tao, X. He, S. Yi, Y. Deng, *Smart Mater. Struct.* **2019**, *28*, 095021.
[8] M. Ben Salem, H. Hussein, G. Aiche, Y. Haddab, P. Lutz, L. Rubbert, P. Renaud, *J. Micro-Bio Rob.* **2019**, *15*, 65.
[9] K. Foroutan, A. Jalali, H. Ahmadi, *J. Sound Vib.* **2019**, *447*, 155.
[10] S. Kamrava, D. Mousanezhad, H. Ebrahimi, R. Ghosh, A. Vaziri, *Sci. Rep.* **2017**, *7*, 46046.
[11] Y. Gerson, S. Krylov, B. Ilic, D. Schreiber, *Finite Elements Anal. Des.* **2012**, *49*, 58.
[12] R. Addo-Akoto, J.-H. Han, *J. Intell. Mater. Syst. Struct.* **2018**, *30*, 506.
[13] P. Rothemund, A. Ainla, L. Belding, D. J. Preston, S. Kurihara, Z. Suo, G. M. Whitesides, *Sci. Rob.* **2018**, *3*, eaar7986.
[14] B. Xu, Y. Qiao, Y. Li, Q. Zhou, X. Chen, *Appl. Phys. Lett.* **2011**, *98*, 221909.
[15] B. Xu, Y. Qiao, T. Park, M. Tak, Q. Zhou, X. Chen, *Energy Environ. Sci.* **2011**, *4*, 3632.

[16] X. Lachenal, S. Daynes, P. M. Weaver, *J. Intell. Mater. Syst. Struct.* **2014**, *25*, 744.

[17] X. Lachenal, P. M. Weaver, S. Daynes, *Proc. R. Soc. A* **2012**, *468*, 1230.

[18] A. F. Arrieta, V. v. Gemmeren, A. J. Anderson, P. M. Weaver, *Smart Mater. Struct.* **2018**, *27*, 025006.

[19] M. W. Hyer, *J. Compos. Mater.* **1981**, *15*, 296.

[20] M. W. Hyer, *J. Compos. Mater.* **1981**, *15*, 175.

[21] V. Chillara, M. Dapino, *Composites, Part B* **2017**, *111*, 251.

[22] B. Wang, K. S. Fancey, *Mater. Lett.* **2015**, *158*, 108.

[23] S. Daynes, C. Diaconu, K. Potter, P. Weaver, *J. Compos. Mater.* **2010**, *44*, 1119.

[24] S. Daynes, K. Potter, P. Weaver, *Compos. Sci. Technol.* **2008**, *68*, 3431.

[25] H. Li, F. Dai, P. Weaver, S. Du, *Compos. Struct.* **2014**, *116*, 782.

[26] M. R. Schultz, M. W. Hyer, *J. Intell. Mater. Syst. Struct.* **2003**, *14*, 795.

[27] C. Bowen, R. Butler, R. Jervis, H. Kim, A. Salo, *J. Intell. Mater. Syst. Struct.* **2007**, *18*, 89.

[28] P. Portela, P. Camanho, P. Weaver, I. Bond, *Comput. Struct.* **2008**, *86*, 347.

[29] M. Gude, W. Hufenbach, C. Kirvel, *Compos. Struct.* **2011**, *93*, 377.

[30] P. F. Giddings, H. A. Kim, A. I. Salo, C. R. Bowen, *Mater. Lett.* **2011**, *65*, 1261.

[31] M. R. Schultz, W. K. Wilkie, R. G. Bryant, *J. Aircr.* **2007**, *44*, 1069.

[32] M.-L. Dano, M. Jean-St-Laurent, A. Fecteau, *Smart Mater. Res.* **2012**, *2012*, 695475.

[33] A. Arrieta, D. Wagg, S. Neild, *J. Intell. Mater. Syst. Struct.* **2011**, *22*, 103.

[34] A. F. Arrieta, O. Bilgen, M. I. Friswell, P. Hagedorn, *J. Intell. Mater. Syst. Struct.* **2013**, *24*, 266.

[35] O. Bilgen, A. F. Arrieta, M. I. Friswell, P. Hagedorn, *Smart Mater. Struct.* **2013**, *22*, 025020.

[36] H. A. Kim, D. N. Betts, A. I. T. Salo, C. R. Bowen, *AIAA J.* **2010**, *48*, 1265.

[37] W. Hamouche, C. Maurini, S. Vidoli, A. Vincenti, *Proc. R. Soc. A* **2017**, *473*, 20170364.

[38] A. J. Lee, A. Moosavian, D. J. Inman, *Mater. Lett.* **2017**, *190*, 123.

[39] A. J. Lee, A. Moosavian, D. J. Inman, *Smart Mater. Struct.* **2017**, *26*, 085007.

[40] A. J. Lee, A. Moosavian, D. J. Inman, presented at *Proc. SPIE 10164, Active and Passive Smart Structures and Integrated Systems*, April **2017**.

[41] S. Krylov, S. Seretensky, *J. Micromech. Microeng.* **2006**, *16*, 1382.

[42] S. Krylov, B. R. Ilic, D. Schreiber, S. Seretensky, H. Craighead, *J. Micromech. Microeng.* **2008**, *18*, 055026.

[43] L. Medina, R. Gilat, B. Ilic, S. Krylov, *Sens. Actuators, A* **2014**, *220*, 323.

[44] X. Chen, S. Meguid, *Proc. R. Soc. A* **2015**, *471*, 20150072.

[45] L. Medina, R. Gilat, S. Krylov, *Int. J. Eng. Sci.* **2017**, *110*, 15.

[46] F. Najar, M. Ghommem, A. Abdelkefi, *Int. J. Mech. Sci.* **2020**, *178*, 105624.

[47] E. G. Loukaides, S. K. Smoukov, K. A. Seffen, *Int. J. Smart Nano Mater.* **2015**, *5*, 270.

[48] K. A. Seffen, S. Vidoli, *Smart Mater. Struct.* **2016**, 25.

[49] Y. Kim, H. Yuk, R. Zhao, S. A. Chester, X. Zhao, *Nature* **2018**, *558*, 274.

[50] X. Hou, Y. Liu, G. Wan, Z. Xu, C. Wen, H. Yu, J. X. J. Zhang, J. Li, Z. Chen, *Appl. Phys. Lett.* **2018**, *113*, 221902.

[51] A. Amor, A. Fernandes, J. Pouget, *Int. J. Non-Linear Mech.* **2020**, 119.

[52] X.-Q. Li, W.-B. Li, W.-M. Zhang, H.-X. Zou, Z.-K. Peng, G. Meng, *Smart Mater. Struct.* **2017**, *26*, 105007.

[53] Z. Zhang, K. Pei, M. Sun, H. Wu, X. Yu, H. Wu, S. Jiang, F. Zhang, *Compos. Struct.* **2020**, *248*, 112506.

[54] H. Li, F. Dai, S. Du, *Compos. Sci. Technol.* **2012**, *72*, 1767.

[55] E. Eckstein, A. Pirrera, P. M. Weaver, *AIAA J.* **2016**, *54*, 1778.

[56] E. Eckstein, A. Pirrera, P. M. Weaver, *Compos. Struct.* **2013**, *100*, 363.

[57] L. Zhou, H. Xie, presented at *2019 20th Int. Conf. on Solid-State Sensors, Actuators and Microsystems & Eurosensors XXXIII (TRANSDUCERS & EUROSENSORS XXXIII)*, Berlin, Germany, June **2019**.

[58] L. Zhou, X. Zhang, Y. Sung, W.-C. Shih, H. Xie, *2018 Int. Conf. on Optical MEMS and Nanophotonics (OMN)*, IEEE, Piscataway, NJ **2018**.

[59] H. Hussein, F. Khan, M. I. Younis, *Smart Mater. Struct.* **2020**, *29*, 075033.

[60] J. M. Jani, M. Leary, A. Subic, M. A. Gibson, *Mater. Des.* **2014**, *56*, 1078.

[61] W. Huang, Z. Ding, C. Wang, J. Wei, Y. Zhao, H. Purnawali, *Mater. Today* **2010**, *13*, 54.

[62] Y. Gandhi, A. Pirondi, L. Collini, *Procedia Struct. Integr.* **2018**, *12*, 429.

[63] R. Panciroli, F. Nerilli, *Procedia Struct. Integr.* **2019**, *24*, 593.

[64] Z. Wei, R. Sandstroröm, S. Miyazaki, *J. Mater. Sci.* **1998**, *33*, 3743.

[65] Y. Osada, A. Matsuda, *Nature* **1995**, *376*, 219.

[66] A. Lendlein, S. Kelch, *Angew. Chem., Int. Ed.* **2002**, *41*, 2034.

[67] T. Chen, K. Shea, *3D Print. Addit. Manuf.* **2018**, *5*, 91.

[68] H. Y. Jeong, E. Lee, S. Ha, N. Kim, Y. C. Jun, *Adv. Mater. Technol.* **2019**, *4*, 1800495.

[69] Q. Zhao, X. Yang, C. Ma, D. Chen, H. Bai, T. Li, W. Yang, T. Xie, *Mater. Horiz.* **2016**, *3*, 422.

[70] G. Kocak, C. Tuncer, V. Bütün, *Polym. Chem.* **2017**, *8*, 144.

[71] Z. Han, P. Wang, G. Mao, T. Yin, D. Zhong, B. Yiming, X. Hu, Z. Jia, G. Nian, S. Qu, *ACS Appl. Mater. Interfaces* **2020**, *12*, 12010.

[72] M. Camacho-Lopez, H. Finkelmann, P. Palffy-Muhoray, M. Shelley, *Nat. Mater.* **2004**, *3*, 307.

[73] A. Lendlein, H. Jiang, O. Jünger, R. Langer, *Nature* **2005**, *434*, 879.

[74] A. H. Gelebart, D. J. Mulder, G. Vantomme, A. P. Schenning, D. J. Broer, *Angew. Chem., Int. Ed.* **2017**, *56*, 13436.

[75] Z. Jiang, M. L. Tan, M. Taheri, Q. Yan, T. Tsuzuki, M. G. Gardiner, B. Diggle, L. A. Connal, *Angew. Chem.* **2020**, *132*, 7115.

[76] G. Y. Gu, J. Zhu, L. M. Zhu, X. Zhu, *Bioinspir. Biomim.* **2017**, *12*, 011003.

[77] T. Chen, O. R. Bilal, K. Shea, C. Daraio, *Proc. Natl. Acad. Sci. USA* **2018**, *115*, 5698.

[78] S. Nishikawa, Y. Arai, R. Niiyama, Y. Kuniyoshi, *IEEE Rob. Autom. Lett.* **2018**, *3*, 1018.

[79] B. Gorissen, D. Melancon, N. Vasios, M. Torbati, K. Bertoldi, *Sci. Rob.* **2020**, *5*, eabb1967.

[80] S.-P. Jung, G.-P. Jung, J.-S. Koh, D.-Y. Lee, K.-J. Cho, *J. Mech. Rob.* **2015**, *7*, 021010.

[81] Y. Tang, Y. Chi, J. Sun, T.-H. Huang, O. H. Maghsoudi, A. Spence, J. Zhao, H. Su, J. Yin, *Sci. Adv.* **2020**, *6*, eaaz6912.

[82] Z. Zhang, X. Li, X. Yu, H. Chai, Y. Li, H. Wu, S. Jiang, *Compos. Struct.* **2019**, *229*, 111422.

[83] D. Lunni, M. Cianchetti, C. Filippeschi, E. Sinibaldi, B. Mazzolai, *Adv. Mater. Interfaces* **2020**, *7*, 1901310.

[84] H. Zhang, J. Sun, J. Zhao, *2019 Int. Conf. on Robotics and Automation (ICRA)*, Montréal, Canada, May **2019**.

[85] Y. Chi, Y. Tang, H. Liu, J. Yin, *Adv. Mater. Technol.* **2020**, *5*, 2000370.

[86] Y. Ke, C. Castro, J. H. Choi, *Annu. Rev. Biomed. Eng.* **2018**, *20*, 375.

[87] S. Nummelin, B. Shen, P. Piskunen, Q. Liu, M. A. Kostiainen, V. Linko, *ACS Synth. Biol.* **2020**, *9*, 1923.

[88] H. Ijas, S. Nummelin, B. Shen, M. A. Kostiainen, V. Linko, *Int. J. Mol. Sci.* **2018**, *19*, 2114.

[89] L. Zhou, A. E. Marras, H. J. Su, C. E. Castro, *Nano Lett.* **2015**, *15*, 1815.

[90] L. Zhou, A. E. Marras, C. E. Castro, H.-J. Su, *J. Mec. Rob.* **2016**, *8*, 051013.

[91] A. Ghosh, D. Paria, H. J. Singh, P. L. Venugopalan, A. Ghosh, *Phys. Rev. E: Stat., Nonlinear, Soft Matter Phys.* **2012**, *86*, 031401.

[92] Z. Chen, *2013 13th IEEE Int. Conf. on Nanotechnology (IEEE-NANO 2013)*, Beijing, China, August **2013**.

[93] J. Casals-Terre, A. Fargas-Marques, A. M. Shkel, *J. Microelectromech. Syst.* **2008**, *17*, 1082.

[94] M. A. A. Hafiz, L. Kosuru, A. Ramini, K. N. Chappanda, M. I. Younis, *Micromachines* **2016**, *7*, 191.

[95] Q. Chen, Y. Haddab, P. Lutz, presented at *2010 IEEE/RSJ Int. Conf. on Intelligent Robots and Systems*, Taipei, Taiwan, October **2010**.

[96] H. Hussein, I. Bouhadda, A. Mohand-Ousaid, G. Bourbon, P. Le Moal, Y. Haddab, P. Lutz, *Sens. Actuators, A* **2018**, *271*, 373.

[97] I. Bouhadda, A. Mohand-Ousaid, G. Bourbon, P. Le Moal, P. Lutz, H. Hussein, Y. Haddab, *2018 IEEE/RSJ Int. Conf. on Intelligent Robots and Systems (IROS)*, IEEE, Madrid, Spain, October **2018**.

[98] H. Hussein, V. Chalvet, P. Le Moal, G. Bourbon, Y. Haddab, P. Lutz, *2014 IEEE/ASME Int. Conf. on Advanced Intelligent Mechatronics*, Besançon, France, July **2014**.

[99] S.-W. Huang, F.-C. Lin, Y.-J. Yang, *Sens. Actuators, A* **2020**, *310*, 111934.

[100] H. M. Ouakad, M. I. Younis, *J. Sound Vib.* **2014**, *333*, 555.

[101] E. G. Loukaides, R. W. C. Lewis, C. R. Bowen, *Smart Mater. Struct.* **2019**, *28*, 02LT02.

[102] Z. Vangelatos, G. X. Gu, C. P. Grigoropoulos, *Extreme Mech. Lett.* **2019**, *33*, 100580.

[103] L. Wang, Y. Yang, Y. Chen, C. Majidi, F. Iida, E. Askounis, Q. Pei, *Mater. Today* **2018**, *21*, 563.

[104] J. T. Overvelde, T. A. de Jong, Y. Shevchenko, S. A. Becerra, G. M. Whitesides, J. C. Weaver, C. Hoberman, K. Bertoldi, *Nat. Commun.* **2016**, *7*, 10929.

[105] W. Ma, Z. Zhang, H. Zhang, Y. Li, H. Wu, S. Jiang, G. Chai, *Smart Mater. Struct.* **2019**, *28*, 025028.

[106] E. T. Filipov, G. Paulino, T. Tachi, *Proc. R. Soc. A* **2016**, *472*, 20150607.

[107] J. L. Silverberg, J. H. Na, A. A. Evans, B. Liu, T. C. Hull, C. D. Santangelo, R. J. Lang, R. C. Hayward, I. Cohen, *Nat. Mater.* **2015**, *14*, 389.

[108] A. Gillman, K. Fuchi, P. R. Buskohl, *Int. J. Solids Struct.* **2018**, *147*, 80.

[109] A. Rafsanjani, D. Pasini, *Extreme Mech. Lett.* **2016**, *9*, 291.

[110] P. Bhovad, J. Kaufmann, S. Li, *Extreme Mech. Lett.* **2019**, *32*, 100552.

[111] A. Pagano, T. Yan, B. Chien, A. Wissa, S. Tawfick, *Smart Mater. Struct.* **2017**, *26*, 094007.

[112] A. P. Milojević, N. D. Pavlović, *J. Intell. Mater. Syst. Struct.* **2015**, *27*, 1306.

[113] C. Jianguo, Z. Xiaowei, Z. Ya, F. Jian, T. Yongming, *J. Mech. Des.* **2015**, 137.

[114] Q. Liu, J. Huang, B. Xu, *J. Mech. Phys. Solids* **2019**, *133*, 103722.

[115] Q. Liu, B. Xu, *ACS Appl. Mater. Interfaces* **2020**, *12*, 43058.

[116] M. Safaei, H. A. Sodano, S. R. Anton, *Smart Mater. Struct.* **2019**, *28*, 113001.

[117] Y. Jia, *J. Intell. Mater. Syst. Struct.* **2020**, *31*, 921.

[118] B. Kathpalia, D. Tan, I. Stern, A. Erturk, *Smart Mater. Struct.* **2017**, *27*, 015024.

[119] S. F. A. Michael I Friswell, Onur Bilgen, Sondipon Adhikari, Arthur W Lees, Grzegorz Litak, *J. Intell. Mater. Syst. Struct.* **2012**, *23*, 1505.

[120] L. Van Blarigan, J. Moehlis, *Chaos* **2016**, *26*, 033107.

[121] A. Garg, S. Dwivedy, *Proc. Eng.* **2016**, *144*, 592.

[122] W. Liu, F. Formosa, A. Badel, A. Agbossou, G. Hu, *Smart Mater. Struct.* **2016**, *25*, 115045.

[123] M. Derakhshani, T. A. Berfield, K. D. Murphy, *Nonlinear Dyn.* **2019**, *96*, 1429.

[124] T. Huguet, A. Badel, M. Lallart, *Smart Mater. Struct.* **2019**, *28*, 115009.

[125] B. Andò, S. Baglio, A. R. Bulsara, V. Marletta, A. Pistorio, *IEEE Trans. Instrum. Meas.* **2017**, *66*, 1067.

[126] B. Andò, S. Baglio, A. Bulsara, V. Marletta, A. Pistorio, *Proc. Eng.* **2015**, *120*, 1024.

[127] A. Emad, M. A. Mahmoud, M. Ghoneima, M. Dessouky, *Smart Mater. Struct.* **2016**, *25*, 115006.

[128] A. Erturk, D. J. Inman, *J. Sound Vibr.* **2011**, *330*, 2339.

[129] A. S. De Paula, D. J. Inman, M. A. Savi, *Mech. Syst. Signal Process.* **2015**, *54*, 405.

[130] Y. Gao, Y. Leng, A. Javey, D. Tan, J. Liu, S. Fan, Z. Lai, *Smart Mater. Struct.* **2016**, *25*, 115032.

[131] Y. Leng, Y. Gao, D. Tan, S. Fan, Z. Lai, *J. Appl. Phys.* **2015**, *117*, 064901.

[132] Y. Gao, Y. Leng, S. Fan, Z. Lai, *Smart Mater. Struct.* **2014**, *23*, 095003.

[133] K. A. Singh, M. Pathak, R. J. Weber, R. Kumar, *IEEE Trans. Sonics Ultrason.* **2018**, *65*, 2184.

[134] D. Zhao, M. Gan, C. Zhang, J. Wei, S. Liu, T. Wang, *Mater. Res. Express* **2018**, *5*, 085704.

[135] G. Wang, W.-H. Liao, B. Yang, X. Wang, W. Xu, X. Li, *Mech. Syst. Signal Process.* **2018**, *105*, 427.

[136] C. Lan, W. Qin, *Mech. Syst. Signal Process.* **2017**, *85*, 71.

[137] P. Podder, D. Mallick, A. Amann, S. Roy, *Sci. Rep.* **2016**, *6*, 37292.

[138] W. Wang, J. Cao, C. R. Bowen, D. J. Inman, J. Lin, *Appl. Phys. Lett.* **2018**, *112*, 213903.

[139] M. Hwang, A. F. Arrieta, *Sci. Rep.* **2018**, *8*, 3630.

[140] H. Deng, Z. Wang, Y. Du, J. Zhang, M. Ma, X. Zhong, *IEEE/ASME Trans. Mechatronics* **2019**, *24*, 282.

[141] S. A. Emam, D. J. Inman, *Appl. Mech. Rev.* **2015**, *67*, 060803.

[142] R. Xu, S. Kim, *J. Phys.: Conf. Ser.* **2015**, *660*, 012013.

[143] P. Harris, C. R. Bowen, H. A. Kim, G. Litak, *Eur. Phys. J. Plus* **2016**, *131*, 109.

[144] A. J. Lee, D. J. Inman, *J. Intell. Mater. Syst. Struct.* **2018**, *29*, 2528.

[145] A. J. Lee, D. J. Inman, *J. Sound Vib.* **2019**, *446*, 326.

[146] A. F. Arrieta, P. Hagedorn, A. Erturk, D. J. Inman, *Appl. Phys. Lett.* **2010**, *97*, 104102.

[147] D. N. Betts, H. A. Kim, C. R. Bowen, D. J. Inman, *Appl. Phys. Lett.* **2012**, *100*, 114104.

[148] D. Betts, H. Kim, C. Bowen, D. Inman, presented at 53rd AIAA/ASME/ASCE/AHS/ASC Structures, Structural Dynamics and Materials Conf. 20th AIAA/ASME/AHS Adaptive Structures Conference 14th AIAA, Honolulu, Hawaii, USA, April **2012**.

[149] Z.-Q. Lu, D. Shao, Z.-W. Fang, H. Ding, L.-Q. Chen, *J. Vib. Control* **2019**, *26*, 779.

[150] S. Shan, S. H. Kang, J. R. Raney, P. Wang, L. Fang, F. Candido, J. A. Lewis, K. Bertoldi, *Adv. Mater.* **2015**, *27*, 4296.

[151] X. Tan, S. Chen, S. Zhu, B. Wang, P. Xu, K. Yao, Y. Sun, *Int. J. Mech. Sci.* **2019**, *155*, 509.

[152] J. Hua, H.-s. Lei, C.-f. Gao, D.-n. Fang, presented at *2019 13th Symposium on Piezoelectrcity, Acoustic Waves and Device Applications (SPAWDA)*, Harbin, China, January **2019**.

[153] C. S. Ha, R. S. Lakes, M. E. Plesha, *Mater. Des.* **2018**, *141*, 426.

[154] C. Winkelmann, S. S. Kim, V. La Saponara, *Compos. Struct.* **2010**, *93*, 171.

[155] M. J. Frazier, D. M. Kochmann, *J. Sound Vib.* **2017**, *388*, 315.

[156] C. Ren, D. Yang, H. Qin, *Materials* **2018**, *11*, 1078.

[157] B. Haghpanah, L. Salari-Sharif, P. Pourrajab, J. Hopkins, L. Valdevit, *Adv. Mater.* **2016**, *28*, 7915.

[158] A. Rafsanjani, A. Akbarzadeh, D. Pasini, *Adv. Mater.* **2015**, *27*, 5931.

[159] X. Zhang, X. Tian, L. Xiao, X. Li, L. Chen, *Appl. Energy* **2018**, *228*, 450.

[160] D.-A. Wang, J.-H. Chen, H.-T. Pham, *Sens. Actuators, A* **2013**, *189*, 481.

[161] A. Cherkaev, S. Leelavanichkul, *Int. J. Damage Mech.* **2011**, *21*, 697.

[162] H. Y. Jeong, S. C. An, I. C. Seo, E. Lee, S. Ha, N. Kim, Y. C. Jun, *Sci. Rep.* **2019**, *9*, 324.

[163] V. Vetriselvi, M. Geetha, K. Dhanalakshmi, presented at *2018 8th IEEE India Int. Conf. on Power Electronics (IICPE)*, Jaipur, India, December **2018**.

Yunteng Cao is currently a Ph.D. candidate in the Department of Civil and Environmental Engineering at Massachusetts Institute of Technology (MIT). He received his B.E. degree in Engineering Mechanics from Shanghai Jiao Tong University (China) in 2013 and M.E. in solid mechanics from Xi'an Jiaotong University (China) in 2016. His research focuses on advanced materials and structures, biopolymers and material delivery to plants and precision agriculture.

Guoliang Huang is currently a Huber and Hellen Croft Chair professor of mechanical and aerospace engineering at University of Missouri-Columbia. He received his Ph.D. degree from University of Alberta, Canada, in 2004. Dr. Huang works in the broad area of Solid Mechanics and Architected Materials in particular the new frontiers of structural dynamics, topological mechanics, wave propagation, and dynamical behaviors of composite materials, both man-made and formed naturally. Dr. Huang's research has been funded by NSF, Air Force of Scientific Research, Army Research Office, Office of Naval Research, Department of Energy, NASA, and major industries.

Changyong Cao is currently an Assistant Professor of Packaging, Mechanical Engineering, and Electrical & Computer Engineering at Michigan State University, where he is directing the *Laboratory for Soft Machines & Electronics*. He received his Ph.D. degree in Mechanical Engineering and Materials Science from the Australian National University (ANU) in 2014, and then worked as a postdoctoral associate for three years at Duke University, USA. His research interests include solid mechanics, soft (active) materials, soft/hybrid robotics, flexible and stretchable electronics, energy devices, and 3D/4D printing of multifunctional materials.